Determination of Porin Channel Activity and Evolution of Targeting Signals in Plant Peroxisomes

by

Pradeep Soni

Thesis submitted in fulfilment of the
requirements for the degree of
Doctor of Philosophy
(PhD)

Faculty of Science and Technology
Department of Mathematics and Natural Science

2013

University of Stavanger
N-4036 Stavanger
Norway
www.uis.no

ISBN 978-82-7644-521-3
ISSN 1890-1387

PhD thesis no. 184

Contents

Acknowledgements

I would like to express my deepest gratitude to my supervisor Prof. Peter Ruoff without whose guidance and support, it would have been impossible for me to carry out this study. I will always be indebted for his unconditional assistance and invaluable comments.

I am also very thankful to my co-supervisors Prof. Sigrun Reumann and Prof. Cathrine Lillo for their kind cooperation. Special thanks to Prof. Bjørn Hjertager for his much appreciated help and to Prof. Roland Benz, University of Würzburg, Germany for allowing me to conduct part of my research work in his lab.

I would also like to thank my friends and colleagues at CORE: Dr. Amr Kataya, Dugassa Nemie-Feyissa, Dr. Behzad Heidari, Dr. Kristine M. Olsen, Aline Benichou, Dorde Nikolic, Chimuka Mwaanga, Altinai Adilbayeva, Dr. Gopal Chowdhary, Dr. Rajneesh Singhal, Manish budathoki, Mohammed Gebriel, Dr. Xiang Ming Xu, Dr. Daniela Gargano, Dr. Jodi Grødem, Dominik Piston, Janine Arnold, Dr. Clemens Furmes, Dr. Ingunn W. Jolma and Dr. Xiao-Yu Ni.

Lastly, I am very grateful to Almighty God and His representatives in the form of family members for their never ending love and care.

Abstract

Peroxisomes are eukaryotic organelles traditionally known for their roles in fatty acid metabolism and generation and removal of hydrogen peroxide. Several new functions are being ascribed to these organelles with the help of genetic and proteomic based studies. Despite showing the diversity in metabolic functions, peroxisomes from different sources share certain common features related to protein import pathways and the transfer of metabolites across them.

The majority of peroxisome matrix proteins are imported by peroxisome targeting signals PTS 1 and 2. All the proteins containing PTS2 have been found to be replaced by PTS1 in *C.elegans* and *P.tricornutum* suggesting higher preference to PTS1 in these organisms. One aim of the present study was to determine if a similar transition of targeting signals from PTS2 to PTS1 has also occurred in plants during the course of evolution. This was studied by taking protein orthologs from both lower photosynthetic organisms including mosses and algae and higher plants containing monocots as well as dicots. In total five groups of proteins could be constructed assuming an increased affinity to PTS1 in higher plants and their targeting signals were analyzed by *in vivo* subcellular localization studies. The results showed a higher preference to PTS2 signal by proteins from lower plants while the corresponding protein sequences from higher plant orthologs displayed higher affinity to PTS1 signal. It is also suggested that the evolution of targeting signals in plants may not end to exclusive PTS1 proteins like *C.elegans* but rather dual signal proteins containing both PTS1 and PTS2 signals either on one protein or on two different but interacting proteins.

The peroxisomal membranes are predicted to contain the porin like channels that regulate the transfer of solutes involved in various metabolic reactions. However, the molecular basis of such a channel in plants is not known. Thus, the leaf peroxisomes were isolated from

Arabidopsis and subjected for electrophysiological characterization with the help of planar lipid bilayer technique. The results showed the pore forming activity in the peroxisomal membrane fractions with the average single channel conductance corresponding to 0.5 nS in 1 M KCl. In addition, two peroxisomal membrane proteins AtPMP22 and AtPEX11-D were also overexpressed using *Pichia* as a heterologous system and were subjected for lipid bilayer analysis. The experiments suggested a porin activity in the purified fractions containing the recombinant proteins.

The study presented in this thesis will help to understand the evolution of targeting signals in plant peroxisomes and may expand our knowledge related to protein import pathways. The pore forming activity observed in Arabidopsis leaf peroxisomes and in the overexpressed recombinant proteins AtPMP22 and AtPEX11-D may help in better understanding of porin channels in plant peroxisomes and also in finding the molecular basis of the reported channel activity. This in turn may shed more light on our current information about transport properties of this organelle.

List of Publications

1. **Babujee, L., Wurtz, V., Ma, C., Lueder, F., Soni, P., Van Dorsselaer, A., Reumann, S.** (2010). The proteome map of spinach leaf peroxisomes indicates partial compartmentalization of phylloquinone (vitamin K1) biosynthesis in plant peroxisomes, Journal of Experimental Botany, 61, 1441-1453.

Abbreviations

ABC	ATP binding cassette
ACO	Aconitase
ACX	Acyl-CoA oxidase
ADP	Adenosine di-phosphate
APS	Ammonium persulfate
APX	Ascorbate peroxidase
ASC	Ascorbate
ATP	Adenosine tri-phosphate
CaMV	Cauliflower mosaic virus
CAT	Catalase
CBB	Comassie brilliant blue
CE	Crude extract
Co-A	Coenzyme A
CSY	Citrate synthase
DHAR	Dehydroascorbate reductase
DPhPC	Diphytanoyl phosphatidylcholine
DTT	Dithiothreitol
ER	Endoplasmic reticulum
EYFP	Enhanced yellow fluorescent protein

GGT	Glutamate:glyoxylate amino transferase
GOX	Glycolate oxidase
GR	Glutathione reductase
GSH	Glutathione
GST	Glutathione-S-transferase
H_2O_2	Hydrogen peroxide
His	Histidine
HPR	Hydroxypyruvate reductase
IAA	Indole-3-acetic acid
IBA	Indole butyric acid
ICL	Isocitrate lyase
JA	Jasmonic acid
KAT	Ketoacyl-CoA thiolase
LACS	Long chain acyl-CoA synthetase
nS	nano (10^{-9}) Siemens
MDAR	Monodehydroascorbate reductase
MDH	Malate dehydrogenase
MF	Membrane fraction
MFP	Multifunctional protein
MLS	Malate synthase

NS	Naphthoate synthase
NTA	Nitrilo acetic acid
PCR	Polymerase chain reaction
PEX	Peroxin
PF	Purified fraction
PG	Phosphoglycolate
PMP	Peroxisome membrane protein
PMSF	Phenyl methyl sulfonyl fluoride
POPC	Palmitoyl oleoylglycero phospho choline
POPE	Palmitoyl oleoylglycero phospho ethanolamine
PTD	Peroxisomal targeting domain
PTFE	Polytetrafluoroethylene
PTS	Peroxisome targeting signal
RE	Restriction endonuclease
ROS	Reactive oxygen species
SDS	Sodium dodecyl sulfate
SGT	Serine:glyoxylate amino transferase
TEMED	N’-tetramethylethane-1,2-diamine

List of Figures

List of Tables

1. Introduction

1.1 Peroxisomes

Peroxisomes are single membrane-bound tiny organelles (0.1-1µm in diameter) which are found in almost all eukaryotic organisms ranging from simple unicellular algae to highly evolved multicellular species (Purdue and Lazarow, 2001). They were first isolated and characterized by Christian de Duve who came across them while studying carbohydrate metabolism in rat liver cells (De Duve and Baudhuin, 1966). The two most widely distributed and well conserved functions of peroxisomes include the detoxification of reactive oxygen species (ROS) and the break-down of fatty acids by β-oxidation pathway. The functions of peroxisomes depend upon the organism, cell type and even environmental conditions, signifying the highly dynamic nature of this organelle (Lanyon-Hogg *et al*., 2010). Owing to this specialization in their functions, peroxisomes are often called with different names. For example, in plants they are broadly categorized as leaf peroxisomes, glyoxysomes and unspecialized peroxisomes. While leaf peroxisomes are involved in the process of photorespiration for recycling phosphoglycerate from phosphoglycolate, glyoxysomes helps in metabolizing acetyl Co-A via glyoxylate cycle. Yeast peroxisomes are unique sites of methanol-metabolism and penicillin biosynthesis (van der Klei *et al*., 2006; Bartoszewska *et al*., 2011). Mammalian peroxisomes regulate synthesis of plasmalogens (ether-linked phospholipids) and cholesterol (Wanders *et al*., 2010) and also play an important role in the degradation of very long chain dicarboxylic polyunsaturated fatty acids (Nguyen *et al*., 2008). In some protozoans like *Trypanosoma* and *Leishmania*, peroxisomes contain glycolytic enzymes and are called as glycosomes (Opperdoes, 1987). In certain filamentous fungi, peroxisomes are known as Woronin bodies where they seal septal pores occurred during hyphal injury and thereby restricting the loss of cytoplasm to the site of injury (Jedd and Chua,

2000). Figure 1-1 gives an overview of the diverse metabolic functions played by peroxisomes in different tissues and organisms.

Despite the profound diversity in their metabolic functions, peroxisomes from different sources show similarity in morphology, biogenesis and in the metabolite transport pathways (Antonenkov and Hiltunen, 2012).

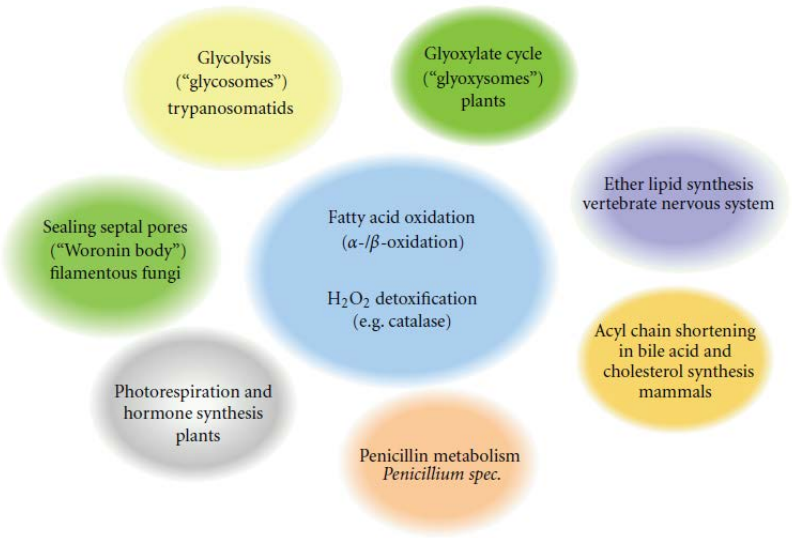

Figure 1-1: Overview of peroxisomal functions

Peroxisomes are involved in many different metabolic reactions. The conserved functions of peroxisomes including fatty acid metabolism and H_2O_2 degradation are displayed in the centre while the specialized metabolic pathways in different organisms and tissues are shown in the periphery. Figure taken from (Till *et al.*, 2012).

1.1.1 Functions of plant peroxisomes

Plant peroxisomes are highly dynamic organelles which are involved in several biochemical processes. In addition to the already known functions such as fatty acid metabolism, detoxification reactions, photorespiration and glyoxylate cycle, many new functions have been ascribed in the recent past with the help of genetic (Lipka *et al*., 2005; Boisson-Dernier *et al*., 2008) bioinformatic (Lingner *et al*., 2011) and proteomic based studies (Wiese *et al*., 2007; Eubel *et al*., 2008; Reumann *et al*., 2009).

1.1.1.1 Fatty acid metabolism

Fatty acid degradation in plants, unlike in mammals, takes place exclusively in the peroxisomes with the help of β-oxidation pathway. The peroxisome ABC transporter PXA1, ATP/ADP transporters PNC1/2 and two long chain acyl-Co-A synthetases (LACS6/7) regulate fatty acid import into the peroxisomes and their activation to corresponding Co-A esters before they are metabolised (Zolman *et al*., 2001; Fulda *et al*., 2004; Linka *et al*., 2008). Each cycle of the β-oxidation pathway results in the shortening of fatty acyl-CoAs by two carbon residues with the help of core enzymes acyl-CoA oxidase (ACX), multifunctional protein (MFP) and 3-ketoacyl Co-A thiolase (KAT). The schematic representation of the β-oxidation cycle is shown in Figure 1-2. In addition to these core enzymes, many auxiliary enzymatic activities are also required for β-oxidation of unsaturated fatty acids which contain double bonds at various places (even- or odd-numbered carbon atoms). Two of these auxiliary enzyme activities were described for cucumber MFP showing Δ(3),Δ(2)-enoyl-CoA-isomerase and 3-hydroxylacyl-CoA epimerase activities (Behrends *et al.*, 1988). Later, using *Arabidopsis* it was shown that Δ(3,5)Δ(2,4)-enoyl-CoA isomerase is required for β-oxidation of fatty acids having double bonds at odd numbered carbons (Goepfert *et al.*, 2005) and enoyl-CoA hydratase 2 is required for degradation of cis-unsaturated

fatty acids with double bonds at even number carbon atoms (Goepfert *et al.*, 2006).

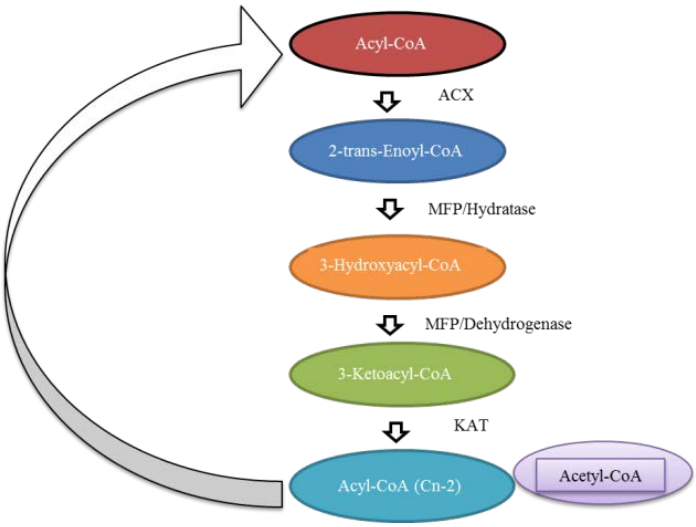

Figure 1-2: β-oxidation pathway for fatty acid metabolism

Fatty acids are degraded in peroxisomes by a four step cyclic process starting from oxidation of Acyl-CoA followed by hydration, dehydrogenation and thiolysis resulting into the formation of a shortened fatty acid and acetyl-CoA.

1.1.1.2 Glyoxylate cycle

The glyoxylate cycle involves the conversion of acetyl-CoA derived from fatty acid β-oxidation into 4-carbon compounds which can be further converted into hexoses by the process of gluconeogenesis or into sucrose which is required for growing seedling tissue (Graham, 2008). The enzymes involved in this pathway include citrate synthase (CS), aconitase (ACO), isocitrate lyase (ICL), malate synthase (MLS) and malate dehydrogenase (MDH). This cycle allows plants to use

lipids as a source of energy during seed germination. In a similar manner like tricarboxylic acid cycle, the glyoxylate cycle also starts with CSY that transfers acetyl-CoA to oxaloacetate leading to the production of citrate, which is then converted into isocitrate by ACO. The isocitrate is cleaved by the activity of ICL into glyoxylate and succinate, a characteristic feature of this cycle. The cycle continues with MLS catalysing the synthesis of malate from glyoxylate and acetyl-CoA. Malate is finally dehydrogenised by MDH into oxaloacetate. The schematic representation of the glyoxylate cycle is shown in Figure 1-3.

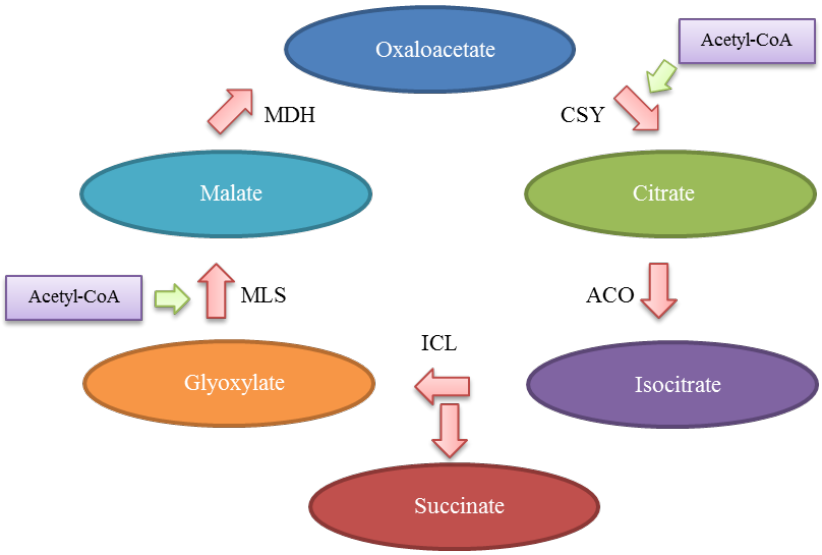

Figure 1-3: Glyoxylate cycle

The glyoxylate cycle in peroxisomes starts with the synthesis of citrate from acetyl-CoA and oxaloacetate which is then converted into isocitrate. Isocitrate cleave to succinate and glyoxylate and in the end malate which is formed from glyoxylate and acetyl-CoA is converted to oxaloacetate.

1.1.1.3 Photorespiration

Photorespiration results from the oxygenase reaction catalysed by ribulose-1,5-bisphosphate carboxylase/oxygenase (Rubisco) and forms phosphoglycolate. It occurs in all oxygen producing photosynthetic organisms and serves as a major carbon-recovery system (Bauwe *et al.*, 2010; Maurino and Peterhansel 2010). This metabolic pathway recycles the toxic compound phosphoglycolate into phosphoglycerate with the help of several enzymatic reactions which are distributed in chloroplast, peroxisomes and mitochondria. Leaf peroxisomes play a major role in photorespiration by harbouring six out of the eleven enzymes that include glycolate oxidase (GOX), catalase (CAT), glutamate:glyoxylate aminotransferase (GGT), serine:glyoxylate aminotransferase (SGT), hydroxypyruvate reductase (HPR) and malate dehydrogenase (MDH) (Kaur *et al*., 2009; Hu *et al*., 2012). All of these enzymes have been suggested to be present as multi-protein complexes facilitating substrate channelling and thereby minimizing leakage of metabolic intermediates across peroxisomal membranes (also see 1.2) (Heupel *et al.*, 1991; Heupel and Heldt, 1994).

1.1.1.4 Hormone biosynthesis

Plant peroxisomes are also involved in the synthesis of hormones such as jasmonic acid (JA) and indole-3-acetic acid (IAA). Biosynthesis of JA takes place in two organelles, starting in the chloroplasts and ending in the peroxisomes. The chloroplast helps in the degradation of polyunsaturated fatty acids by releasing JA precursor, 12-oxo-phytodienoic acid (OPDA). OPDA is then transferred to the peroxisomes via peroxisomal ABC transporter PXA1 where it is reduced into 3-oxo-2-(2'-[Z]-pentenyl) cyclopentane-1-octanoic acid (OPC:8) by OPDA reductase (Schaller *et al.*, 2000; Theodoulou *et al.*, 2005). OPC:8 is activated by OPC:8 Co-A ligase 1 (OPCL1) which after three rounds of β-oxidation is converted into JA-CoA and finally when thioesterases cleave Co-A moiety, JA is formed (Koo *et al.*, 2006; Schilmiller *et al.*, 2007). Another phytohormone, IAA is

synthesized exclusively in peroxisomes. Similar to JA, IAA is also produced from its precursor indole butyric acid (IBA) that is assumed to be imported into peroxisomes via PXA1 transporter where is metabolised to indoleacetyl-CoA by the enzymatic reactions similar to fatty acid β-oxidation. The IAA-CoA thus generated is hydrolysed by enoyl-CoA hydratase to release the active auxin IAA (Strader *et al.*, 2011; Zolman *et al.*, 2007; Zolman *et al.*, 2008).

1.1.1.5 Detoxification

Several reactive oxygen species (ROS) are produced during the various oxidative metabolic pathways such as photorespiration, fatty acid β-oxidation and polyamine oxidation which take place inside the peroxisomes. These reactive molecules are comprised of superoxides and hydrogen peroxide (H_2O_2) and are very toxic to the cell environment. These molecules are thus required to be detoxified in order to prevent any cellular damage. H_2O_2 is degraded in peroxisomes primarily by catalase which converts it into water and oxygen molecules. In addition, plant peroxisomes also convert H_2O_2 into water with the help of ascorbate-glutathione cycle involving ascorbate peroxidase (APX), monodehydroascorbate reductase (MDAR), dehydroascorbate reductase (DHAR) and glutathione reductase (GR) (Yamaguchi *et al.*, 1995; Lisenbee *et al.*, 2005). Glutathione-S-transferase (GST), superoxide dismutase and peroxiredoxins are the other antioxidants required for reactive species metabolism (Almagro *et al.*, 2009). Figure 1-4 show the schematic representation of the events occurring in the synthesis and degradation of H_2O_2. These reactive species when present in less amount also act as cellular messengers with probable roles in intra- and inter-cellular communication *(*del Rio *et al.*, 2006).

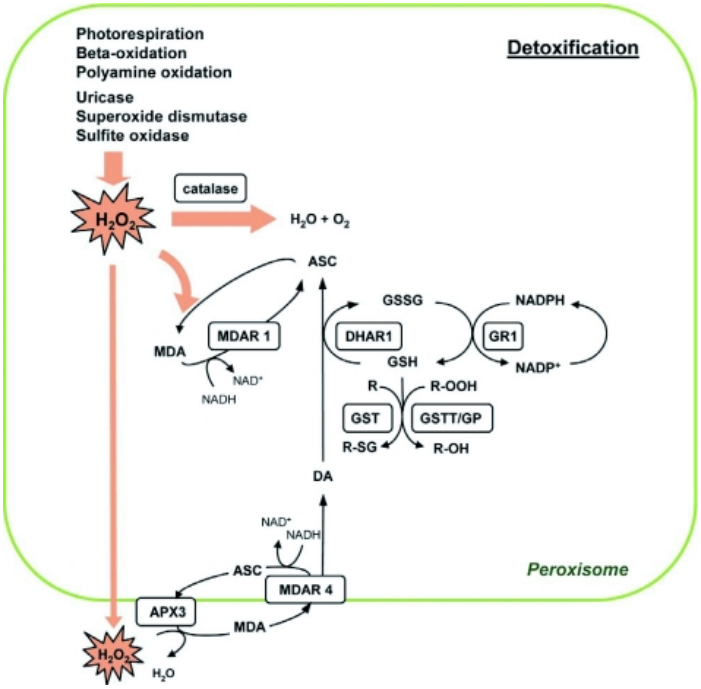

Figure 1-4: Role of peroxisomes in detoxification reactions

H_2O_2 is a very toxic substance that is produced by several oxidative reactions and may damage surrounding enzymes and membrane lipids. It is degraded within peroxisomes in two ways- by catalase and ascorbate (ASC)-glutathione (GSH) cycle. Figure taken from (Kaur *et al.*, 2009).

1.1.1.6 Plant defense

Recent studies have suggested the role of peroxisomes in plant innate immunity. It has been reported that the *PEN2* gene encoding glycosyl hydrolase is responsible for conferring resistance against a broad spectrum of non-adaptive pathogens (Lipka *et al.*, 2005). Furthermore, it was shown that peroxisomes accumulate at penetration sites of fungal pathogens and defects in the *PEN2* gene leads to a loss of penetration resistance (Koh *et al.*, 2005; Lipka *et al.*, 2005). It is suggested that PEN2 possibly hydrolyses 4-methoxy-indole-3-methylglucosinolate which further downstream leads to activation of callose deposition and

plant resistance against pathogens (Clay *et al*., 2009). Recently it was reported that *enhanced disease resistance 1* (*edr1)* gene in Arabidopsis functions in pre-invasive nonhost resistance. The *edr1* mutant also exhibited enhanced susceptibility to host-adapted pathogens, including *Colletotrichum higginsianum* and necrotrophic *Alternaria brassicicola* (Hiruma *et al*., 2011). It has also been shown that pathogen infection in plants leads to an increased accumulation of ROS within peroxisomes which induce hypersensitive reactions that appear to play an important role in plant defense responses (Taler *et al*., 2004; Del Rio, 2011).

1.1.2 Peroxisomes biogenesis

Peroxisome biogenesis is considered to be regulated by two distinct mechanisms. New peroxisomes can either be formed *de novo* from the endoplasmic reticulum (Mullen and Trelease, 2006) or from pre-existing peroxisomes by the process of proliferation and division (Lazarow and Fujiki, 1985; Motley and Hettema, 2007). The proteins that play role in peroxisome biogenesis are designated as peroxisome biogenesis factors or PEROXINS (PEX) (Distel *et al*., 1996). In studies related to peroxisome biogenesis, three peroxins (PEX3, PEX16 and PEX19) have been studied in greater detail. These proteins are very important for the initial steps in assembly of peroxisome membrane and their maintenance. Loss of these proteins result in mutants lacking the organelle while re-introduction of functional protein into these mutants restores the peroxisomes and thereby supporting the *de novo* synthesis model of peroxisome biogenesis (South and Gould, 1999; Hoepfner *et al*., 2005; Kim *et al*., 2006). However, it was also suggested that peroxisomes are generated from pre-existing organelles either by undergoing proliferation, the substantive increase in peroxisome number which is induced in response to external stimuli or constitutively by replication/division (Yan *et al*., 2005). A three step process consisting of peroxisome elongation, constriction and fission is considered to regulate both peroxisome proliferation and division (Kaur

and Hu, 2009). Proteins belonging to the family of PEX11, dynamin related protein (DRP) and to the Fission1 (Fis1) play key roles in peroxisome biogenesis. These proteins are evolutionarily conserved in fungi, plants and mammals suggesting similar mechanisms of peroxisome biogenesis in these organisms (Kaur *et al*., 2009). However, some additional peroxisome division factors were reported recently which also regulate peroxisome proliferation but act independently of PEX11, DRPs and FIS1 proteins (Aung and Hu, 2011).

1.1.2.1 Matrix protein import

The absence of genomic DNA in peroxisomes implies that all peroxisomal proteins are nuclear encoded and required to be imported from cytoplasm (Lazarow and Fujiki, 1985). As shown in Fig. 1-5, these peroxisomal proteins contain specific amino acid sequences which act as targeting signals and regulate the protein import pathway. There are mainly two types of peroxisome targeting signals - PTS1 and PTS2 that are used for the import of most of the peroxisomal matrix proteins (Subramani, 1993). The PTS1 signal is usually composed of three amino acids and is located at the C-terminal end of the protein. Since 1987, when it was first identified as the 'SKL' motif in firefly luciferase (Gould *et al*., 1987), several tri-peptide motifs have been reported for the import of peroxisomal proteins in various organisms (Gould *et al*., 1988; Kragler *et al*., 1998). A consensus sequence for PTS1 proteins, initially proposed as (S/A/C)-(K/R/H)-L (Gould *et al*., 1989), was modified by putting methionine as the last amino acid in the tri-peptide motif thus changing the consensus sequence to (S/A/C)-(K/R/H)-(L/M) (Kragler *et al*., 1998). But some proteins have been reported to follow the consensus sequence only partially (Reumann *et al*., 2007). In addition, it has been found that sequences immediately upstream to the tri-peptide motif also contribute to specificity, especially when they deviate from the consensus sequence (Ma and Reumann, 2008).

In comparison to the PTS1, lesser proteins require the PTS2 targeting signal for their import. Moreover, the PTS2 signal differs in many aspects from the PTS1 dependent protein import. Firstly, the PTS2 is located at or near the N-terminal end rather than at the C-terminal end of the protein. Secondly, the PTS2 sequence motif is normally composed of the nine amino acids in comparison to the tri-peptide motif of PTS1. Finally, the PTS2 signal (unlike the PTS1 signal) is usually cleaved off after import of protein into the peroxisomes. The PTS2 signal is composed broadly of the consensus sequence (R/K)-(L/V/I)-X_5-(H/Q)-(L/A/F) where X denotes any amino acid (Purdue and Lazarow, 2001). Indigoidine synthase A (IndA), His triad family proteins (HIT 2/3), Naphthoate synthase (NS) and peroxisomal-3-ketoacyl-CoA thiolase (PKT 2/3/4) are some of the plant proteins containing the PTS2 signal for their import into the peroxisomes.

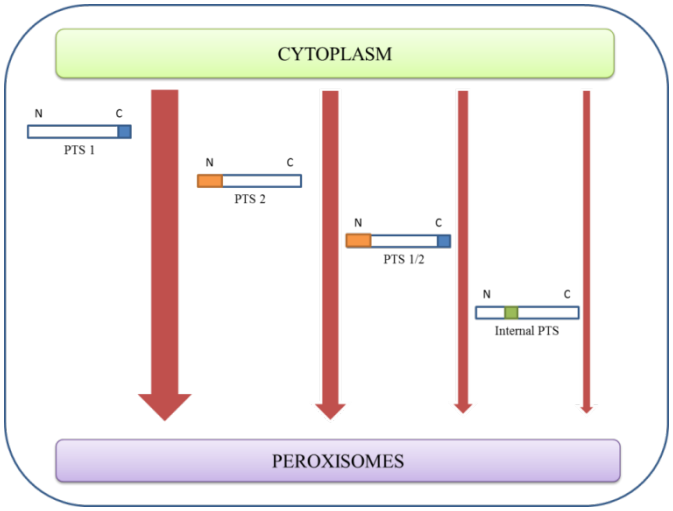

Figure 1-5: Peroxisome targeting signals for protein import

The import pathway for peroxisomal matrix proteins is regulated by amino acid sequences known as peroxisome targeting signals PTS. The majority of proteins are imported by PTS1 and PTS2 signals located at C and N terminal end of the protein respectively. Some proteins contain both PTS 1/2 while few proteins contain PTS located in middle, away from both terminal ends.

Introduction

The whole process for protein import can be broadly divided into five steps as shown in Figure 1-6. The first step includes the recognition of the matrix protein (also termed as cargo) by the different cytosolic receptor and co-receptors. The second step involves the docking of cargo-receptor complexes at the peroxisomal membrane. The membrane translocation of cargo-receptor complex starts during the third step with release of cargo taking place in the fourth step and finally, the receptors are recycled back into the cytoplasm to perform the next round of import cycle. The proteins containing the PTS1 and PTS2 signals are recognised by PEX5 and PEX7 receptors respectively. Both the pathways are interconnected in plants with PEX5 also acting as a co-receptor for PTS2 proteins and by the PEX7 requirement in enhancing the stability of PEX5. The cargo-loaded receptors associate with the peroxisomal membrane via the docking complex which consists of PEX13, PEX14 and PEX17 (Chang *et al*., 1999; Fan *et al*., 2005). Three models have been suggested to describe the possible modes of cargo translocation. The simple shuttle model proposes that the receptor is partially exposed to the peroxisomal lumen for cargo unloading (Marzioch *et al.*, 1994), the extended shuttle model suggests the complete entry of the receptor-cargo complex inside the peroxisomes which is then followed by unloading of cargo (Dammai and Subramani, 2001; Kunau, 2001) whereas the transient pore concept postulates that the receptor proteins may also act as pores through which the receptor-cargo complex passes and enters into the organelle, subsequently releasing the cargo (Erdmann and Schliebs, 2005). The docking complex is connected via PEX8 to the RING-finger motif containing PEX2, PEX10 and PEX12 (Agne *et al*., 2003). The protein complex composed of PEX1, PEX6, PEX4 and PEX22 is involved in the ubiquitination of receptor proteins which are then finally exported to the cytoplasm in order to initiate another import cycle (Collins *et al*., 2000; Zolman *et al*., 2005).

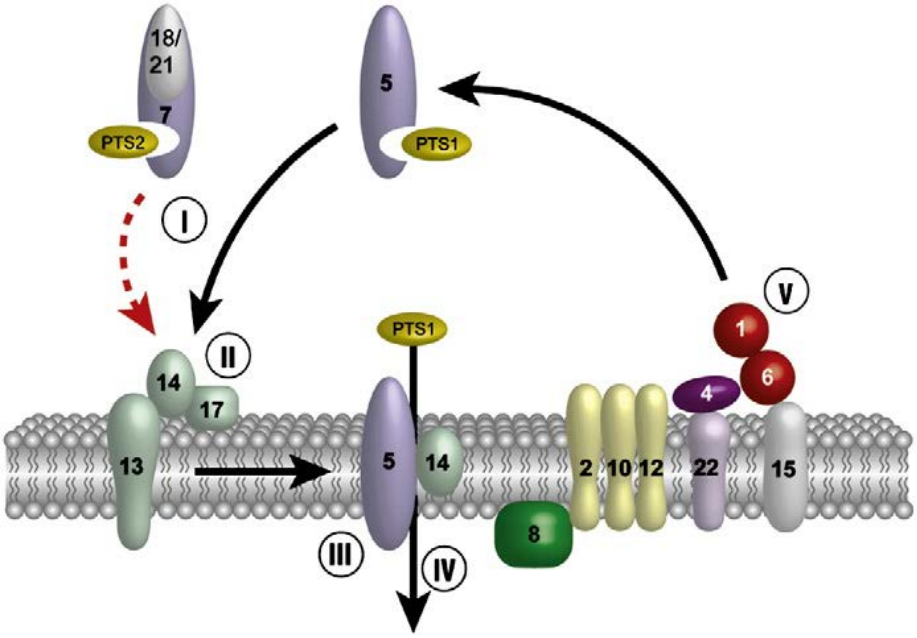

Figure 1-6: Matrix protein import pathway

Matrix protein import cycle consisting of (I) receptor cargo interaction (II) docking of cargo loaded receptors to peroxisomal membrane (III) cargo translocation (IV) cargo entry inside the peroxisomes and (V) receptor release to the cytoplasm. Figure taken from (Rucktäschel *et al.*, 2011).

In addition to PTS 1 and 2, there are other mechanisms also for protein import but these different types of import procedures are used by only few proteins. In some cases, a protein has an internal PTS such as shown by catalase in plants where the signal is located at -13 to -11 from the C-terminal end (Kamigaki *et al*., 2003; Oshima *et al*., 2008). There are few proteins which are localized to more than one organelle. These dual localized proteins include alanine:glyoxalate aminotransferase (AGT), acetoacetyl-CoA thiolase and 3-hydroxy-3-methylglutaryl CoA (HMG-CoA) lyase in mammals (Ashmarina *et al*., 1999; Olivier *et al*., 2000; Danpure, 2006) and carnitine-acyl-

transferase in yeast (Tanaka and Ueda, 2000). There are few proteins that do not carry any of the two targeting signals and are assumed to be imported either by a PTS3 targeting signal as reported for *S. cerevisiae* acyl CoA oxidase (Klein *et al*., 2002) or with the help of other PTS-containing subunits, a process also known as piggy-backing that is proposed for import of carnitine acetyltrasnferase (CAT) subunits and enoyl-CoA isomerase (Eci1p) in *S. cerevisiae* (Elgersma *et al*., 1995; Yang *et al*., 2001).

Usually all organisms require both the PTS1 and PTS2 targeting signals for the import of peroxisomal proteins. However, there are no proteins that contain PTS2 in nematode *Caenorhabditis elegans* (Motley *et al*., 2000) and as recently reported in diatom *Phaeodactylum tricornutum* (Gonzalez *et al*., 2012). It is assumed that PTS2 is an ancient form of target signal in these organisms and PTS1 might have probably evolved from PTS2 during the course of evolution. Not much is known about the evolution of targeting signals in higher organisms. Further analysis of the targeting signals of both types (PTS1 and PTS2) using homologous sequences from different plant species ranging from lower photosynthetic organisms such as algae and mosses and highly evolved plants like monocots and dicots will be very important to understand the evolutionary significance of these targeting pathways in plants (Also see section 3.2).

1.1.2.2 Membrane protein import

The peroxisomal membrane protein (PMP) import follows a distinct pathway as compared to the import of matrix proteins. There are two broad categories in which all PMPs are classified based on their import routes: Group I includes those PMPs that are targeted directly from cytoplasm to peroxisomes such as PEX10, PEX2, PMP22 (Fujiki *et al*., 1984; Sparkes *et al*., 2005) whereas Group II comprises of the PMPs which are imported indirectly via the endoplasmic reticulum (ER) to the peroxisomes such as PEX3, PEX16 and PEX22 (Sparkes *et al*., 2005; Fujiki *et al*., 2006; Van Ael and Fransen, 2006) as shown in

Figure 1-7. The peroxisomal targeting signal for membrane protein is designated as mPTS and it is never proteolytically cleaved upon import. The mPTSs are usually composed of two functional domains including a targeting element and a membrane anchoring region. As the name suggests, the targeting element directs the import of PMPs to peroxisomes while the anchoring region is required for the permanent insertion of the protein into the peroxisomal membrane. The anchoring region can have either a transmembrane region in case of integral membrane proteins or a protein interaction site for peripheral membrane proteins. The targeting element present in mPTS of PMPs belonging to group I include a binding site for PEX19 which acts as a soluble receptor for newly synthesized PMPs and upon binding, targets them to the peroxisome membrane (Sacksteder *et al.*, 2000; Rottensteiner *et al., 2004).* PEX19 also functions as PMP-specific chaperon and is proposed to bind to and stabilize the PMPs and prevent their aggregation (Jones *et al.*, 2004). PEX19 is also known to play role in Group II PMPs specially in transportation of PEX3 from endoplasmic reticulum to peroxisome membrane and in matrix protein import by regulating the assembly of PTS-receptor docking complexes (Fransen *et al.*, 2004; Hoepfner *et al.*, 2005).

AtPMP22 and AtPEX11 are integral membrane proteins of plant peroxisomes and belong to group 1 of PMPs which are directly sorted to the peroxisomes (also see section 1.2). Membrane proteins belonging to group II are targeted to the peroxisome membrane in a distinct mechanism. The mPTSs of such proteins lack the PEX19 binding site in their targeting signal and instead has a membrane anchoring region. It is also observed that sometimes the mPTS of different proteins are similar and are functionally interchangeable as reported in PEX3 and PEX22 (Halbach *et al.*, 2009). PEX3 plays a very important role in import of group I PMPs by acting as a docking factor and binds with complex of PEX19-PMP at the peroxisome membrane (Fang *et al.*, 2004). PEX3 has also been shown as peroxisomal receptors for class V

myosin and for peroxisome retention factor Inp1p, thus emphasizing their role in peroxisome movement and inheritance at least in yeast (Chang *et al.*, 2007; Chang *et al.*, 2009).

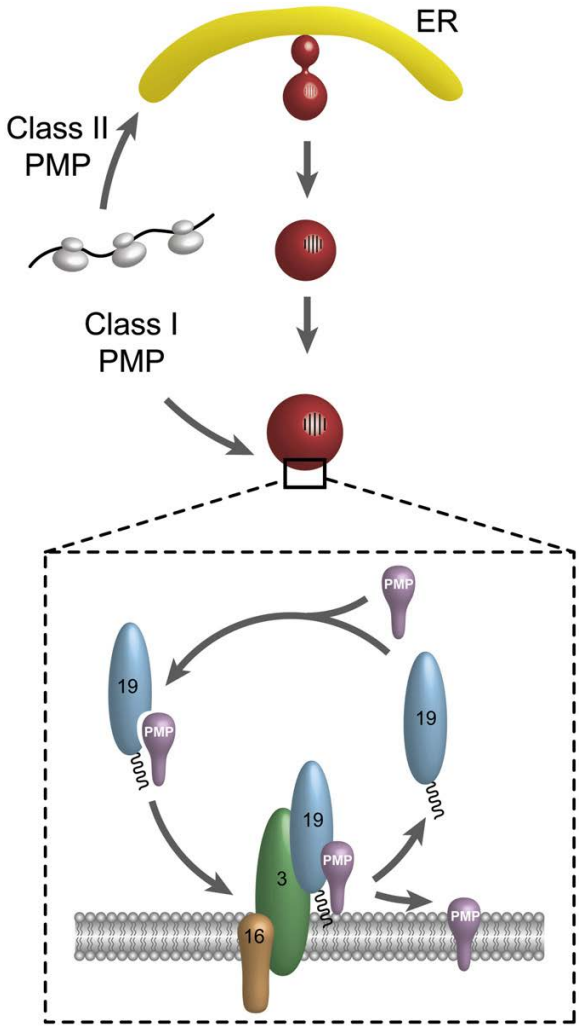

Figure 1-7: Import of peroxisome membrane proteins

Import of Class I PMP takes place in association with Pex19 protein whereas Class II proteins are sorted indirectly via endoplasmic reticulum. Figure taken from (Girzalsky *et al.*, 2010).

It is not well understood how the PMPs belonging to class II are imported from the cytoplasm to the ER and then from ER into the peroxisomes. However, recently it was shown that the Sec61p translocon along with Get3p complex is required for targeting PMPs to the ER where the ER associated secretory molecules which include Sec20p, Sec39p and Dsl1p play role in the exit of PEX3 from the ER (Perry *et al.*, 2009; van der Zand *et al.*, 2010).

1.2 Pore forming activity in peroxisomes

All the metabolic reactions require several specific metabolic intermediates. These molecules need to be exchanged between different cells and its compartments. There are mainly two modes by which the metabolites are transferred across the peroxisomal membranes. The transfer of metabolites via ion channels is usually non selective and allows a large number of water soluble metabolites. Transporters are commonly involved in the transfer of specific solutes. The metabolite transfer via channels is driven by a concentration gradient and is thus a passive transport whereas the transfer of solutes via transporters is against their concentration gradient which results in an active process of transfer. The mechanism by which different metabolites are transferred across peroxisomal membrane is assumed to be well conserved across different species. The electrophysiological approaches using 'Planar Lipid Bilayer' and 'Patch-clamp' techniques have been very successful for studying the transportation activities of peroxisomal membrane proteins.

The presence of channel forming activity has been reported in peroxisomes from different organisms including mammals, insects, fungi and plants. It is considered that the porin like channels are involved in the transfer of the majority of metabolic intermediates across peroxisomal membranes. Initial reports suggested the presence of pore forming activity in peroxisomes from rat liver (Labarca *et al.*, 1986) and yeast (Sulter *et al.*, 1993). These reports were however not conclusive due to relatively low purity of peroxisomes and using low

concentration of the electrolyte (0.1-0.3 M KCl) in measuring the electrophysiological properties of the channel (Antonenkov and Hiltunen, 2006). The channel forming activities were described in plant peroxisomes using membranes of spinach leaf peroxisomes (Reumann *et al.*, 1995) and also in glyoxysomes of castor bean endosperm (Reumann *et al.*, 1997). These reports suggested the presence of porin like channels in peroxisomes showing the average single channel conductance of 0.3-0.35 nS in 1 M KCl electrolyte which is considerably different from the single channel conductance of porin channels of mitochondria (2-4 nS) and of chloroplast (7-8 nS) in 1 M KCl. The channels are selective for anions with permeability ratio of pCl^-/pK^+ near to 20. Moreover, the channels show nonlinear dependence of single channel conductance to the concentration of electrolyte suggesting that these channels belong to the category of specific porins where permeability properties are determined by charge effect at a selectivity filter. The channel from spinach leaf peroxisomes display high stability constant for the binding of dicarboxylic anions such as malate, oxaloacetate, succinate, 2-oxoglutarate suggesting their role in the transfer of metabolic intermediates of photorespiration (Reumann *et al.*, 1998). Figure 1-8 shows the possible mechanisms by which the different metabolites are transferred during photorespiration pathway.

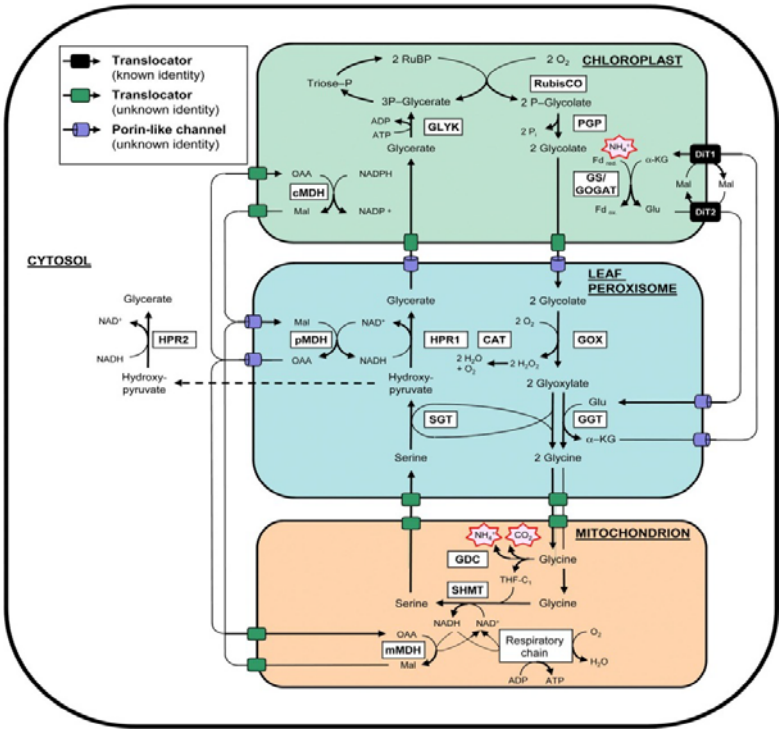

Figure 1-8: Porin like channel for metabolite transfer across peroxisomes during photorespiration

The photorespiratory cycle for salvage of phosphoglycolate is comprised of several enzymatic reactions distributed in chloroplast, peroxisomes, mitochondria and cytosol. The transfer of metabolic intermediates across peroxisomal membranes other than serine and glycine is assumed to take place via porin like channels. Figure taken from (Hu *et al*., 2012).

Two porin-like channels with distinct electrophysiological properties were also discovered in mammalian peroxisomes. These channels are of single channel conductance of 1.3 nS and 2.5 nS in 1 M KCl electrolyte. Moreover, both channels showed cation selectivity with permeability ratio of pK^+/pCl^- value around 4 (Antonenkov *et al.*, 2005). Similarly, two channels were also reported from electrophysiological studies of peroxisomal preparations from *S. cerevisiae* displaying average single channel conductance equivalent to

0.2 and 0.6 nS in 1 M KCl electrolyte. It was proposed that the higher conductance channel is actually a homodimer of two low conductance channels (Grunau *et al.*, 2009). Additionally, a higher conductance channel of 4 nS was also observed upon induction by DTT. It was suggested that this channel is involved in the transfer of bulky products possibly of glyoxylate cycle (Antonenkov *et al.*, 2009). Recently the channel forming activities were also reported from glycosomes showing an average single channel conductance of 1, 2 and 7.5 nS in 3 M KCl (Gualdron-López *et al.*, 2012).

Since the porin channel found in peroxisomes of different organisms such as yeast, mammals, glycosomes and plants vary in their electrophysiological properties, it will be interesting to see if the porin channel also varies in different plants. Despite of being a model plant Arabidopsis has not been investigated for the presence of porin channel of peroxisomes and to see whether the electrophysiological properties differ in comparison with spinach plants where the previous studies were conducted.

The exact molecular basis of these channel forming activities is largely unknown. PMP22 was the first mammalian peroxisomal protein discovered to be responsible for channel activity. This protein is encoded by *Pxmp2* and is an abundant peroxisomal membrane protein of mass 22 kDa. The channel showed conductance equal to 0.45nS, 0.9nS and 1.3 nS and was suggested to be a homotrimer (Rokka *et al.*, 2009). It shows weak cation selectivity (pK/pCl equal to 2.3) allowing diffusion of small solutes up to 300Da. The channels with conductance of 1.3 nS were found to be absent in knockout mice confirming PMP22 protein as a channel protein. In addition to PMP22, proteins belonging to PEX11 family are also predicted to be channel forming proteins regulating the transmembrane movement of medium chain fatty acids (van Roermund *et al.*, 2000).

1.3 Thesis goals

The thesis goals were divided into four main points that were studied in the course of this study:

I. To investigate the evolution of peroxisome targeting signals (PTS) in plants – Usually, the matrix proteins require either PTS1 or PTS2 for their import from cytoplasm to peroxisomes. Out of these two signals, PTS1 is most abundant with only one-third of the proteins containing PTS2 in case of plants. The ratio of PTS2 to PTS1 proteins is very less in case of mammals and fungi. The absence of PTS2 in *C.elegans* and diatoms suggested the transition of targeting signals, from PTS2 containing proteins converting into PTS1 proteins. Thus, one of the aim of the current study was to elucidate if there is a transition of targeting signals in protein orthologs from lower and higher photosynthetic species and if yes, then to understand which targeting signal is preferred over other.

II. Electrophysiological characterization of the porin channel in *Arabidopsis* leaf peroxisomes – The plant peroxisomes have been shown to contain the pore forming activity with the possible role in the transfer of metabolic intermediates that participate in several metabolic reactions occurring within peroxisomes (See 1.2). Despite of being the model plant, there has been no report describing the channel activity in Arabidopsis. Thus, it will be crucial to characterize the pore forming activity using Arabidopsis leaf peroxisomes.

III. Overexpression of two Arabidopsis peroxisome membrane proteins, AtPMP22 and AtPEX11D in *Pichia pastoris*- As mentioned above, the plant peroxisomes have been shown to display the ion-channel activity but till date, the molecular basis of the channel activity is unknown. The PMP22 has been

recently shown to be responsible for channel activity in case of mammalian peroxisomes and proteins belonging to PEX11 family are predicted to be involved in transfer of fatty acids in yeast peroxisomes. Since the membrane proteins are highly conserved in case of peroxisomes from different organisms, the Arabidopsis homologs of these two proteins were chosen for overexpression studies using *Pichia pastoris* as a heterologous expression system.

IV. Electrophysiological characterization of the purified AtPMP22 and AtPEX11D proteins – Lastly if the two Arabidopsis membrane proteins AtPMP22 and AtPEX11-D are able to be overexpressed and purified, it would be very interesting to see if the protein fractions display the pore forming activity which may further help in finding the molecular basis of the porin like channel reported in plant peroxisomes.

2. Materials and Methods

2.1 Materials

2.1.1 Organisms

Table 2-1: List of Organisms

Organism	Strain/ Genotype	Description	Reference/ Source
Bacteria	*Escherichia coli* JM109	F′ (traD36, proAB+ lacIq, Δ(lacZ)M15) endA1 recA1 hsdR17(rk -, mk+) mcrA supE44 λ- gyrA96 relA1 Δ(lac-proAB) thi-1	Kindly provided by Dr. Ioannis Livieratos, MAICh, Greece.
Yeast	*Pichia pastoris* SMD1163	*(his4 pep4 prb1)* strain (Invitrogen), was made His+ with the incorporation of pPIC3.5 vector	Kindly provided by Dr. Silke Grunau, University of Oulu, Finland
Plant	Arabidopsis *Col-0*	wild type plant of ecotype columbia	Lehle seeds, USA

2.1.2 Media and Buffer

Table 2-2: Media and Buffer composition

Media	**Composition**
Luria Bertani (LB) for bacteria	1% tryptone, 0.5% yeast extract and 1% NaCl (1.5% agar)
YPD for yeast	1% yeast extract, 2% peptone, 2% dextrose (2% agar)
YPDS for yeast	1% yeast extract, 2% peptone, 2% dextrose and 1 M sorbitol (2% agar)
Buffer	**Composition**
Hoagland solution	1mM KH_2PO_4, 5 mM KNO_3, 5 mM $Ca(NO_3)_2.4H_2O$, 2 mM $MgSO_4.7H_2O$, 1 uM Fe-EDTA, 46.23 uM H_3BO_3, 9.2 uM $MnCl_2.4H_2O$, 0.36 uM $CuSO_4.5H_2O$, 0.77 uM $ZnSO_4.7H_2O$ and 0.12 uM $Na_2MoO_4.H_2O$
TAE (1X)	40 mM Tris-acetate and 1 mM EDTA, pH 8.0
TSS	85% LB, 10% PEG 8000 (w/v), 5% DMSO and 50mM $MgCl_2$, pH 6.5
BMGY	1% yeast extract, 2% peptone, 100 mM potassium phosphate, pH 6.0, 1.34% yeast nitrogen base, 0.00004% biotin and 1% glycerol
BMMY	1% yeast extract, 2% peptone, 100 mM potassium phosphate, pH 6.0, 1.34% yeast nitrogen base, 0.00004% biotin and 0.5% methanol
SDS loading buffer (1X)	60mM Tris-HCl pH 6.8, 10% (v/v) glycerol, 2% (w/v) SDS, 5% (v/v) β-mercaptoethanol, 0.025% bromophenol blue

SDS running buffer (1X)	250 mM Tris-HCl, 192 mM glycine and 0.1% (w/v) SDS
Breaking buffer	50 mM sodium phosphate, pH 7.4, 1mM PMSF, 1 mM EDTA and 5% glycerol
Solubilization buffer	50 mM Tris-HCl, pH 7.5, 30% glycerol and 300 mM NaCl
Lysis buffer	50 mM NaH_2PO_4, 300 mM NaCl, 10 mM imidazole, pH adjusted to 8.0 using NaOH
Washing buffer	50 mM NaH_2PO_4, 300 mM NaCl, 20 mM imidazole, pH adjusted to 8.0 using NaOH
Elution buffer	50 mM NaH_2PO_4, 300 mM NaCl, 250 mM imidazole, pH adjusted to 8.0 using NaOH

2.1.3 Vectors

pCAT-EYFP: It is composed of pCAT which is a pUC based vector harbouring the Cauliflower mosaic virus (CaMV) 35S promotor with a duplicated enhancer region and a 35S polyadenylation site, 35S-PA and the enhanced yellow fluorescent protein (EYFP) cloned between NotI and XbaI sites. The vector map is shown in Figure 6-1. The vector was largely used for cloning the inserts required for subcellular localization analysis. The vector was kindly provided by Prof. Martin Fulda, Germany (Fulda *et al*., 2002). Several modifications were made in this vector for different combinations of subcloning the gene of interest.

pCAT-SKL137: It is a pCAT vector containing 137 aa region flanked between restriction endonucleases NcoI and XbaI. This vector was used for subcloning PTS1 domain constructs.

pCAT-DECR: This vector was made by removing the 137 aa region from pCAT-SKL137 and fusing the DECR protein (At3g12790/800) in pCAT vector. The inserts can be cloned using RE sites for NcoI, SacI

and XbaI. This vector was used for subcloning PTS2 domain constructs.

pCAT-EYFP-Hin1R: The vector is composed of pCAT-EYFP containing Hin1R gene (AT1g54540) for the cloning of inserts using endonucleases NotI/SacI, NotI /SacII and NotI/XbaI. This vector was used for subcloning PTS1 full length proteins.

pCAT-PTD2-EYFP: The vector is composed of Glyoxalase I (At1g11840) domain (DNRRFLHVVYR) and was created (this study) in order to clone the PTS2 domain constructs in front of EYFP in pCAT vector with the help of *Nco*I, *Sac*I in the front and *Sac*II in the back of PTS2 domain.

PWEN99: This vector is composed of red fluorescence protein (RFP) fused with PTS1 tripeptide motif SKL> and was used as a positive control for labelling the peroxisomal localization (Matre *et al*., 2009). It was kindly provided by Prof. Cathrine Lillo, Norway.

pPICZ A: It is a 3.3 kb expression vector (Invitogen ™) used to express recombinant proteins in *Pichia pastoris*. It is composed of a 5′ fragment containing the AOX1 promoter for tightly regulated, methanol-induced expression of the gene of interest and Zeocin™ resistance gene for selection in both *E. coli* and *Pichia* (Ellis *et al*., 1985; Baron *et al*., 1992). The vector map is shown in Figure 6-2. The Arabidopsis membrane proteins AtPMP22 and AtPEX11-D were subcloned using pPICZ A.

2.1.4 Enzymes and commercial kits

Table 2-3: List of commercial kits

Commercial kit	Source
GeneJET plasmid mini prep kit	Fermentas, Germany
GeneJET gel extraction kit	Fermentas, Germany
Illustra GFX PCR DNA and Gel Band Purification Kit	GE Healthcare, England
pGEM®-T Easy Vector System	Promega, USA
Wizard® Plus SV Minipreps DNA purification system	Promega, USA
Expand High Fidelity PCR system	Roche, Germany
Quick-change Site-Directed Mutagenesis Kit	Stratagene, USA
Pichia EasyComp ^{TM} Kit	Invitrogen, USA
Amersham ECl^{+} Western Blot kit	GE Healthcare, England
DNA and Protein ladders	Fermentas, Germany
Restriction endonucleases	Fermentas, Germany

2.2 Methods

2.2.1 Plant material and growth conditions

2.2.1.1 *Arabidopsis* seed sterilization

Surface sterilization of *Arabidopsis* seeds was carried out in a sterile chamber. Seeds were soaked in a 1 ml solution of 70% (v/v) ethanol and 0.05% (v/v) Triton X-100 for 10 min with occasional shaking. They were then washed twice in 100% ethanol for 10 min and dried on a sterile filter paper.

2.2.1.2 Standard growth conditions

Arabidopsis seeds were sown on a mixture of commercial soil (P-jard, LOG/Oslo, Norway) and Perlite in the ratio of 3:1 respectively. After sowing seeds, they were stratified at 4°C in the dark for 1-2 days before being transferred to standard growth conditions i.e. at ~22°C with a light intensity of 100-150 µmol m^{-2} s^{-1} in a 16/8 h cycle (referred to as long-day conditions). The soil was treated weekly with Hoagland nutrient solution, if required (Hoagland and Arnon, 1950). The trays containing seeds were covered with a plastic dome for few days to maintain humidity until germination.

2.2.2 Molecular biology techniques

2.2.2.1 PCR

Fragments of DNA were amplified using the polymerase chain reaction (PCR) (Mullis and Faloona, 1987). For each PCR reaction, the primers were designed taking into consideration the annealing temperature and that the GC content at the 5' and 3' ends should be suitable for primer annealing. PCR reactions consisted of a 94°C denaturation step, for 1minute, a primer-annealing step, which was variable depending on the specific primers, and an elongation step at 72°C, for a time depending on the length of the DNA to be amplified and the rate of polymerization of the DNA polymerase used. Analytical PCR was performed for the confirmation of the products using homemade thermostable DNA polymerase from *Thermus aquaticus* (Taq DNA polymerase) whereas preparative PCR was performed, after the product confirmation, using Hi-fidelity DNA polymerase (Expand High-Fidelity^{PLUS}, Roche Applied sciences). The PCR reaction mixture consisted of 5 µl of 10x Taq buffer (500 mM KCl, 100 mM Tris-HCl (pH 9.0), 1.0% Triton X-100), 5 µl of 25 mM $MgCl_2$, 1 µl of 10 mM dNTP mix, 1 µl of Taq polymerase (1 U/µl) or 1.25 Units of High fidelity polymerase), 1 µl each of forward and reverse primers (10 µM) and water to make up the final volume equal to 50 µl.

2.2.2.2 Agarose Gel Electrophoresis

The electrophoretic separation of DNA for analytical and preparative purposes was done in horizontal agarose gels with 1x TAE (40 mM Tris-acetate and 1 mM EDTA, pH 8.0) as a running buffer. DNA samples were mixed with 6x DNA loading buffer (Fermentas, Germany) and were run in a gel made up of 1% (w/v) melted agarose solution in 1x TAE and electrophoresed usually at 90 V. A standard 1 kb DNA ladder (Fermentas, Germany) was always run alongside the samples to determine size and amount of the DNA fragments. Visualization of DNA was done under UV light (260 nm) and images were taken with the help of Gel Doc instrument (GE Healthcare). When a preparative gel was run and particular band fragments were needed to be cut out, detection was done using larger wavelength of UV light (320 nm). The PCR and Gel Extraction Purification kit (Fermentas, Germany) was used to recover DNA from agarose gels. The eluted fragments were always verified by analytical gel electrophoresis as described above.

2.2.2.3 Gene Cloning

2.2.2.3.1 Cloning PTS1 domain constructs

The PTS1 domain constructs were prepared by cloning PTS1 domain containing spacer region of 7 amino acids in the back of pCAT-EYFP vector such that it is fused with the C terminal end of EYFP. The resulting constructs were denoted as 'EYFP-Ct 10 aa-protein name'. The forward primer used was complementary to the 5' region of EYFP whereas the reverse primer containing PTS1 domain was complementary to 3' region of EYFP. The forward and reverse primer contained Nco I and Xba I restriction sites respectively. The PCR amplification was done using pCAT-EYFP-CKI as a template and the amplified fragment was put into empty pCAT obtained by removing SKL137 fragment from the destination vector pCAT SKL137. The primer details required to clone PTS1 domains is shown in Table 6-1.

2.2.2.3.2 Cloning PTS2 domain constructs

The PTS2 domain constructs were cloned in front of EYFP in pCAT-EYFP vector such that the domain is fused with the N- terminal end of EYFP. The forward primer was chosen to be complementary to 5' region of EYFP and had 15 amino acids containing corresponding PTS2 domain whereas the reverse primer used was complementary to the 3' EYFP. The resulting constructs were denoted as 'Nt 15 aa-protein name-EYFP'. The forward and reverse primers contained Sac I and Xba I restriction sites respectively. The PCR amplification was done using pCAT-PTD2-EYFP as a template and the amplified fragment was put into empty pCAT which was obtained by removing DECR fragment from the destination vector pCAT-DECR. The primer details required to clone PTS2 domains is shown in Table 6-1.

2.2.2.3.3 Cloning AtPMP22 and AtPEX11-D

The Arabidopsis peroxisomal membrane proteins AtPMP22 and AtPEX11-D were cloned using the multiple cloning site (MCS) of the pPICZ A expression vector. The forward primers were complementary to N-terminal end of the insert and were also designed to contain 10 *histidine* amino acids in front of the gene of interest whereas the reverse primers were complementary to the C terminal end of the corresponding genes to be cloned. The forward and reverse primers contained sites for Sfu I and Apa I restriction enzymes respectively. The primer details are given in Table 6-1.

PMP22 Homolog full length construct was cloned in the back of EYFP using pCAT-EYFP-Hin1R vector such that the construct is fused to the C-terminal end of EYFP. The forward primer used was complementary to N-terminal region of the gene and C-terminal end of EYFP and the reverse primer used was complementary to C-terminal end of the gene of interest. The forward and reverse primers contained Not I and Xba I endonuclease sites respectively.

2.2.2.4 Gene transfer into competent *E. coli* cells

E. coli cells are not competent by nature i.e. they are unable to take up foreign DNA from the environment. Therefore, competent *E. coli* (JM109 strain) cells were made competent before they were transformed.

2.2.2.4.1 Preparation of competent *E. coli* cells

For the preparation of competent cells the bacterial strain was first streaked onto LB plate (with suitable antibiotic, if required) and incubated over night at 37°C. A single colony was picked and inoculated in 5 ml of LB broth and incubated at 37°C at 220 rpm overnight. From this overnight grown culture 1% inoculum was transferred to LB medium and was grown at 37°C at 220 rpm until an OD_{600} of 0.5 was reached. The culture was chilled on ice for 20 min followed by centrifugation at 1500 rpm for 5 min at 4°C. The pellet was re-suspended gently (without vortexing) in 10 ml (for 100 ml of culture) of ice cold TSS buffer (85% LB, 10% PEG 8000 (w/v), 5% DMSO and 50 mM $MgCl_2$ pH 6.5). The cells were distributed in 150 µl aliquots and frozen in liquid nitrogen and stored at -80°C for long term storage.

2.2.2.4.2 Transformation of *E. coli* cells

An aliquot of competent *E. coli* cells (see previous section) was thawed on ice and 50 ng of plasmid DNA was added. The mixture was incubated on ice for 20 min after which the cells were given a heat shock for 90 s at 42°C and then returned to ice where it was incubated for 2-3 min. 500 µl of LB medium was added to the cells and the suspension was mixed on a roller for 1-2 hours at 37°C to allow plasmid replication and expression of the antibiotic resistance gene. 200-400 µl of culture was spread on LB agar plates supplemented with appropriate antibiotic. The plates were kept for overnight incubation at 37°C.

2.2.2.4.3 Colony PCR

Direct colony PCR was used to screen for successful plasmid transformation into *E. coli* cells. A 50 µl PCR reaction mixture was prepared similar to preparative PCR with the difference that the *E. coli* colony was used as a DNA template rather than plasmid. The primer combination used was such that one primer would be vector-specific while the other would be insert-specific. Once the mix was made, a bacterial colony was picked up using sterile toothpick and inoculated into the PCR mix and finally the PCR reaction mixture was subjected to PCR amplification as described above.

2.2.2.5 Site-directed mutagenesis (SDM)

The QuikChange ® Site-Directed Mutagenesis Kit was used to perform point mutation required to replace the histidine amino acid at position twenty to valine in the PTS2 domain construct of NS/ECHId. The primers containing the desired mutation were designed following the manufacturer recommendations (also see Table 6-1 for primer details) and the mutation was performed using *PfuTurbo* ® DNA polymerase. The *Dpn* I endonuclease was used for digesting the parental DNA template containing the methylated and hemimethylated DNA and to select for mutation-containing synthesized DNA. The nicked vector DNA containing the desired mutations was transformed into XL1-Blue supercompetent cells supplied by the manufacturer. The resulting clone was then sequenced for confirming the specific mutation at the desired place.

2.2.2.6 Gene transfer into competent Yeast cells

The Arabidopsis membrane proteins after cloning in pPICZ A expression vector were overexpressed using *Pichia* as a heterologous expression system. This process required different methods than that of *E.coli* gene transformations and to check the positive transformed clones.

2.2.2.6.1 Preparation of *Pichia* competent cells

The *Pichia* competent cells were prepared by following the chemical method described in the *Pichia* EasyComp™ Kit (Invitrogen). A single colony of *Pichia* strain (SMD1163 + pPIC3.5K) was inoculated into 10 ml of YPD and was grown overnight at 28°C in a shaking incubator at 250 rpm. The next day, the culture was diluted to OD_{600} of 0.1-0.2 in 10 ml YPD and cells were grown at 28°C to OD_{600} of 0.6-1.0. After this, the cells were pelleted by centrifugation at 500 g for 5 min at RT and the pellet was re-suspended in 10 ml of Solution 1 (EasyComp™ Kit). The cells were again pelleted by centrifugation at 500 g for 5 min at RT and the competent cells were obtained by re-suspending the pellet in 1 ml of Solution 1. The competent cells were distributed in 100 µl aliquots and were stored at -80°C.

2.2.2.6.2 Gene transformation of *Pichia*

The *Pichia* cells were chemically transformed using the EasyComp™ kit (Invitrogen). 5 µg of AtPMP22 and AtPEX11 constructs cloned in pPICZ A expression vector were linearized with *Pme*I and then added to a 100 µl aliquot of *Pichia* competent cells and were mixed after adding 1 ml of solution 2 (EasyComp™ Kit). The transformation reaction was incubated at 30°C for 1 h (with intermittent mixing) and later at 42°C for 10 min. The cells were split equally in two micro-centrifuge tubes containing 1 ml of YPD in each tube and were incubated at 30°C for 1 h. After that, the cells were centrifuged at 3000 g for 5 min at RT and the pellet was re-suspended in 500 µl of solution 3 (EasyComp™ Kit). The cells were combined and centrifuged again at 3000 g for 5 min at RT before finally re-suspending the pellet in 100 µl of solution 3 and spreading on YPDS + Zeocin plates.

2.2.2.6.3 Colony PCR of *Pichia* transformants

The transformed colonies of *Pichia* were checked for the insert with the help of colony PCR following the method described in detail elsewhere (Akada *et al*., 2000). In brief, a single colony of *Pichia* was taken and

mixed in 20 µl of 0.25% SDS before heating at 90°C for 3 min. The culture was centrifuged at 5000 g for 30 sec and 4 µl of the supernatant was added to the PCR reaction mixture containing 5 µl of 10X Taq Buffer, 5µl of 25 mM $MgCl_2$, 1 µl of 10 mM dNTP mix, 1 µl each of forward and reverse primers, 3 µl of 20% Triton X-100, 1 µl of Taq polymerase (1 U/µl) and water to make final volume of the mixture equal to 50 µl.

2.2.2.7 DNA Sequencing

The new recombinant constructs isolated using Wizard® Plus SV Minipreps DNA purification system () were confirmed for the presence of the desired gene of interest by sequencing the nucleotides. The DNA sequencing was done by sending samples (600-700 ng DNA with 20 pmol primer) to the Seqlab (Göttingen, Germany).

2.2.3 *In vivo* subcellular localization analyses

The targeting signals of various putative peroxisomal proteins were evaluated by performing *in vivo* subcellular localization analyses. The reporter- fused proteins obtained by cloning either the full length and/or domain constructs in pCAT-EYFP vectors were analyzed upon transient gene expression in onion epidermal cells with the help of inverted fluorescence microscopy.

2.2.3.1 Preparation of gold particles for bombardment

50 mg of gold particle (Bio-Rad) was re-suspended in 1 ml of 100% ethanol. It was vortexed thoroughly for 3-4 min followed by centrifugation at 10000 g for 30 sec. The supernatant was discarded and the pellet was washed with 100% ethanol thrice. After the last washing step the pellet was re-suspended in 1 ml of sterile nano-pure water and centrifuged at 10000 g for 30 sec. The supernatant was discarded and pellet was re-suspended in 1 ml of sterile nano-pure water. It was then distributed as 50 µl aliquots in 1.5 ml micro-centrifuge tubes and stored at -20°C until further use.

2.2.3.2 Coating gold particles with DNA

A 50 µl aliquot of gold particle was taken out from the freezer and kept on ice to thaw. Following chemicals were then added onto the gold particle: 5 – 10 µg of plasmid DNA, 50 µl of 2.5 M Calcium chloride and 20 µl of 0.1 M spermidine. After the addition of each component it was vortexed thoroughly. It was then centrifuged at 10000 g for 30 sec. The supernatant was discarded and the pellet was re-suspended in 250 µl of 100% ethanol, vortexed for 1.5 min and centrifuged at 10000 g for 30 sec. The supernatant was removed and the pellet was washed thrice with 250 µl of 100% ethanol. After the last wash the pellet was re-suspended in 50 µl of 100% ethanol and stored at -20°C until use. For each shot 5 – 10 µl of sample was used.

2.2.3.3 Transient expression in onion epidermal cells

Onions were cut into pieces and placed on a wet tissue in Petri dishes. These whole pieces were bombarded using a Biolistic Particle Delivery System (BioRad, USA) with 1100 psi rupture discs (briefly rinsed by ethanol) under a vacuum of 0.1 bars. After bombardment the samples were incubated over-night in dark at room temperature. Onion epidermal cell layers were peeled and transferred to glass slides for examining under fluorescence microscopy (Fulda *et al.,* 2002). The onion epidermal cell layers were kept for cold incubation at 4°C for up to 7 days while keeping the sample humid.

2.2.3.4 Microscopy

Fluorescence image acquisition was performed on a Nikon TE-2000U inverted fluorescence microscope equipped with an Exfo X-cite 120 fluorescence illumination system (Exfo) and filters for YFP (exciter HQ500/20, emitter S535/30), CFP (exciter D436/20, emitter D480/40), a dual YFP/CFP filter with single-band exciters (Chroma Technologies), Texas red filter set for RFP: 31004, and chlorophyll autofluorescence (exciter HQ630/30, emitter HQ680/ 40, Chroma Technologies, Rockingham, VT, USA). All images were captured

using a Hamamatsu Orca ER 1394 cooled CCD camera. Volocity II software (Improvision, Coventry, UK) was used to capture 0.5 μm Z-sections to generate extended focus images.

2.2.4 Protein overexpression and purification studies

2.2.4.1 Membrane protein expression

The *Arabidopsis* membrane proteins AtPMP22 and AtPEX11-D were expressed by following the slightly modified protocol described elsewhere (Egawa *et al*., 2009). The AtPMP22 and AtPEX11-D were expressed by inoculating single colony of respective yeast constructs into 20 ml of BMGY medium (1% yeast extract, 2% peptone, 100 mM potassium phosphate, pH 6.0, 1.34% yeast nitrogen base, 4 x 105% biotin and 1% glycerol) in a 250 ml baffled flask. The culture was grown overnight in an incubator shaker at 28°C and 250 rpm to an OD_{600} of around 10. On the next day, the cells were pelleted down by centrifugation at 3000 g for 10 min at 4°C and were re-suspended in 200 ml of BMMY medium (1% yeast extract, 2% peptone, 100 mM potassium phosphate, pH 6.0, 1.34% yeast nitrogen base, $4x10^{-5}$% biotin and 0.5% methanol) in a 2-L baffled flask to an initial OD_{600} of 1 and grown at 30°C for 24 h using an incubator-shaker at 250 rpm. The cells were harvested by centrifugation at 5000 g for 10 min at 4°C and immediately frozen in liquid nitrogen. The samples were stored at -80°C till further use.

2.2.4.2 Isolation of crude cell extract and enrichment for membrane proteins

The frozen cell pellet was thawed and re-suspended in 20 ml breaking buffer (50 mM sodium phosphate, pH 7.4, 1 mM EDTA, 5% glycerol, and freshly added 1 mM PMSF). Acid washed glass beads of size 0.5 mm were added to the cell suspension. The mixture was vortexed for 30 sec and incubated on ice for another 30 sec. The process was repeated around 7 times by alternate vortexing and cooling. Finally the

sample was centrifuged at 1500 g for 10 min at 4°C to obtain the crude cell extract in the form of supernatant. The cell extract was further enriched for membrane proteins by centrifuging at 100,000 g for 1 hr at 4°C. The supernatant, cytosolic fraction was discarded and the pellet (membrane) fraction was harvested for subsequent purification. The pellet was homogenized in solubilization buffer (50 mM Tris–HCl, pH 7.5, 30% glycerol and 0.3 M NaCl) and diluted to a total protein concentration of 2-3 mg/ml and solubilized by adding 0.4% Triton X-100 at the final concentration. The crude cell extract, the cytosolic fraction and the membrane fraction were analyzed by SDS–PAGE and Western blotting.

2.2.4.3 Determination of protein concentration

The protein concentration was determined by the Bradford Protein Assay (Bradford, 1976). The micro assay was performed by adding 200 µl of 5X Roti-Quant reagent to the 800 µl solution of water containing appropriate amount of protein. The absorbance was measured at 595 nm with the Bio-Rad SmartSpec 3000 UV/Vis Spectrophotometer. Protein concentration was calculated using a standard curve of bovine serum albumin.

2.2.4.4 Protein precipitation

Membrane proteins are usually expressed in limited amounts and therefore need to be concentrated before analyzing with SDS-PAGE and/or Western blotting. The diluted protein samples were concentrated by following the method described elsewhere in detail (Wessel and Flügge, 1984). In brief, 400 µl of methanol was added initially to 100 µl of protein sample and was mixed shortly using a vortex. Later100 µl of chloroform was added and vortexed for a short time. Finally, 300 µl of H_2O was added and vortexed as before. The mixture was then centrifuged for 1 min at 9000 g. The supernatant was removed avoiding disruption of the interphase containing proteins. To the remaining solution, 300 µl of methanol was added and homogenized using a

vortex. The sample was centrifuged for 2 min at 9000 g. The supernatant was discarded and the protein pellet was dried at room temperature for 10 min before suspending it in smaller amount of the buffer.

2.2.4.5 SDS-Polyacrylamide gel electrophoresis

SDS-PAGE (sodium dodecyl sulfate-polyacrylamide gel electrophoresis), in which proteins are separated based on polypeptide length, was used to detect the overexpressed proteins. The electrophoresis was done using a discontinuous buffer system, in which a non-restrictive large pore gel, called stacking gel, is layered over a separating gel called the resolving gel. The composition of the stacking gel used was 125 mM Tris-HCl pH 6.8, 4% (w/v) acrylamide, 0.1% (w/v) SDS, 0.05% (w/v) APS and 0.15% (v/v) TEMED while that of the resolving gel was 0.38 M Tris-HCl pH 8.8, 10% (w/v) acrylamide 0.1% (w/v) SDS, 0.05% (w/v) APS, 0.07% TEMED. The protein samples were mixed with 1X SDS loading buffer [60 mM Tris-HCl pH 6.8, 10% (v/v) glycerol, 2% (w/v) SDS, 5% (v/v) β-mercaptoethanol, 0.025% bromophenol blue] and boiled at 95°C for 5 min and then cooled on ice. The samples were then loaded onto the stacking gel. Unstained or pre-stained protein marker (Fermentas, Germany) was run alongside the samples and used as a size reference. The gels were fitted in a Mini-PROTEAN II cassette (BioRad) filled with SDS running buffer [250 mM Tris-HCl, 192 mM glycine and 0.1% (w/v) SDS] and electrophoresed first at 80 V until they reached the end of the stacking gel, after which the voltage was increased to 150 V.

2.2.4.6 Coomassie staining

To visualize all proteins on an SDS-PAGE gel, the gel was incubated in Coomassie stain solution (50% (v/v) methanol, 10% (v/v) glacial acetic acid, 0.5% (w/v) Coomassie Brilliant Blue R250) for 2 hrs at room temperature with gentle agitation. The gels were de-stained in distilled water overnight.

2.2.4.7 Western blotting

The Western blot technique was used to detect the expressed membrane proteins AtPMP22 and AtPEX11-D using primary antibody against the His-tag attached to the proteins. The proteins were analyzed by this technique at different steps of expression and purification including the crude cell extracts, membrane fractions and after Ni-NTA affinity chromatography.

Blotting: Initially the proteins were separated in an acrylamide gel by SDS-PAGE. Afterwards, the proteins were electro-transferred to a nitrocellulose membrane. For the transfer of proteins from the gel to the membrane, the cassette and tank were prepared as described by the manufacturer (Bio-Red). The gel (towards cathodic side) and the membrane on top of the gel were sandwiched between two times 3-layers of Whatman filter papers. All the components of the cassette were pre-soaked with cold transfer buffer (25 mM Tris-HCl, 192 mM glycine and 20% methanol) before placing inside the tank filled with transfer buffer. The transfer was performed overnight at 20 mV in the cold room at 4°C.

Immunodetection: After protein blotting, the membrane was rinsed thrice for 5 min in PBS buffer (0.8% NaCl, 0.02% KCl, 0.144% Na_2HPO_4, 0.024% KH_2PO_4, pH 7.4). Later the remaining area of the membrane was incubated in PBS buffer containing 5% dry milk powder and 0.02% Tween-20 for 30 min to 1 hr in order to avoid unspecific antibody binding to the membrane. After the blockage the membrane was treated with primary antibody (Anti-His) for 3 hrs on a rocker at RT. The antibody was diluted by 1:5000 times in PBS containing 1% BSA. The membrane was washed thrice in PBS for 10 min each time. After that, the membrane was again incubated for 1 hr in secondary antibody (Protein A-HRP) diluted to 1:10000 in PBS containing 0.05% Tween-20. The membrane was washed twice in PBS before analyzing by chemi-luminescence.

Development: The membrane was placed inside an X-ray cassette where the electro-chemi-luminescence reagents were added. The membrane was developed with the "ECL-detection kit" (GE healthcare). The membrane was incubated with the mixture of 1 ml solution A and 0.025 ml solution B for 1-2 minute. The excess solution was removed and an X-ray film was exposed to the membrane in a dark room. After exposure for 1-10 min, the film was submersed first in the developing solution (Kodak), rinsed with water and then immersed in the fixing solution (Kodak) and finally rinsed again with water before letting it dry.

2.2.4.8 His tag purification with Ni-NTA affinity chromatography

This method of protein purification is based on the binding affinity of Nickel Nitrilo acetic acid (Ni-NTA) resins to the His-tag associated with the protein. While cloning the *Arabidopsis* membrane proteins AtPMP22 and AtPEX11-D into pPICZ A expression vector, a His-tag consisting of 10 histidine amino acids was attached in front of the gene. The purification was done in a batch culture under native conditions ('the Qiaexpressionist manual' 2003). 100 µl of Ni-NTA matrix (Qiagen) was first equilibrated with 400 µl of lysis buffer (50 mM sodium phosphate, pH 8, 300 mM NaCl and 10 mM imidazole) or solubilisation buffer and was further loaded with 250 µl solubilized membrane fraction and was kept at 4°C with slow stirring for 1 hr. The sample was centrifuged at 1000 g for 10 sec and the flow-through was saved to check binding efficiency. The pellet was washed thrice with 400 µl of washing buffer (50 mM sodium phosphate, pH 8, 300 mM NaCl and 20 mM imidazole) by incubating at 4°C with slow stirring for 30 min each time. The flow-through obtained upon centrifugation at 1000 g for 10 sec were pooled and stored to check binding efficiency. The His-tagged protein was eluted twice with 200 µl of elution buffer (50 mM sodium phosphate, pH 8, 300 mM NaCl and 250 mM imidazole) upon centrifugation at 1000 g for 10 sec. The eluted protein

along with the unbound fraction and the washed fraction were analyzed by SDS-PAGE and Western blot.

2.2.5 Isolation of Arabidopsis leaf peroxisomes

Leaf peroxisomes from *Arabidopsis* plants were isolated following the protocol described elsewhere in detail (Reumann *et al.*, 2007). All steps were performed at 4°C. About 60 g of fresh leaves from eight to ten weeks old *Arabidopsis* plants were ground in 120 ml grinding buffer (170 mM Tricine-KOH, pH 7.5, 1 M sucrose,1% BSA, 2 mM EDTA, 5 mM DTT, 10 mM KCl, 1 mM $MgCl_2$, 0.5% PVP40 and freshly added 0.1 mM PMSF) using a mortar and a pestle. The suspension was filtered through two layers of Mira cloth. Cell debris and chloroplasts were removed by centrifugation of the homogenate at 7500 rpm for 1 min in a Sorvall SS34 rotor (Sorvall RC5B). Approximately 17 ml of supernatant was loaded onto eight Percoll-sucrose density gradients containing 15% and 38% Percoll and 36% (w/w) sucrose solutions. All solutions were prepared in TE buffer (20 mM Tricine-KOH, pH 7.5, and 1 mM EDTA) and Percoll solutions were supplemented with 0.75 M sucrose and 0.2% (w/v) BSA. The gradient was formed of the following solutions from top to bottom: 3 ml of 15% Percoll, 9 ml of 38% Percoll, 2 ml mixture of 38% Percoll and 36% [w/w] sucrose at a ratio of 2:1 and 1:2, and 3 ml of 36% (w/w) sucrose in TE buffer). The samples were differentially centrifuged for 12 min at 10,500 rpm and 20 min at 15,000 rpm (Sorvall SS34 rotor). The supernatant was sucked off using Pasteur pipette and vacuum pump. The fractions at the bottom (around 2 ml) of all eight gradients were combined and diluted in 36% (w/w) sucrose in TE buffer to the final volume of 80 ml. The diluted solution was further sedimented by centrifugation for 30 min at 18,000 rpm (Sorvall SS34 rotor), yielding the leaf peroxisomes. The supernatant was sucked off with the help of Pasteur pipette and vacuum pump and the peroxisomal fractions were combined to final volume of 5ml. The organelles were gently homogenized and loaded on top of a discontinuous sucrose density gradient (1 ml 41% [w/w], 1 ml 44%

[w/w], 1 ml 46% [w/w], 2 ml 49% [w/w], 0.5 ml 51% [w/w], 1 ml 55% [w/w], and 1 ml 60% [w/w] sucrose in TE buffer) and centrifuged for 120 min at 25,000 rpm in Beckman 41Ti rotor (Beckman coulter Ultracentrifuge). The leaf peroxisome fraction enriched in membrane proteins, visible as a sharp white band above 55% (w/w) sucrose, was harvested and supplemented with 1 mM PMSF. The peroxisomal fractions were stored in small aliquots at -80 ˚C.

2.2.6. Planar Lipid bilayer assay

The planar lipid bilayer technique is used to investigate the pore forming activity of a membrane protein. The simplified set up for planar lipid bilayer is shown in Figure 2-1.

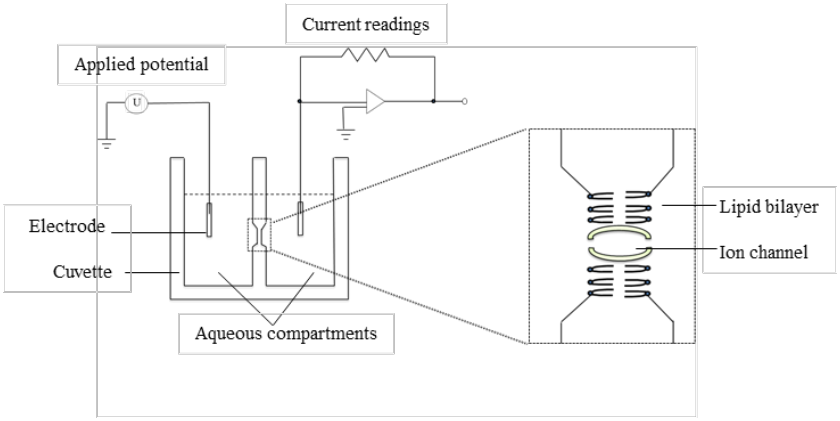

Figure 2-1: Simplified set-up for lipid bilayer experiments

This technique is also called as ‘black lipid bilayer assay’ due to the black colour of the artificial membrane when it forms a single lipid bilayer. This method is based on the ion-impermeable properties of lipid membranes. A typical bilayer has a very high resistance of 10^9 ohm and thus the electrical current is almost zero in the absence of any channel forming proteins. But when pore forming proteins get inserted

in the membrane, they form holes through which the increased flow of ions take place which in-turn increases the bilayer conductance. The particular conductance of each porin depends on the size of the hole formed in the membrane. Insertions of porins in the membrane can be measured in terms of increasing-conductance steps with a typical value depending on the porin. Porins differ from each other in conductance and other electrophysiological properties. For example, the single channel conductance of mitochondrial porins is around 2-4 nS while a porin from plastids has higher conductance of 7-8 nS (Reumann *et al.*, 1995). Some porins are either selective for anions or cations. Some of them have a rigid structure that resists high voltages without any changes in conductance while some others are specialized in the transport of certain specific type of molecules. The following electrophysiological properties of the porin channels can be estimated by conducting lipid bilayer assays.

2.2.6.1. Single channel conductance

Each pore forming protein has a characteristic single channel conductance value. The conductance is determined by the amount of ions transferred across the pore/channel formed by the protein upon insertion into the lipid bilayer. This ion flow in turn depends upon the channel diameter, channel internal charges and oligomeric constitution of a porin. The entry of ion channels in the bilayer is measured in a step wise increase in bilayer conductance where each step corresponds to the insertion of a single channel into the lipid bilayer. The single channel conductance of the porin is defined as the most common conductance value observed in a protein sample. Mathematically, the conductance of a porin can be defined as

Materials and Methods

$$G = \frac{I}{V_a} \qquad (1)$$

where G = conductance (S)
I = current (A)
V_a = applied voltage (V)

In the bilayer setup at Prof. Benz's lab in Würzburg, Germany the increase in bilayer current was first amplified and transformed in voltage, which was then actually registered in the chart recorder. This output voltage is directly proportional to the current (I). Thus the current is also represented as

$$I = \frac{V_{out}}{V_{amp}} \qquad (2)$$

where V_{out} = output voltage (V)
V_{amp} = amplification factor (VA^{-1})

Upon substituting equation (2) in (1), the conductance is equal to

$$G = \frac{V_{out}}{V_{amp}.V_a} \qquad (3)$$

Since the record paper where the output voltage was registered is divided into 100 boxes, the conductance per box (G_b) results from dividing the full scale of the register (V_f) by 100 and thus calculated as given in equation 4. Finally, the single channel conductance of a porin is determined by multiplying the conductance per box to the height of the peak in terms of increment in the number of boxes in the record paper after the insertion of each porin channel in the membrane.

$$G_b = \frac{V_f}{V_{amp}.V_a.100} \quad (4)$$

where G_b = Conductance per box (S)

V_f = full scale of the register (V)

Whereas in our lab, when using the Ionovation Compact device with the help of EPC10 amplifier and Patchmaster software, it showed automatically the increase in current (pA) at a specific voltage (mV) and thus the conductance (G) was directly calculated upon dividing the current by voltage.

2.2.6.2. Ion selectivity

The ion selectivity of a porin was estimated mainly by two ways. In the first case, the porins were tested in different concentrations of KCl and in different electrolytes to gain some insight into the ion transport through them. This method gives an indication about the preference of a channel towards a specific type of ion. Porins are divided into two types, general diffusion porins and substrate-specific porins depending upon the relation between the solute flow through a porin and the bulk concentration of the solute in the salt solution (fig). General diffusion porins show linear relation between the solute flow and the bulk concentration of the electrolyte whereas in case of specific porins, the transported molecules have different binding sites in the channel. The channel becomes saturated at a particular solute concentration and thus it displays non-linear solute flow with respect to the solute concentration. Using the planar lipid bilayer technique, the solute flow is observed in terms of single channel conductance, thus the channel selectivity for ions is displayed by the relationship between single channel conductance and the salt concentration.

Materials and Methods

The ion selectivity is determined at a more precise level by conducting reverse potential measurements described in detail elsewhere (ref). These measurements are done in an asymmetric condition where the two compartments of the chamber contain the different concentrations of the same electrolyte. The type of ion for which the porin shows specificity is preferentially transported to the diluted side of the chamber to equilibrate the concentration creating a potential difference. The potential difference works against the concentration gradient. This process stops when the electrochemical potential is equal in both sides. That membrane potential at which the flux is zero is called as reverse potential which can be calculated using the Goldmann-Hodgin-Katz flux equation

$$V_{rev} = \frac{RT}{F} \ln \frac{\sum_{cations} P_{+} C_{+}^{cis} + \sum_{anions} P_{-} C_{-}^{trans}}{\sum_{cations} P_{+} C_{+}^{trans} + \sum_{anions} P_{-} C_{-}^{cis}} \qquad (5)$$

where
V_{rev} = Reverse potential
R = Gas constant
T = Thermodynamic temperature
F = Faraday constant
P_{+} = Permeability of the corresponding cation
P_{-} = Permeability of the corresponding anion
$C_{\pm}^{cis/trans}$ = Concentration of the corresponding ion on either side

Upon transformation and using only potassium and chloride ions, the above equation can also be written as

$$\frac{P_{K^+}}{P_{Cl^-}} = \frac{[Cl^-]_{cis} - [Cl^-]_{trans} . e^{\frac{F.V_{rev}}{R.T}}}{[K^+]_{cis} . e^{\frac{F.V_{rev}}{R.T}} - [K^+]_{trans}} \qquad (6)$$

2.2.6.3 Voltage dependence

Few porins are opened only at a narrow range of voltage and get closed at membrane potential outside this range whereas some others are more stable and remain open at a wide range of voltage. The opening and closing of porin at given voltage range is characteristic of that particular porin. Moreover, the porins also differ in their behaviour at positive and negative membrane potential. This kind of voltage dependency of the channel was determined by conducting experiments at a wide range of voltage usually between -100 mV to +100 mV. These studies give indication about the symmetric or asymmetric or no voltage dependence of the porin.

2.2.6.4 Substrate specificity

The mechanism of solute transport through specific porins including the peroxisomal channel can be explained by the simple two-barrier, one site model (Benz and Hancock, 1987). It assumes a binding site in the centre of the specific porin channel. The rate constant k_1 describes the movement of the substrate molecules from the aqueous phase of concentration c, across the barrier to the central binding site and the inverse motion is described by the rate constant k_{-1}. The stability constant of the binding between a substrate molecule and the binding site is K

$$K = \frac{k_1}{k_{-1}} \qquad (7)$$

Also, it is assumed that the channel is a single file channel which means that only one substrate molecule can bind to the binding site at a given time and that no substrate or ions can pass the channel when the binding site is occupied (Benz *et al.,* 1987). This means that a substrate can enter the channel only when the binding site is free. The channel (P) is open when no substrate (S) is bound and closed when it is

occupied by a substrate S to form the non-conducting substrate-channel complex (PS)

$$P + S \underset{k_{-1}}{\overset{k_1 c}{\rightleftharpoons}} PS \qquad (8)$$

In the presence of a solute of concentration c (identical concentrations on both sides) the probability that the binding site is occupied is given by p and that it is free by 1-p

$$p = \frac{K.c}{1+K.c} \qquad (9)$$

$$1 - p = \frac{1}{1+K.c} \qquad (10)$$

The conductance of a membrane containing many specific porins in the presence of a solute with the stability constant K and solute concentration c, is given by the probability that the binding site is free

$$G(c) = \frac{G_{max}}{1+K.c} \qquad (11)$$

Where G_{max} is the membrane conductance before the start of the solute addition to the aqueous phase when all channels are in the open configuration and G(c) is the conductance at the solute concentration c.

The equation (11) can also be written as

$$\frac{G_{max}-G(c)}{G_{max}} = \frac{K.c}{1+K.c} \qquad (12)$$

Thus, the stability constant for solute binding can be derived from titration experiments. The titration curve is analyzed by using Lineweaver-Burke plots. The half saturation constant Ks, is given by the inverse stability constant 1/K.

To test if a porin is specific for a substrate, binding assays were done in which a bilayer was first saturated with a porin sample. When the porin insertions in the membrane reached a stationary phase, 1µl of substrate solution (0.5 – 1 M) was added to each side of the chamber under stirring conditions. A few minutes waiting is required to see if there is an effect in the membrane conductance. The idea is that if the porin transports a substance specifically through the membrane the ion flux will be interrupted thereby decreasing the total membrane conductance. When the conductance became stable again the same was repeated by adding increasing amounts (2, 4, 8, 16, 32, 64 and 128 µl) of the substrate to both the compartments of the chamber without disturbing the bilayer and the binding constant was calculated as explained above.

2.2.6.5 Procedure

The lipid bilayer measurements in Prof. Roland Benz's lab in Würzburg, Germany were performed by following the procedure described in detail elsewhere (Benz *et al.*, 1978). The key components of the bilayer set-up are shown in Figure 2-2. The instrumentation consists of a Teflon chamber with two aqueous compartments connected by a small circular hole. The hole has a surface area of about 0.4 mm^2. Membrane bilayers were formed by painting a 1% solution of

diphytanoyl phosphatidylcholine (Avanti Polar Lipids) in n-decane onto the hole. The aqueous salt solutions were usually unbuffered and had a pH around 6. The protein samples were treated with 0.5% Genapol (final concentration) before adding to the aqueous phase on both sides of the black membrane. The membrane conductance was measured at a fixed membrane potential of 20 mV with the help of a pair of Ag/AgCl electrodes inserted into the aqueous solutions on both sides of the membrane. All measurements were done at 20°C. Membrane current was measured using home-made current to voltage converter combined with an amplifier. The amplified signal was recorded on a strip chart recorder.

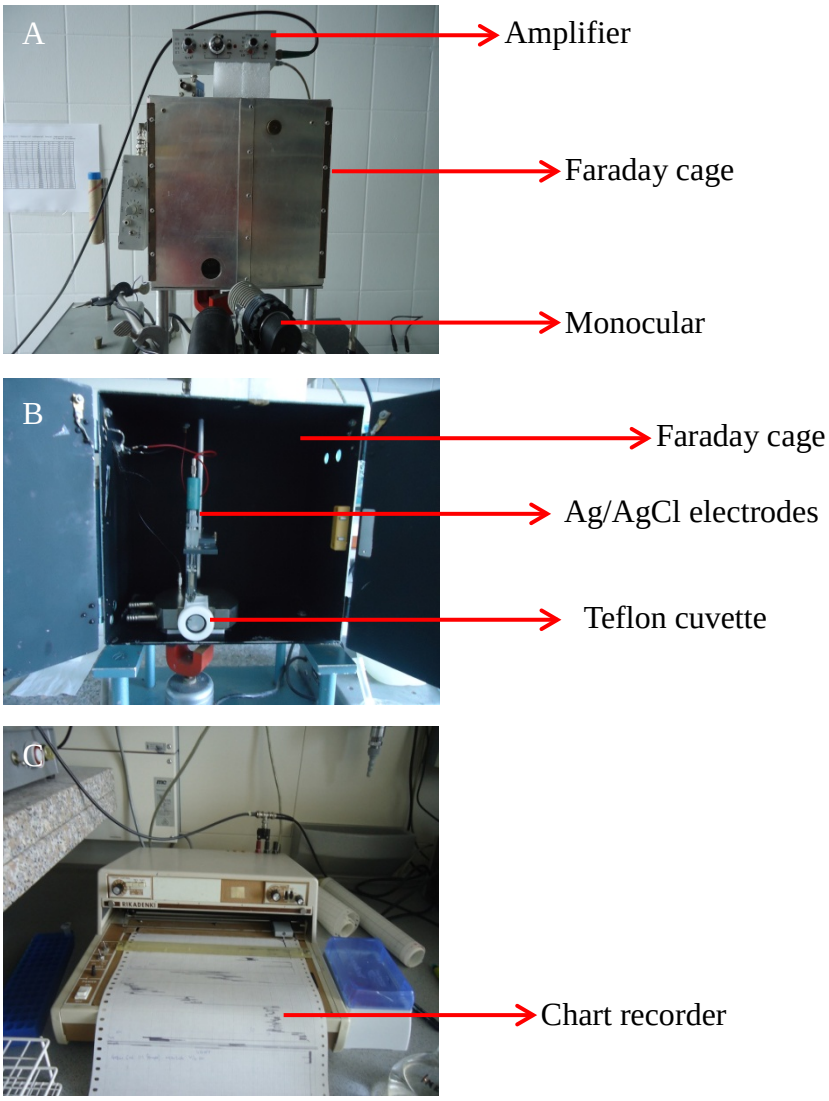

Figure 2-2: Instrumentation for lipid bilayer experiments

The instrumentation in Prof. Benz's lab at Würzburg for conducting planar lipid bilayer assays. The Figure displays the key components - Faraday cage, amplifier and oscilloscope (A), electrodes and cuvette (B) and chart recorder (C). The device was used to measure porin activity in leaf peroxisomes from Arabidopsis plants.

Materials and Methods

The bilayer experiments for measuring channel activity in overexpressed membrane proteins AtPMP22 and AtPEX11-D were conducted using 'Ionovation Compact' device (manufactured by the Ionovation GmbH, Germany) coupled with the HEKA-EPC10 amplifier. Figure 2-3 shows the key components of the ionovation compact device. The data acquisition and analysis were performed using the Patchmaster^{TM} software (HEKA). For such experiments, the disposable bilayer chambers were used consisting of two compartments separated by a PTFE septum. The septum contains a 50 to 100 µm microhole across which the bilayer was formed automatically by the instrument upon adding 1 µl of the lipid solutions to one side of the aqueous chamber. The lipid solutions (1% lipid in n-decane) were composed of either DPhPC or POPE/POPC lipid. The Ag/AgCl electrodes were connected to the compartments with a salt bridge of 1% Agar containing 2 M KCl. The chambers had usually 1.2 ml of 1 M KCl in each compartment unless otherwise mentioned. The capacitance of the bilayer was in the range of 60-80 pF. The increase in bilayer conductance upon insertion of porins was initially recorded at 0 mV and subsequently at different membrane potentials.

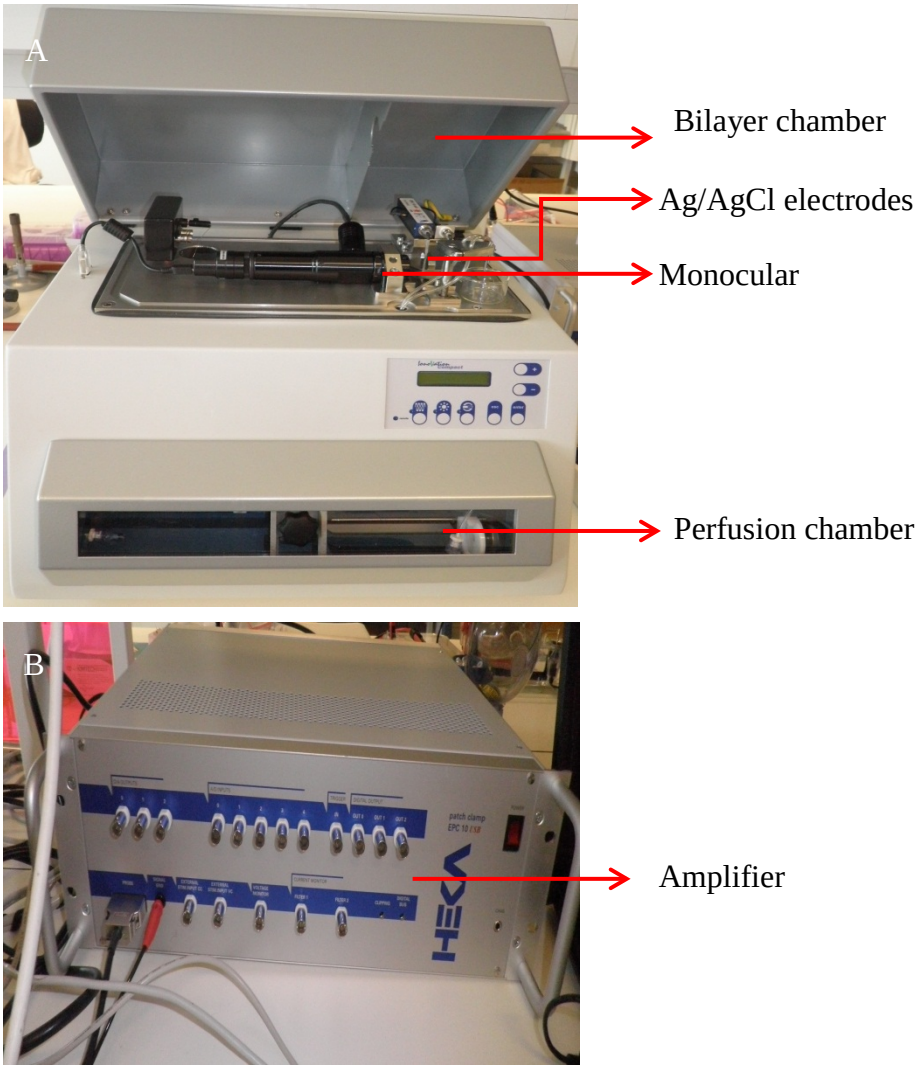

Figure 2-3: The ionovation compact device

The ionovation compact bilayer device showing key components – bilayer chamber, electrodes, monocular and perfusion chamber (A) and EPC10 amplifier (B). The device was used to measure porin activity in purified protein fractions of the peroxisome membrane proteins, AtPMP22 and AtPEX11-D overexpressed in *P.pastoris*.

3. Results and Discussion

3.1 Partial compartmentalization of phylloquinone (vitamin K1) biosynthesis in plant peroxisomes

The first requirement for performing any organelle proteomics is the availability of organelles with sufficient purity and abundance. Isolation of pure peroxisomes has been proved to be very difficult because of their highly fragile nature, low abundance and contamination with neighbouring organelles. Several attempts have been made in recent past for proteomic analysis of plant peroxisomes isolated from the different parts of same plant such as greening and etiolated cotyledons and leaf peroxisomes of Arabidopsis as well as different plants such as soybean cotyledons and spinach leaf peroxisomes. Many proteins were found exclusively in each study signifying the rationale behind the analysis of organelles from different plant species.

The proteome mapping of spinach leaf peroxisomes with the help of protein spots arising from 2-dimensional gels and their subsequent analysis by matrix-assisted laser desorption ionization mass spectrometry (MALDI-MS) and liquid chromatography tandem mass spectrometry (LC-MS/MS) revealed a large number of peroxisomal proteins. The tryptic peptides of three proteins showed high sequence similarity with Arabidopsis proteins containing putative peroxisomal targeting signals including a short chain alcohol dehydrogenase (SDRa, At4g05530) and two enoyl-CoA hydratases/isomerases (ECHIa, At4g16210; NS/ECHId, At1g60550). The predicted PTS1 signals for SDRa (SRL>) and ECHIa (SKL>) and PTS2 signal for NS/ECHId (RLx_5HL) were confirmed by *in vivo* targeting analysis of their peroxisome targeting domain (PTD) fused to EYFP reporter protein.

To confirm that NS/ECHId contain PTS2 (RLx_5HL), the PTD was mutated by performing side directed mutagenesis to replace histidine at position number twenty to valine (H_{20} to V). The mutated PTD

(RLx$_5$VL) was sub-cloned in front of EYFP to make the construct NS/ECHIdΔPTS2–EYFP as described in Materials and Methods. The new construct thus made was checked for *in vivo* subcellular localization and was found to be cytosolic as shown in Figure 3-1, thus confirming the RLx$_5$HL motif as PTS2 for NS/ECHId.

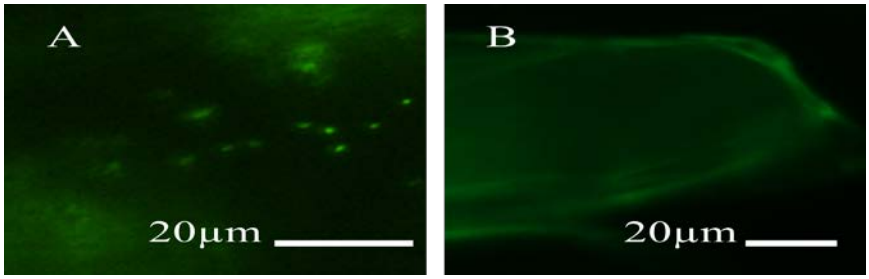

Figure 3-1: *In vivo* subcellular localization of NS/ECHId

The NS/ECHId full length protein fused with EYFP (NS/ECHId-EYFP) is targeted to peroxisomes (A). To validate that the protein contains PTS2, the domain RLx$_5$HL was mutated to RLx$_5$VL by SDM. The mutated NS upon fusing with EYFP was analyzed and found to be localized to cytoplasm instead of peroxisomes (B), confirming the PTS2 domain for the protein localization to peroxisomes.

The single Arabidopsis naphtoate synthase (NS) is orthologous to MenB from cyanobacteria that participates in phylloquinone biosynthesis, a pathway previously assumed to be compartmentalized entirely in chloroplasts. It was also shown that the Arabidopsis orthologs of the MenE (the upstream enzyme of MenB), acyl-CoA activating enzyme isoform 14 (AAE14) is also targeted to peroxisomes by PTS type 1 (SSL>) indicating a novel function of plant peroxisomes in partial compartmentalization of phylloquinone biosynthesis (Babujee *et al*., 2010).

Results and Discussion

3.2 Evolution of peroxisomal targeting signals in plants

There are mainly two types of targeting signals in peroxisomes by which most of the matrix proteins are imported from cytoplasm to peroxisomes. Most of the peroxisomal matrix proteins contain PTS1 signal, whereas only few proteins utilize the PTS2 signal for their import (also see 1.1.2.1). Both PTS1 and PTS2 have been reported in all organisms except the nematode *C.elegans* and the diatom *P.tricornutum* where the usual PTS2 containing proteins have been found to acquire PTS1 suggesting the switching of targeting signals from PTS2 to PTS1. This switching of targeting signals is assumed to result in the complete loss of PTS2 pathway of protein import. The possible reasons behind such a transition are not fully known but it is suggested that probably there is a higher preference for PTS1 in these organisms because of the high degeneracy and relatively simpler targeting signal when compared to PTS2. The other possible reason for the loss of PTS2 can be the alternate localization to other organelles such as mitochondria and cytoplasm instead of peroxisomes (Motley *et al*., 2000). To study whether the switching of PTS2 to PTS1 also takes place in plants, several matrix proteins were sorted into five groups based upon their putative targeting signals and affinity to individual PTSs. The groups are mentioned in Table 3-1. The representative protein orthologs of each group were compared using either full length constructs or targeting domains from lower photosynthetic plants such as mosses and algae as well as from higher plants including monocots and dicots to study the pattern of PTS followed by matrix proteins of plant peroxisomes. This study was done along with other colleagues in the lab and collaborators.

Table 3-1: Protein groups based on their targeting signals

The five protein groups were made depending upon their affinity to targeting signals, specifically in higher plant orthologs. The representative proteins from each group are also shown.

Group No.	Targeting Signals	Representative Proteins
One	only PTS2	NS, PKT3
Two	functional PTS2 and low affinity PTS1	Acd32.1, pMDH, CSY
Three	functional PTS2and high affinity PTS1	ACX, CSY
Four	functional PTS1 and low affinity PTS2	LACS
Five	only PTS1	PfkB IndA

3.2.1 *In vivo* subcellular localization analyses for group one proteins

The proteins belonging to group one includes Peroxisomal-3-ketoacyl-CoA thiolase (PKT); 1,4-Dihydroxy-2-naphthoyl-CoA-synthase/Enoyl-CoA hydratase/isomerase (NS/ECHI); Histidne triad nucleotide binding (HIT) and Transthyretin like protein (TLP). These proteins contain PTS2 in Arabidopsis and other higher plant orthologs. The orthologs in lower eukaryotes were predicted by phylogenetic analyses (data not shown) to also contain functional PTS2 signal.

To confirm that proteins of this group does not contain PTS1 even in higher plants, the PTS1 domain constructs of AtPKT3 (DAR>) and At NS (RRP>) were cloned into pCAT-EYFP-SKL137 vector in the back of EYFP as described in Materials and Methods to allow the PTS1

motif accessible to cellular receptors. The respective plasmid constructs were analysed for localization studies by precipitating them on gold particles and transforming onion cells with the help of biolistic particle delivery system. The bombarded onion epidermal cells were analyzed by inverted fluorescence microscopy after 16-18 hr of incubation at room temperature and also after 5-7 days of cold incubation 4°C. The PTS1 domains of AtPKT3 and AtNS showed only cytosolic localization as shown in the Figure 3-2. The cold incubation did not alter the localization and the proteins remained cytosolic, suggesting that the Arabidopsis PTS1 domains of PKT3 (DAR>) and NS (RRP>) are not able to target the proteins to peroxisomes. Thus, it was shown that the proteins of group one contain only PTS2 signal.

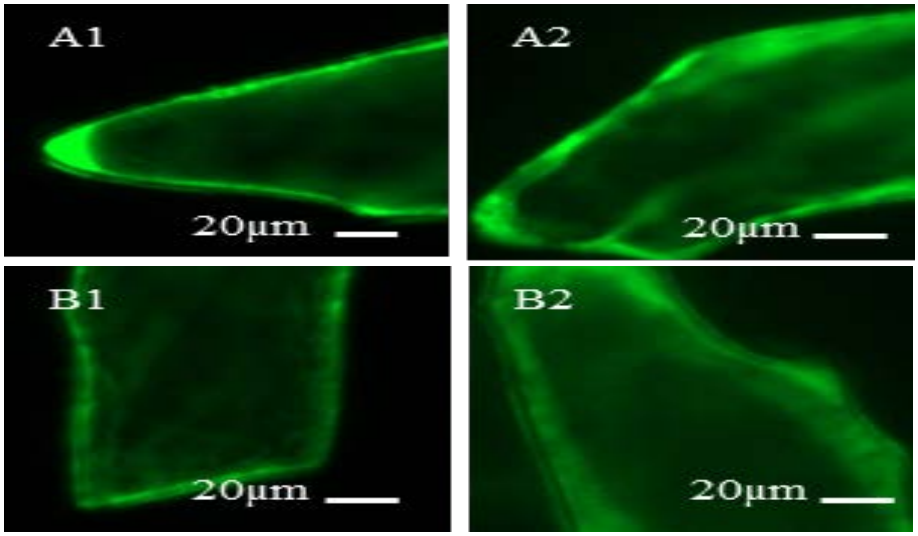

Figure 3-2: *In vivo* subcellular localization of AtPKT3 and AtNS

The PTS1 domain constructs (EYFP-Ct 10aa-AtPKT3 and EYFP-Ct 10aa-AtNS) were made by fusing the PTS1 domain in the back of EYFP and cloning into pCAT-SKL137. The onion epidermal cells were transformed by bombarding the gold particles coated with plasmid DNA. *In vivo* subcellular localization of the transiently expressed protein was analyzed by fluorescence microscopy. The constructs showed cytosolic fluorescence for AtPKT3 and AtNS (A1 and B1 respectively). The cold incubation did not alter the localization (A2 and B2).

3.2.2 *In vivo* subcellular localization analyses for group two proteins

Group two is composed of those proteins which contain mainly PTS2 but also have low affinity for PTS1 specifically in higher plants. The representative proteins chosen for studying this group include Alpha crystalline domain protein (Acd), peroxisomal Malate dehydrogenase (pMDH) and Citrate synthase (CSY). These proteins were investigated using orthologous sequences from both lower plants as well as higher plants.

The Acd32.1 in Arabidopsis has been shown to contain both PTS2 (RLx_5HF) and PTS1 (PKL>) (Ma *et al*., 2006). The half C-terminal domain of AtAcd32.1 fusion protein cloned in the back of EYFP showed cytosolic fluorescence (data not shown, analysed by co-worker) demonstrating that the predicted PTS1 domain alone of AtAcd32.1 is not sufficient enough to localise the protein to peroxisomes and the protein depends mainly on PTS2 for targeting. The protein ortholog from lower plant *Selaginella moellendorfi* was analysed by localization studies of both PTS1 and PTS2 domain of the protein. The PTS1 domain of SmAcd32.1 (PKS>) was cloned into pCAT-EYFP-SKL137 vector in the back of EYFP while the PTS2 domain (RMx_5HL) was cloned in pCAT-PTD2-EYFP in the front of EYFP as described in Materials and Methods. The fusion proteins were then analysed for in-vivo subcellular localization where the PTS1 domain was found to be cytosolic with no effect of cold incubation whereas the PTS2 domain was shown to be localized to peroxisomes as shown in Figure 3-3 which showed that the protein SmAcd32.1 contains only PTS2 and not PTS1.

Similarly the PTS1 domains of AtpMDH1 (AKK>), AtpMDH2.3/4 (SKR>), PppMDH (PKS>), AtCSY1 (TKL>) AtCSY3 (SSV>), SmCSY (PSS>) and PTS2 domain of AtpMDH2.1/4 were cloned. The PTS1 orthologs from higher plants showed cytosolic fluorescence after over-night incubation at RT but localized to peroxisomes upon cold incubation for seven days such as AtpMDH1, AtpMDH2.3/4, AtCSY1

and AtCSY3. However the fluorescence remained cytosolic even after cold incubation for domain constructs SmCSY and PppMDH. The PTS2 domain of AtpMDH2.1/4 was localized to peroxisomes (data not shown, analysed by co-workers).

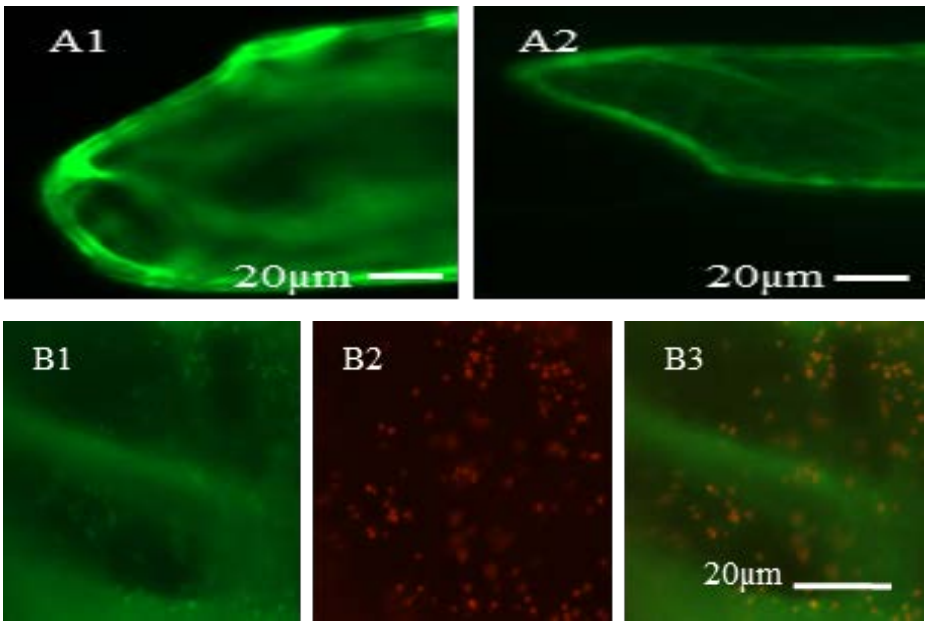

Figure 3-3: *In vivo* subcellular localization of SmAcd32.1

The PTS1 domain construct (EYFP-Ct 10aa-SmAcd32.1) was cloned by fusing the PTS1 tripeptide domain in the back of EYFP. It showed cytosolic fluorescence (A1) with no effect of cold incubation on localization (A2). However, the PTS2 domain construct (Nt 15aa-SmAcd32.1-EYFP) was cloned by fusing the PTS2 domain in the front of EYFP and was localized to peroxisomes (B1). The peroxisome localization of the PTS2 domain construct was confirmed by merging the image (B1) with that of peroxisomal marker protein RFP-SKL> (B2) showing merge in B3.

Thus, it is demonstrated that the Acd32.1, pMDH and CSY proteins mainly contain PTS2 and the orthologs in higher plants also contain low affinity to PTS1 whereas the PTS1 orthologs in lower plants are not functional and hence they are not imported to peroxisomes. The targeting efficiency is low as it required 7 days of incubation at cold,

suggesting that the process of evolution of targeting signals to PTS1 has started in higher plants AtpMDH1, AtpMDH2.3/4, AtCSY1 and AtCSY3 while the lower plant orthologs PppMDH SmCSY and SmAcd32.1 contain only PTS2.

3.2.3 *In vivo* subcellular localization analyses for group three proteins

The proteins belonging to group three are predicted to contain PTS2 and also show high affinity to PTS1. The representatives for this group of proteins include Acyl CoA oxidase (ACX) and Citrate synthase (CSY). The proteins were analysed by using both PTS1 as well as PTS2 domains for subcellular localization.

For this group, the PTS1 domains of Arabidopsis plants AtCSY2 (SAL>), AtACX3 (SSV>), and AtACX6 (SSL>) and one protein from lower plants PpACX 3/6 were cloned and analysed. After over-night incubation at RT, all the fusion proteins from Arabidopsis showed cytosolic localization except AtCSY2 that was found to be localized to peroxisomes. However, in case of AtACX3 and AtACX6 the cold incubation for seven days lead to import of fluorescence into small punctuate structures which were confirmed to be peroxisomes after double labelling and co-localization with RFP-SKL> (data not shown, analysed by co-workers). The lower plant ortholog PpACX3/6 also showed cytosolic fluorescence but the cold incubation did not lead to import of PpACX3/6 into peroxisomes. This suggests that the PTS1 domain of PpACX3/6 is not able to target the protein to peroxisomes, while the PTS1 domains of AtCSY2, AtACX3 and AtACX6 are fully functional and directs the protein to peroxisomes.

The PpACX3/6 and AtCSY2 were also chosen to analyse if they contain PTS2 and thus their PTS2 domains were fused in the front of EYFP in pCAT-PTD2-EYFP vector as explained in material and method and their targeting signals were analyzed. The PTS2 domain of

Results and Discussion

PpACX3/6 (RAx_5HL) displayed peroxisomal localization which was confirmed by double labelling and co-localization with RFP-SKL> as a peroxisomal marker protein as shown in Figure 3-4. Similarly the AtCSY2 domain (RLx_5HL) was also found to be localized to peroxisomes (data not shown, analysed by co-workers).

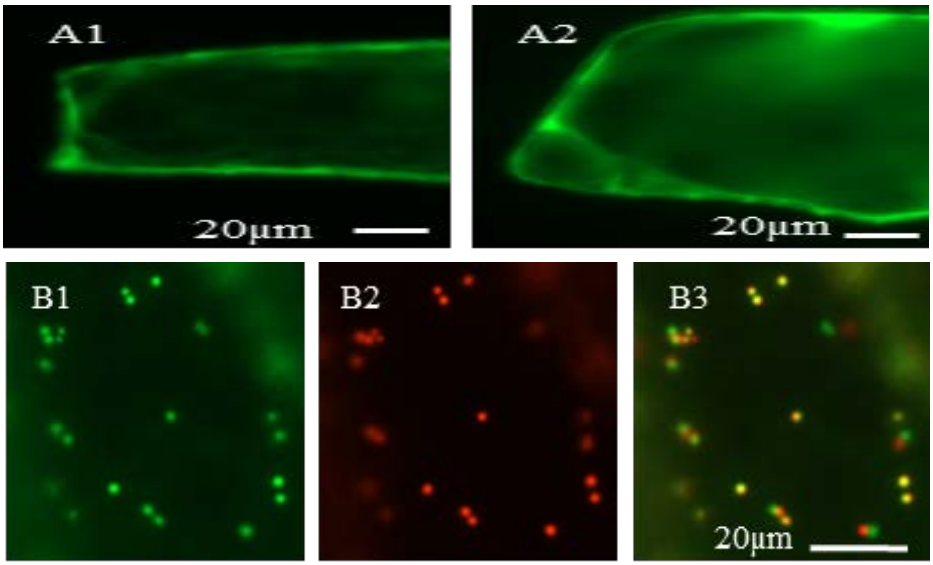

Figure 3-4: *In vivo* subcellular localization of PpACX3/6

The PTS1 domain construct (EYFP-Ct 10aa- PpACX3/6) made by fusing the PTS1 tripeptide domain in the back of EYFP showed cytosolic fluorescence (A1) with no effect of cold incubation on localization (A2) whereas the PTS2 domain construct (Nt 15aa- PpACX3/6-EYFP) made by fusing the PTS2 domain in the front of EYFP was found to be localized to peroxisomes (B1). The onion epidermal cells were transformed by bombarding the gold particles coated with plasmid DNA. *In vivo* subcellular localization of the transiently expressed protein was analyzed by fluorescence microscopy. The peroxisome localization was confirmed by merging the image with that of peroxisomal marker protein RFP-SKL> (B1-B3).

By combining the results of group one and two, it implies that ACX and CSY in lower plants contain PTS2 as the principal targeting signal whereas the higher plant orthologs AtACX3, AtACX6 and AtCSY2 show high affinity to PTS1 also in addition to PTS2.

3.2.4 *In vivo* subcellular localization analyses for group four proteins

The proteins belonging to group four are predicted to contain primarily PTS1 but also show low affinity to PTS2. To study this group the targeting signals of Long Chain Acyl Co-A Synthatase (LACS) were compared in higher plant Arabidopsis and lower plant *Micromonas pusilla* CCMP1545.

Arabidopsis thaliana contain nine isoforms of LACS out of which LACS6 and LACS7 has been found to be localized to peroxisomes. LACS6 contains primarily PTS2 (RIx_5HL), while LACS7 contains high affinity to PTS1 (SKL>) and also shows low affinity for PTS2 (RLx_5HI) (Fulda *et al*., 2002; Fulda *et al*., 2004). The PTS1 domain from lower plant ortholog MpLACS 6/7 (AGR>) was cloned in pCAT-EYFP-SKL137 in the back of EYFP as explained in Materials and Methods. *In vivo* subcellular analysis of the resulting domain construct showed cytosolic localization after over-night incubation at RT and further cold incubation did not lead to import of PTS1 domain construct into the peroxisomes as shown in Figure 3-5 (A1-A2).

To check if the lower plant orthologs utilizes PTS2 for import into the peroxisomes, the PTS2 domain of MpLACS 6/7 (RLx_5HL) was cloned in front of EYFP in the pCAT-PTD2-EYFP vector as explained in material and method. The PTS2 construct was found to be localized in small punctuate structures, which were further confirmed to be peroxisomes by double labelling and co-localization with RFP-SKL> as a peroxisomal marker protein as shown in Figure 3-5 (B1-B3).

Thus, it confirms that LACS belonging to group four is targeted to peroxisome by PTS1 and also PTS2 in higher plant orthologs whereas

the lower plant orthologs still contain the evolutionary old PTS2 only and not PTS1.

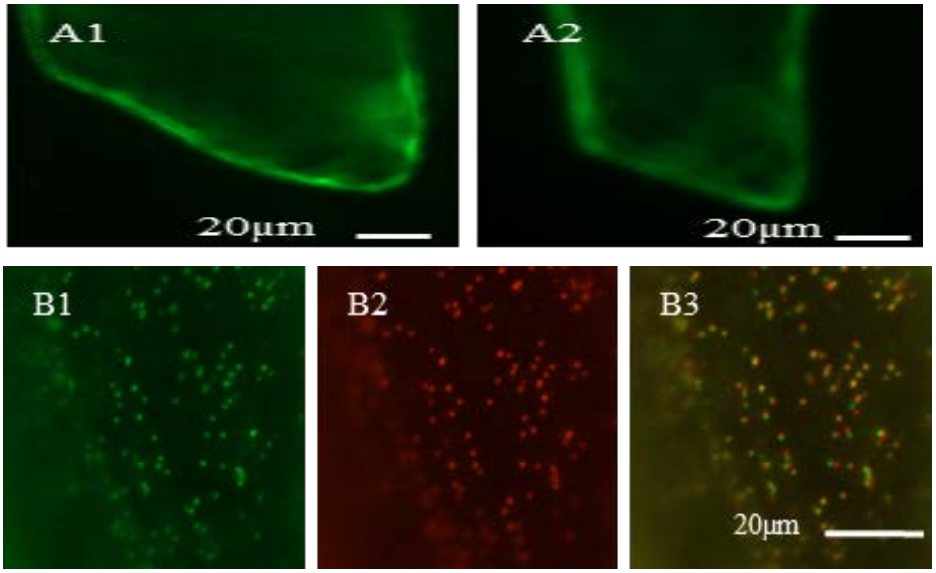

Figure 3-5: *In vivo* subcellular localization of MpLACS 6/7

The PTS1 domain construct (EYFP-MpLACS 6/7-PTS1) made by fusing the PTS1 tripeptide domain in the back of EYFP showed cytosolic fluorescence (A1) with no effect of cold incubation on localization (A2) whereas the PTS2 domain construct (MpLACS 6/7-PTS2-EYFP) made by fusing the PTS2 domain in the front of EYFP was found to be localized to peroxisomes (B1). The onion epidermal cells were transformed by bombarding the gold particles coated with plasmid DNA. *In vivo* subcellular localization of the transiently expressed protein was analyzed by fluorescence microscopy. The peroxisome localization was confirmed by merging the image with that of peroxisomal marker protein RFP-SKL> (B1-B3).

3.2.5 *In vivo* subcellular localization analyses for group five proteins

The proteins belonging to group five are predicted to contain exclusively PTS1 in higher plants but only PTS2 in lower plant

orthologs. The representatives for this group of proteins include Phosphofructokinase B (PfkB) and Indigoidine synthase A (IndA).

The PTS1 domains of PfkB and IndA orthologs were tested in higher plants Arabidopsis and Oryza and in lower plants *Micromonas pusilla RCC299* (for IndA) and *Chlamydomonas reinhardtii* (for PfkB). As expected the lower plant orthologs MspIndA and CrPfkB were found out to be cytosolic while the higher plant orthologs AtPfkB and OsIndA were localized to peroxisomes and likewise the PTS2 domain of MspIndA showed targeting to peroxisomes upon subcellular localization analysis using tobacco protoplasts (data not shown, analysed by co-workers). Thus it is shown that the lower plant orthologs of group five contain PTS2 whereas PTS1 is present in orthologs of higher plants.

To our surprize, the PTS1 domains of AtIndA and OsPfkB showed cytosolic fluorescence indicating the absence of PTS1 in these constructs. But when these protein orthologs were cloned in front of EYFP such that the corresponding PTS1 is blocked, they still localized to peroxisomes. The peroxisomal targeting was observed for AtPfkB and OsIndA even after mutating their PTS1 domains (data not shown, analysed by co-workers).

To analyse if the AtPfkB has PTS2 domain, the first fifty amino acids of the protein were cloned in front of EYFP in pCAT-DECR-EYFP vector and the resulting Nt50-aa-AtPfkB-EYFP was analysed for subcellular localization. The protein showed cytoplasmic fluorescence after overnight incubation at RT and even after cold incubation as shown in Figure and similarly the Nt100-aa-OsIndA also did not localize to peroxisomes (data not shown) confirming the absence of PTS2 in AtPfkB and OsIndA. The two proteins AtPfkB and OsIndA were found to interact with each other using BiFC technique (data not shown, analysed by co-workers).

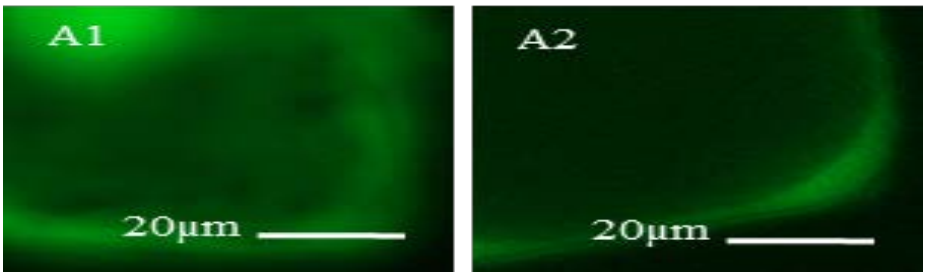

Figure 3-6: *In vivo* subcellular localization of AtPfkB

The PTS2 domain construct (Nt50 aa-AtPfkB-EYFP) was cloned by fusing the first fifty amino acids of the insert in the front of EYFP using pCAT-DECR-EYFP. The onion epidermal cells were transformed by bombarding the gold particles coated with plasmid DNA. *In vivo* subcellular localization of the transiently expressed protein was analyzed by fluorescence microscopy. It was found to be localized to cytoplasm (A1) with no effect of cold incubation of 7 days on the localization (A2).

Thus, the analysis of peroxisome targeting signals in protein orthologs belonging to group number one till five suggests the transition from PTS2 to PTS1 during the course of development from lower photosynthetic plants to higher plant species. It is also possible that the climax of evolution for peroxisomal targeting signals may not be only PTS1 as shown in *C.elegans* and *P.tricornutum* but the dual localization of both targeting signals either on the same protein or on two different but interacting proteins

3.3 Electrophysiological characterization of pore forming activity in Arabidopsis leaf peroxisomes

Isolation and purification of peroxisomes from the Arabidopsis plants has been reported to be extremely difficult in comparison to other plant species such as spinach (*Spinacia oleracea*), pea (*Pisum sativum*) and soybean (*Glycin max*). The process of isolating highly pure intact peroxisomes from the leaves of Arabidopsis is challenging because of

the increased fragility of peroxisomes in aqueous extracts probably due to the high concentration of secondary metabolites and the other reason being the possibility of contamination with neighbouring organelles such as chloroplast and mitochondria because of the pronounced physical association of peroxisomes with mitochondria and chloroplast organelles specifically in the plants belonging to Brassicaceae family.

Enrichment in highly pure peroxisomes from leaves of Arabidopsis was reported upon using a combination of sucrose and percoll for density gradient centrifugation during peroxisome isolation (Reumann *et al.*, 2007). Using the similar strategy, Arabidopsis leaf peroxisomes enriched in membrane proteins were isolated and were subjected for electrophysiological characterization with the help of planar lipid bilayer technique described in Materials and Methods (see section 2.2.6).

Pore forming activity has been observed in peroxisomal membranes isolated from different sources including plants, fungi and mammals (See 1.2). The peroxisomal membrane proteins were solubilised with 0.5% (w/v, final concentration) Genapol X-80 detergent before applying to the aqueous compartment surrounding lipid bilayer for measuring porin activity. As predicted in peroxisomes isolated from Spinach (Reumann *et al.*, 1995), pore forming activity was also observed in Arabidopsis leaf peroxisomes. The average single channel conductance of majority of the channels was observed around 0.5 nS in 1 M KCl as shown in Figure 3-7.

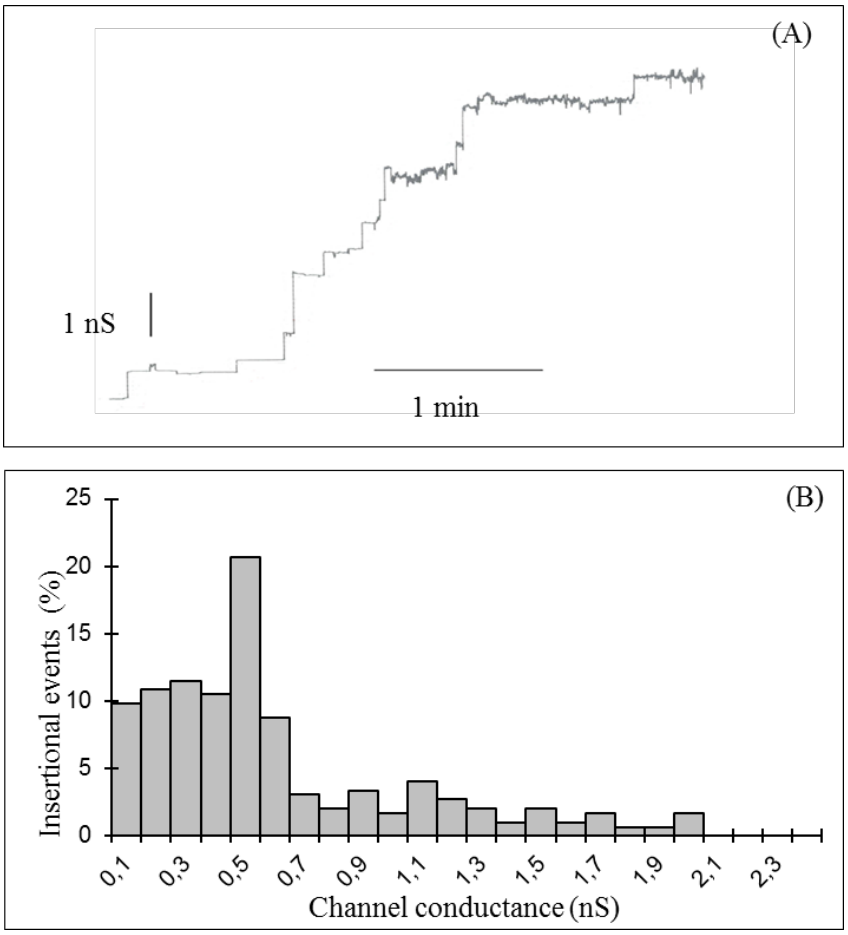

Figure 3-7: Porin activity of Arabidopsis leaf peroxisomes in 1M KCl

Histogram showing the percentage abundance of different single channel conductance measurement observed using solubilised membrane fraction of Arabidopsis leaf peroxisomes (B) with examples of actual insertions in artificial membranes (A). The majority of channels were observed showing average single channel conductance equal to 0.5 nS in aqueous phase containing 1 M KCl. The applied membrane potential was 20 mV and the recordings were done at room temperature. Around 300 insertional events were measured in total.

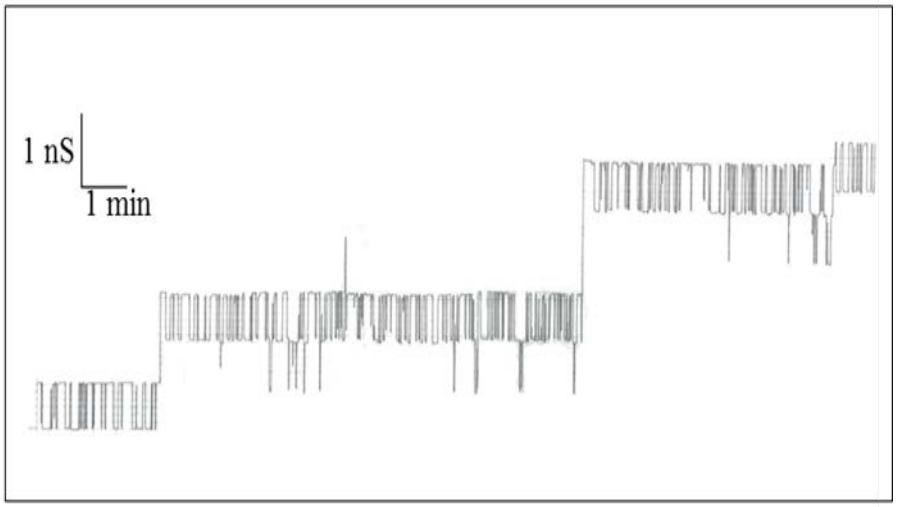

Figure 3-8: The possibility of a dimer state in porin channel

The examples of actual insertions in artificial membranes in aqueous phase containing 1 M KCl showed the possibility of dimer state in the porin channels of Arabidopsis leaf peroxisomes. The applied membrane potential was 20 mV and the recordings were done at room temperature.

The conductance value is slightly higher than 0.3 nS value reported in peroxisomes from spinach but much lesser than conductance values of porins reported from other organelles such as mitochondria (2-4 nS) and chloroplast (7-8 nS) emphasizing that the channel is indeed peroxisomal and not a channel resulting from impurities of neighbouring organelles. The conductance peaks also suggest that the observed porin like channel might be a dimer or trimer as shown in Figure 3-8. Also since the 0.3 nS channel are also observed in significant abundance, there is a possibility that in Arabidopsis the porin like channel shows single channel conductance of 0.3 nS in monomer state and 0.5/0.6 nS in dimer state. The dimer state of channel in Arabidopsis is likely to be more stable giving channel of higher conductance in more quantity.

Results and Discussion

After finding that Arabidopsis leaf peroxisomes contain porin channel in their membranes, the single channel studies were done using different concentrations of the standard electrolyte KCl. It was noticed that the channel conductance is reduced when lower concentration of electrolyte is used. The majority of channels displayed single channel conductance measurement equal to 0.1 – 0.15 nS at 0.1 M KCl as shown in Figure 3-9. The conductance increased slightly to 0.2 nS upon using the 0.3 M KCl as shown in Figure 3-10. However, No significant change in conductance values was observed when 3 M KCl concentration of electrolyte was used compared to that of 1M KCl as shown in Figure 3-11.

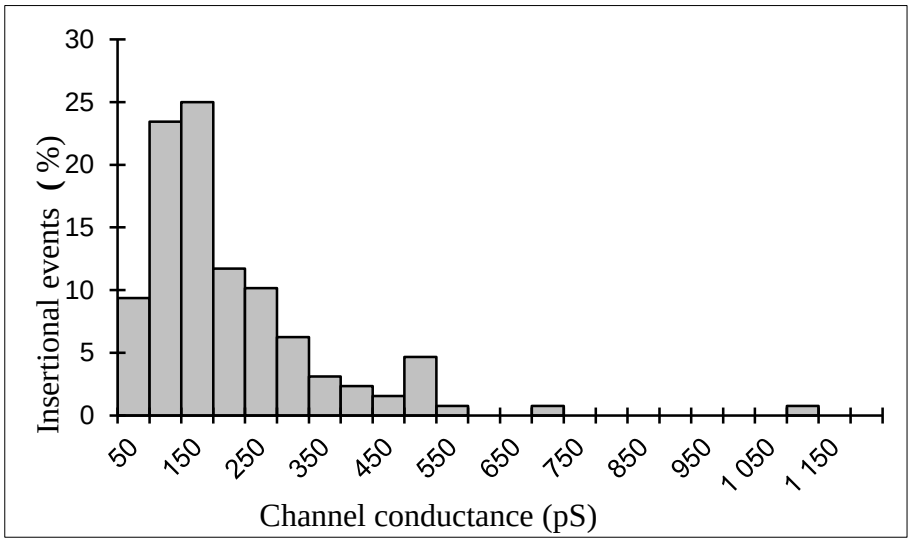

Figure 3-9: Porin activity of Arabidopsis leaf peroxisomes in 0.1 M KCl

Histogram showing the percentage abundance of different single channel conductance measurement observed using solubilised membranes from Arabidopsis leaf peroxisomes. The majority of channels were observed showing average single channel conductance equal to 100-150 pS in aqueous phase containing 0.1 M KCl. The applied membrane potential was 20 mV and the recordings were done at room temperature. Around 128 insertional events were measured in total.

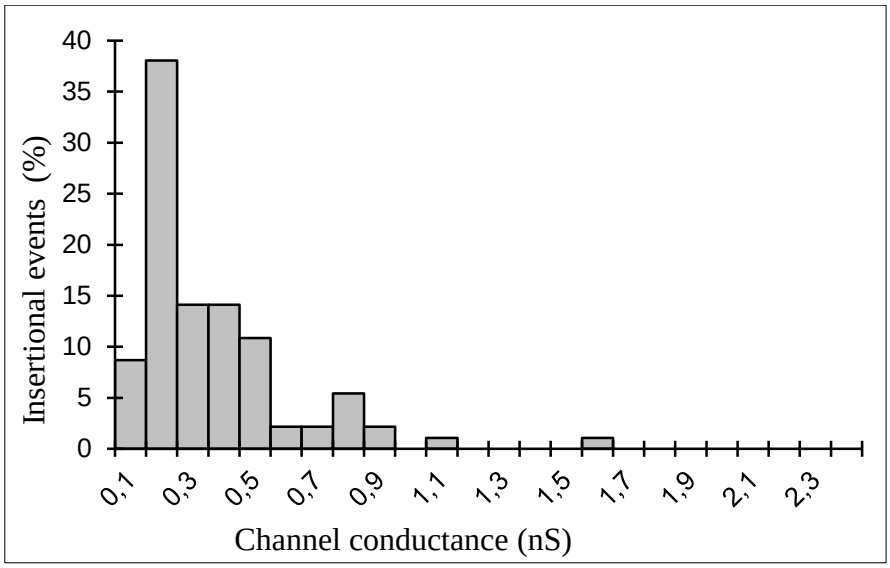

Figure 3-10: Porin activity of Arabidopsis leaf peroxisomes in 0.3 M KCl

Histogram showing the percentage abundance of different single channel conductance measurement observed using solubilised membranes from Arabidopsis leaf peroxisomes. The majority of channels were observed showing average single channel conductance equal to 0.2 nS in aqueous phase containing 0.3 M KCl. The applied membrane potential was 20 mV and the recordings were done at room temperature. Around 92 insertional events were measured in total.

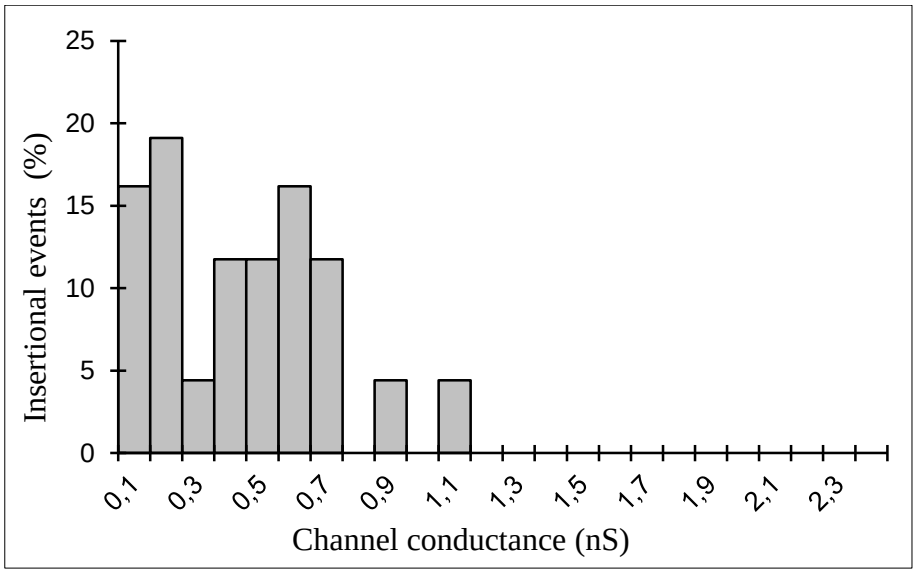

Figure 3-11: Porin activity of Arabidopsis leaf peroxisomes in 3 M KCl.

Histogram showing the percentage abundance of different single channel conductance measurement observed using solubilised membranes from Arabidopsis leaf peroxisomes. The majority of channels were observed showing average single channel conductance equal to 0.2 nS in aqueous phase containing 3 M KCl. The applied membrane potential was 20 mV and the recordings were done at room temperature. Around 68 insertional events were measured in total.

Thus, a nonlinear relationship is observed between the channel conductance and the bulk concentration of the salt comprising the aqueous phase as shown in the Figure 3-12. Thus, it is suggested that the channel is similar to the substrate-specific porin type channel and does not belong to the category of general diffusion porins.

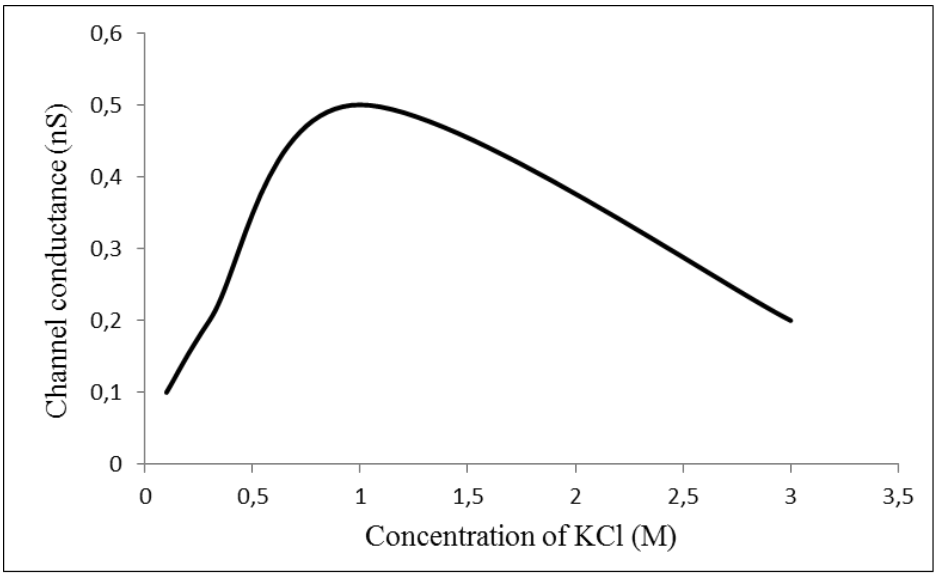

Figure 3-12: Porin activity with respect to salt concentration

The porin-like channel of Arabidopsis leaf peroxisomes showed non-linear correlation between the channel conductivity and the concentration of electrolyte KCl.

The ion selectivity of the channel was determined by measuring the channel conductance in different electrolytes other than KCl. When 1 M LiCl was used, the behaviour of the most of the channels remained almost unchanged as shown in Figure 3-13. Whereas upon using 1 M potassium acetate, the majority of channels displayed reduction in conductance value as shown in Figure 3-14. These experiments suggest the channel to be selective to anions as replacing cation in 1 M LiCl (Li^+ instead of K^+) does not appreciably change the conductance behaviour. However, the channel conductance showed sharp change when anion was replaced in 1 M Potassium acetate (acetate instead of chloride ion) suggesting the channel preference towards anions.

Results and Discussion

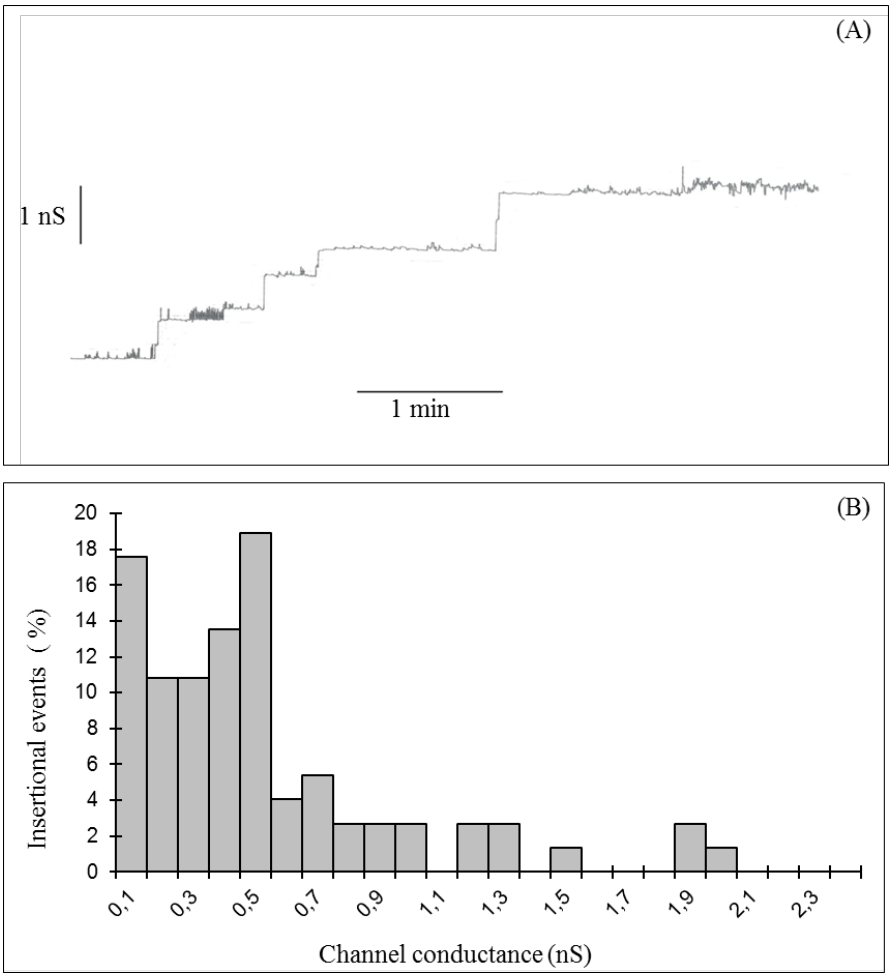

Figure 3-13: Porin activity of Arabidopsis leaf peroxisomes in LiCl

Histogram showing the percentage abundance of different single channel conductance measurement observed using solubilised membranes from Arabidopsis leaf peroxisomes (B) with examples of actual insertions in artificial membranes (A). The majority of channels were observed showing average single channel conductance equal to 0.5 nS in aqueous phase containing 1 M LiCl. The applied membrane potential was 20 mV and the recordings were done at room temperature. Around 74 insertional events were measured in total.

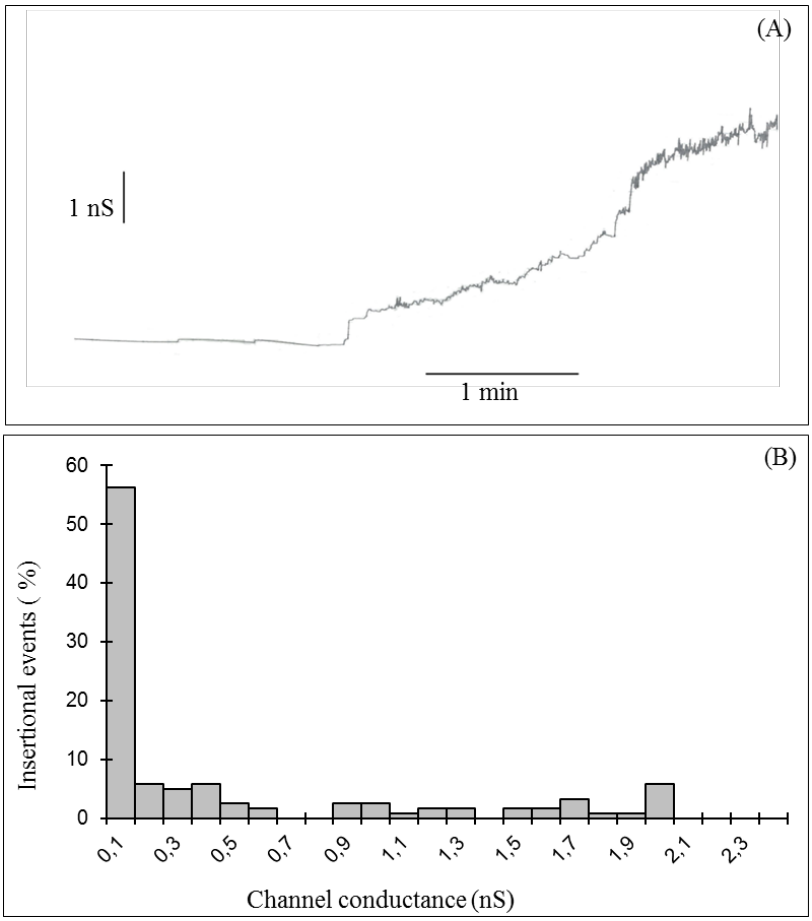

Figure 3-14: Porin activity of Arabidopsis leaf peroxisomes in Potassium acetate.

Histogram showing the percentage abundance of different single channel conductance measurement observed using solubilised membranes from Arabidopsis leaf peroxisomes (B) with examples of actual insertions in artificial membranes (A). The majority of channels were observed showing average single channel conductance equal to 0.5 nS in aqueous phase containing 1 M Potassium acetate, pH 7. The applied membrane potential was 20 mV and the recordings were done at room temperature. Around 121 insertional events were measured in total.

To test further if the channel is specific to certain substrates, the binding assays were done using some of the substrates which are required as

intermediate residues in the metabolic reactions occurring within peroxisomes. The channel showed substrate specificity for succinic acid and citric acid as shown in Figure 3-15 and 3-16 respectively. The half saturation constant for succinic acid was lower (4 mM) in comparison to that of citric acid (34 mM) which shows the higher preference of the channel for succinic acid.

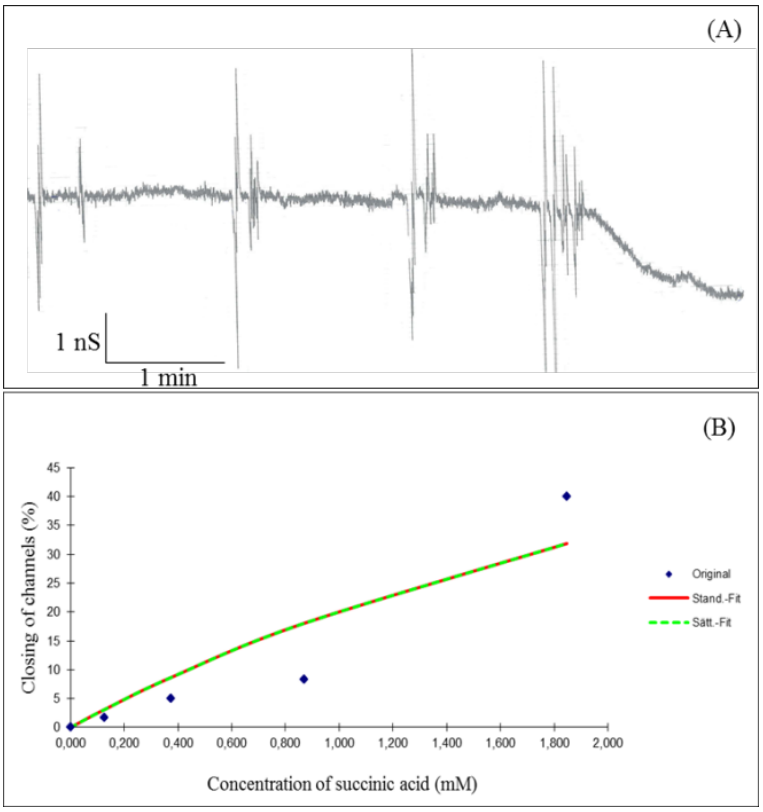

Figure 3-15: Porin specificity to succinic acid

Addition of succinic acid in the aqueous chamber containing 1 M KCl resulted in closure of channels observed by decrease in channel conductance (A). The percentage of total channels that are closed in relation to concentration of succinic acid is also shown (B).

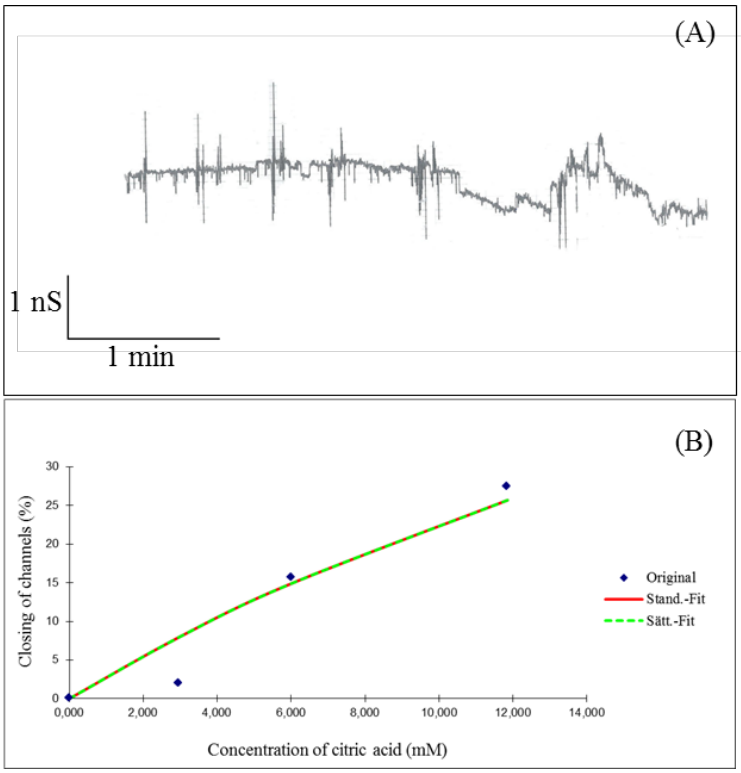

Figure 3-16: Porin specificity to citric acid

Addition of citric acid in the aqueous chamber containing 1 M KCl resulted in closure of channels observed by decrease in channel conductance (A). The percentage of total channels that are closed in relation to concentration of citric acid is also shown (B).

Thus the combined results confirmed the pore forming activity in peroxisomal fractions enriched in membrane proteins when isolated from leaves of Arabidopsis. The bilayer experiments suggested the anion selective porin like channel of 0.5 nS. The channel is found to belong to the category of specific porins with the initial binding assays predicting specificity towards carboxylic acid residues. More binding assays using larger number of substrates will help in better understanding of the predicted channel specificity and on larger scale in the transfer of metabolites across peroxisomes.

Results and Discussion

3.4 Overexpression and purification of AtPMP22 and AtPEX11D

Arabidopsis peroxisomal membrane protein of molecular weight 22 kDa (AtPMP22) is an integral component of the membranes of all peroxisomes. AtPMP22 protein sequence analysis showed its relationship to mammalian PMP22/Mpv17 family of PMPs sharing around 55-57 % amino acid similarity and 28-30 % identity (Tugal *et al*., 1999). Further characterization of the targeting signal of AtPMP22 revealed direct sorting of the protein from cytoplasm to peroxisomes (Murphy *et al*., 2003) putting it under group 1 of PMPs (See introduction). The presence of four putative trans-membrane domains (TMDs) has been suggested with both of its N- and C- termini facing the cytosol. It was also observed that AtPMP22 contains probably a single mPTS and that all four TMDs are required for efficient targeting to peroxisomes (Murphy *et al*., 2003).

In addition to AtPMP22, other abundant membrane proteins of plant peroxisomes include AtPEX11 family of proteins. Arabidopsis plants possess five isoforms of PEX11 designated as AtPEX11- A to E. Amino acid sequence alignment showed that AtPEX11- C, D and E are highly similar to each other with average 75 % identity and 92 % similarity. Similar to AtPMP22, four TMDs have been predicted for AtPEX11-B to E with both terminal ends facing cytosolic side of the peroxisomal membrane. However, AtPEX11-A is predicted to contain three TMDs with N and C termini towards cytosolic and matrix side of the membrane respectively (Lingard and Trelease, 2006). The overexpression and suppression studies using individual and sub family of PEX11 genes revealed their role in peroxisome proliferation and division. It was also observed that overexpression of different isoforms of AtPEX11 results in many unique properties with enhancement in peroxisomal duplication by AtPEX11- A and E, peroxisome elongation by AtPEX11-C and D and in aggregation of peroxisomes by AtPEX11-B (Lingard and Trelease, 2006). It was observed that reduction in the

total number of peroxisomes takes place upon decreasing each of the PEX11 gene individually and increment in peroxisome abundance and size happens upon overexpressing PEX11 genes (Orth *et al*., 2007). In addition to the peroxisome proliferation and division, some other functions have also been suggested for the PEX11 proteins such as the modification in peroxisomal membranes through phospholipid binding, metabolite transport and in recruitment of downstream proteins (Fagarasanu *et al*., 2007). It was also suggested that in yeast peroxisomes PEX11p is primarily involved in transfer of metabolites whereas the role in peroxisome proliferation and division is only secondary to the proteins belonging to PEX11 family (van Roermund *et al*., 2000).

Thus, the further characterization of AtPEX11 proteins is very important to understand the probable role of these proteins, specifically in transfer of certain metabolites. Since there is maximum similarity between porin enriched peptides and AtPEX11-D, we decided to overexpress this membrane protein and also measure the electrophysiological properties of the purified protein.
Recently it was reported that PMP22 act as channel forming protein in mammalian peroxisomal membrane (Rokka *et al*., 2009) (See 1.2 for more detail). No protein has been described till now to explain the pore forming activity observed in plant peroxisomes. Since the peroxisomal proteins related to biogenesis and transportation of proteins and metabolites are conserved irrespective of the source of peroxisomes such as plants, mammals, fungi etc. (See introduction) there is a possibility that the Arabidopsis homolog of PMP22 may also act as channel forming unit. Thus in addition to AtPEX11-D, we also decided to overexpress and characterize AtPMP22.

Both the membrane proteins of peroxisomes AtPMP22 and AtPEX11-D were overexpressed in Pichia pastoris by following a similar strategy used by Egawa *et al* (Egawa *et al*., 2009). Briefly, the AtPMP22 and AtPEX11-D were subcloned in pPICZ A expression vector such that a

Results and Discussion

10-histidine tag is introduced in front of the open reading frame of the insert under the control of the AOX1 promoter and were transformed first in *E.coli* and then in *Pichia pastoris* by following the regular molecular biology techniques explained in material and methods. The Figure 3-17 shows the colony PCR results of transformed clones in *P.pastoris*.

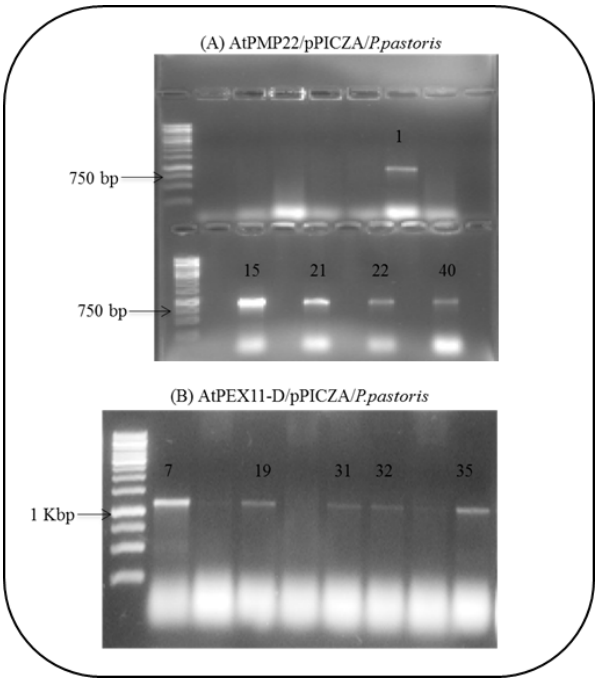

Figure 3-17: Colony PCR of *Pichia* transformants

Colony PCR of *Pichia* transformants (A) AtPMP22 (B) AtPEX11-D. The clone numbers 1, 15, 21, 22 and 40 for AtPMP22 and clone numbers 7, 19, 31, 32 and 35 for AtPEX11-D were found out to contain the insert after the yeast colonies were analysed by Colony PCR using vector specific (5' and 3' AOX) primers.

The expression of the recombinant constructs was performed in *P.pastoris* using BMGY/BMMY media (Material and methods) and the crude extract of the proteins (CE) was obtained by lysis of yeast cells

with the help of Glass-beads and Breaking Buffer. The membrane proteins were enriched by centrifugation of CE at 100,000g and then homogenizing the pellet in membrane solubilisation buffer. The corresponding fraction is designated as membrane fraction (MF). The expressed AtPMP22 and AtPEX11 proteins were analysed by SDS-PAGE and staining with CBB, and by Western blotting. The AtPMP22 and AtPEX11-D proteins were not observed upon CBB stained gels because of lesser amount of the membrane proteins but seen at appropriate place upon determination by Western blot which is a more sensitive technique than CBB staining of protein gels. The Western blot analysis was done using primary antibody against poly-histidine tag that was cloned upstream of AtPMP22 and AtPEX11-D genes. The protein fractions from different clones varied in total protein amount as shown in Figure 3-18. The fractions showing maximum protein concentration were used for further studies.

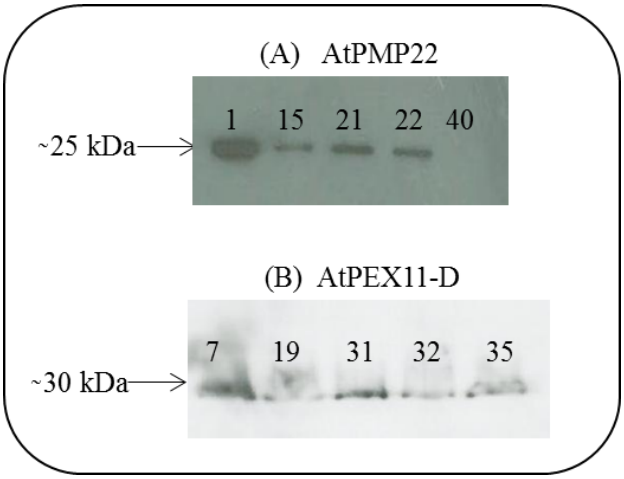

Figure 3-18: AtPMP22 and AtPEX11-D proteins

Protein bands of different AtPMP22 (1, 15, 21, 22 and 40) and AtPEX11-D (7, 19, 31, 32 and 35) clones are shown in A and B respectively. The crude extracts of different clones were observed by Western blotting with clone no. 1 for AtPMP22 and no. 7 and 31 for AtPEX11-D expressing more proteins than others.

Results and Discussion

The AtPMP22 and AtPEX11-D fractions containing the crude extract of the expressed proteins were further purified by centrifuging the respective crude extracts at 100,000g to obtain the membrane fraction by following the procedure as described in Materials and Methods (see section 2.2.4.2). To confirm that AtPMP22 and AtPEX11-D are expressed in membranes and not as soluble proteins, the different fractions obtained by centrifuging crude extract were analysed by western blotting. The presence of overexpressed proteins was only found in membrane fraction and not in supernatant as shown in Figure 3-19.

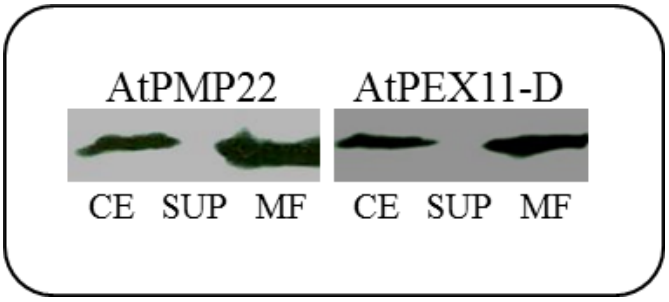

Figure 3-19: Membrane fraction containing the overexpressed AtPMP22 and AtPEX11-D

The presence of overexpressed proteins AtPMP22 and AtPEX11-D is in the membrane fraction of the *Pichia* proteins. The Western blot analysis of crude extract (CE), supernatant (SUP) and the membrane fraction (MF) of AtPMP22 and AtPEX11-D clearly show the absence of the overexpressed proteins in the supernatant fraction which was obtained from the crude extract after centrifugation at 100,000g to get membrane pellet.

After enriching AtPMP22 and AtPEX11-D proteins in membrane fractions, they were purified by Ni-NTA affinity chromatography. The membrane fractions containing AtPMP22 or AtPEX11-D were purified in batch cultures under native conditions (see 2.2.4.8) and were analysed by SDS-PAGE and Western blotting.

The AtPMP22 and AtPEX11-D fractions obtained after Ni-NTA affinity chromatography were relatively more purified than corresponding membrane fractions as shown in Figure 3-20 and 3-21 respectively.

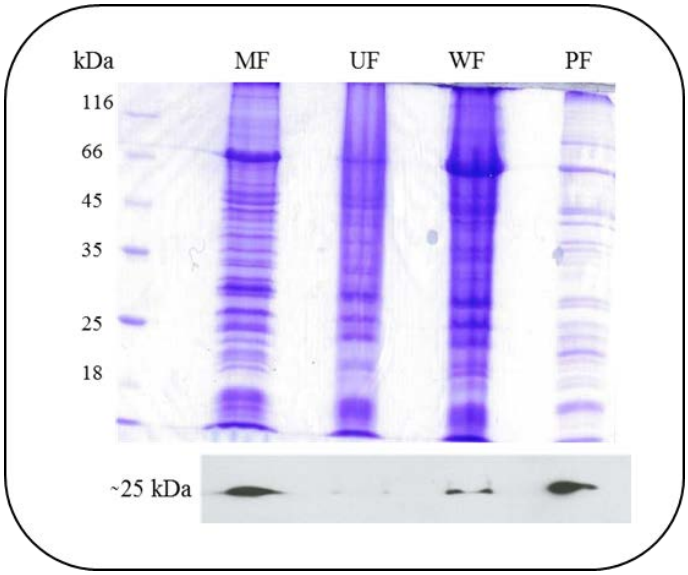

Figure 3-20: Ni-NTA purification of AtPMP22

The different fractions obtained while purifying the AtPMP22 membrane fraction (MF) by Ni-NTA column chromatography including unbound fraction (UF), wash fraction (WF) and purified fraction (PF) obtained by eluting the bound protein from the resin are shown after analysis by SDS-PAGE and Western blotting.

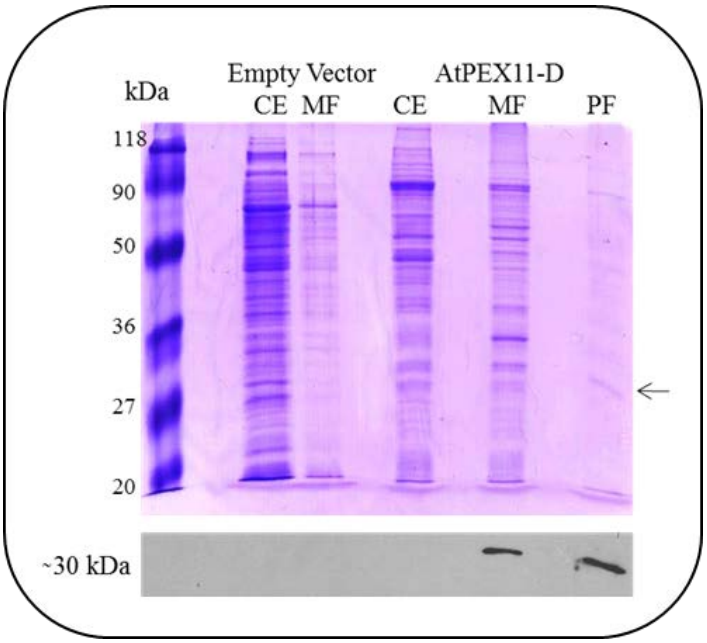

Figure 3-21: Ni-NTA purification of AtPEX11-D

The different fractions obtained during overexpression and purification of the AtPEX11-D protein including the crude extract (CE), membrane fraction (MF) and purified fraction (PF) obtained by Ni-NTA purification are compared with CE and MF of empty vector control and are shown after analysis by SDS-PAGE and Western blotting.

However, the samples could not be purified to utmost purity and showed non-specific proteins when analysed by SDS-PAGE. The further purification of AtPMP22 and AtPEX11-D will be important to understand their properties.

3.5 Electrophysiological characterization of AtPMP22 and AtPEX11-D

The two Arabidopsis peroxisomal membrane proteins AtPMP22 and AtPEX11-D obtained after overexpressing them in *Pichia* (also see section 3.4), were subjected for electrophysiological measurements to determine the channel activity of the recombinant proteins fractions.

The expression vector pPICZ A without containing the gene of interest was used as a negative control. The empty vector was introduced in *Pichia pastoris* to obtain the total protein of non-recombinant yeast to compare with the protein expression profile of the over-expressed peroxisomal membrane proteins AtPMP22 and AtPEX11D.

The crude extract of the protein and the enriched membrane fraction from the empty vector control was obtained in a similar manner as done for the over-expressed membrane proteins. The membrane fraction was then treated with 0.5% to 4% of final concentration of Genapol X-80 detergent and analyzed using planar lipid bilayer technique as described in Materials and Methods (see section 2.2.6). The membrane fraction displayed the channel forming activity upon reconstitution in the artificial lipid bilayer and using the ionovation compact unit for bilayer assays. The protein samples were found to take long time before insertion into the bilayer. Total twelve insertion events were measured in case of protein fractions containing empty vector control using new bilayer each time. The majority of channels showed average single channel conductance equal to 0.1 and 0.2 nS in 1 M KCl as shown in Figure 3-22. The channels corresponding to single channel conductance of 0.3 and 0.6 nS were also observed in considerable amount. The pore forming proteins reported in peroxisomes from yeast *S. cerevisiae* contain two types of channels displaying the average conductance of 0.2 and 0.6 nS in 1.0 M KCl as an electrolyte (Grunau *et al.*, 2009). Thus, the channels of single channel conductance 0.2 and 0.6 nS

observed in proteins expressed by the empty vector control in *Pichia pastoris* can be attributed to the channels predicted from peroxisomes of *S.cerevisiae.*

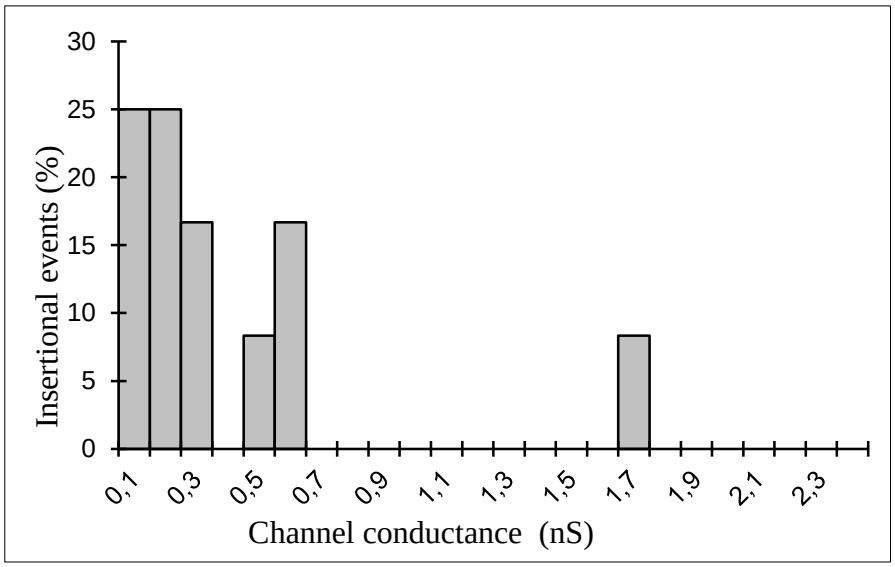

Figure 3-22: Channel activity in membrane fraction of *Pichia* proteins

Histogram showing the percentage abundance of different single channel conductance measurement observed using membrane fractions from Pichia containing empty vector pPICZ A (as a negative control). Protein samples were solubilized with Genapol (1:1, w/v).The majority of channels displayed average single channel conductance equal to 0.1, 0.2 nS in aqueous phase containing 1 M KCl and at membrane potential of 20 mV. The recordings were done at room temperature. Total 12 insertional events were measured using separate bilayer each time.

Further characterization by ion selectivity and voltage dependent assays will help in better understanding of the channels observed in membrane fractions of *Pichia* containing empty pPICZ A expression vector as a negative control.

3.5.1 Single channel conductance measurement of AtPMP22

The purified protein fractions obtained from Ni-NTA affinity chromatography of AtPMP22 membrane fractions were evaluated by planar lipid bilayer analysis. The samples were first solubilized by 0.5% to 1% (w/v, final concentration) Genapol X-80 detergent and then added to the disposable cuvettes which were filled with 1 M KCl electrolyte. The artificial bilayer was formed across the circular hole in the middle of the Teflon septum of the cuvettes. After the reconstitution of the protein sample in the membrane bilayer begin, the single channel conductance of the protein samples were measured by following the procedure described in Materials and Methods (see section 2.2.6).

The purified AtPMP22 protein samples displayed the pore forming activity but the reconstitution frequency of the protein was very less and only few channels could be measured even after many hours of the addition of protein to the bilayer membrane. In total, sixteen channels were measured with the most abundant channels showing 0.1 nS average single channel conductance in 1 M KCl electrolyte and at 20 mV membrane potential. The channels of 0.2 nS conductance were also observed in considerable amount. As mentioned before, the channels of 0.2 nS conductance were reported from peroxisomal fraction of yeast, and also since the purified AtPMP22 protein fraction could not be purified fully and some non-specific protein bands were observed in the SDS-PAGE analysis of the protein samples after they were purified by Ni-NTA column chromatography, it was expected that some of the porin activity showed by the AtPMP22 samples might not belong to AtPMP22 protein and are probably because of other proteins belonging to yeast peroxisomes. Thus it seems that the channel activity of 0.2 nS conductance is from yeast peroxisomes and perhaps the AtPMP22 protein is responsible for the channel activity corresponding to the 0.1 nS single channel conductance. The comparison between the single channel conductance values of AtPMP22 protein fraction and that of empty vector control is shown in Figure 3-23(B).

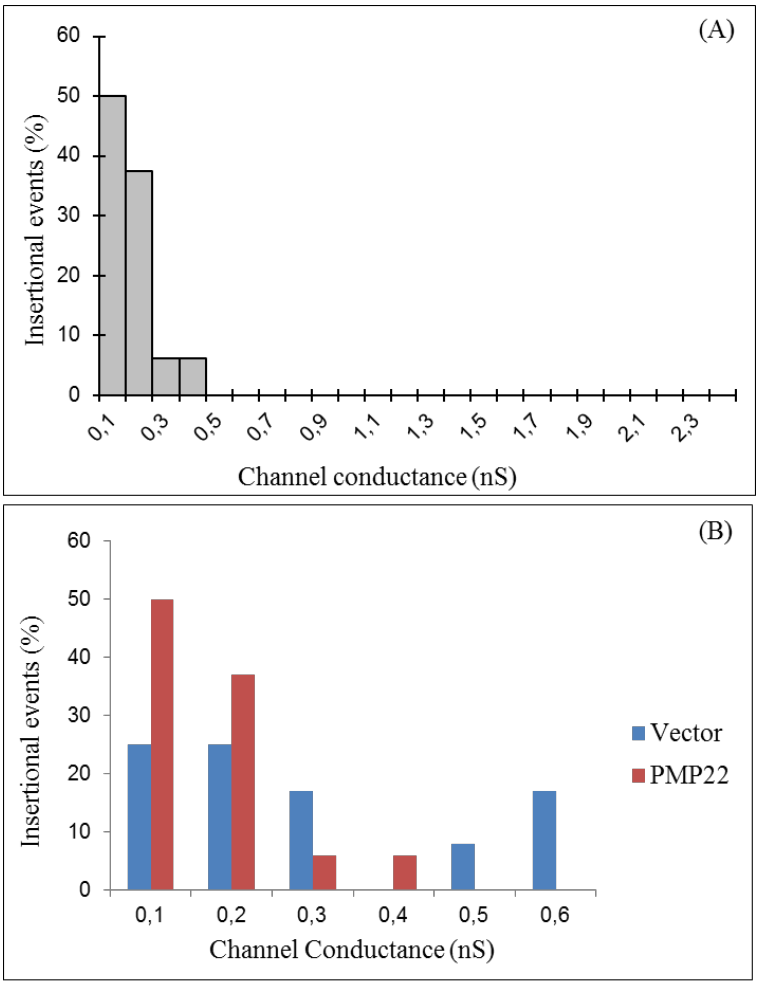

Figure 3-23: Porin activity in AtPMP22 protein

Histogram showing the percentage abundance of different single channel conductance measurement observed using purified fraction of AtPMP22 overexpressed in *Pichia*. Protein samples were solubilized with Genapol (1:1, w/v). The majority of channels displayed average single channel conductance equal to 0.1 nS in aqueous phase containing 1 M KC and at membrane potential of 20 mV. The recordings were done at room temperature. Total 16 insertional events were measured using separate bilayer each time.

3.5.2 Single channel conductance measurement of AtPEX11-D

The membrane fraction of AtPEX11-D before and after purification by Ni-NTA column chromatography were analyzed by planar lipid bilayer analysis as described in Materials and Methods. The single channel conductance measurements using membrane fraction of AtPEX11-D confirmed the presence of pore forming activity. The reconstitution frequency of the protein samples was observed very less and only few insertion events could be measured to determine the channel conductance. In total twenty insertional events were measured. The most abundant channels showed the average conductance equal to 0.3 and 0.6 nS conductance in 1 M KCl electrolyte as shown in Figure 3-24. Some other channels were also observed corresponding to 0.1, 0.2 and 1 nS conductance values. The insertional events showing the single channel conductance values are compared with that of vector control in Fig 3-22. No significant difference was observed between the single channel conductance values of the AtPEX11-D membrane fraction and the empty vector control.

Since the AtPEX11-D membrane fraction showed the pore forming activity, the purified fraction obtained after Ni-NTA column chromatography were also analysed by planar lipid bilayer technique. The insertion activity of the channels in the bilayer membrane was very less but improved slightly comparing to that of AtPEX11-D membrane fraction. In total, twenty nine insertional events were measured with the most abundant channels corresponding to 0.3 nS single channel conductance in 1M KCl electrolyte. The channels of 0.1 nS conductance were also appeared in significant amount.

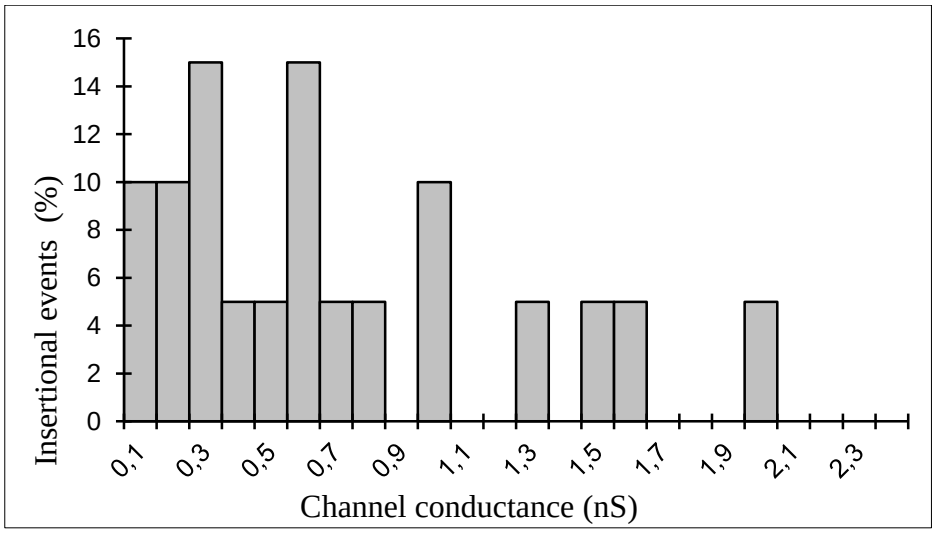

Figure 3-24: Porin activity in membrane fraction of AtPEX11-D

Histogram showing the percentage abundance of different single channel conductance measurement observed using AtPEX11-D membrane fraction (MF) overexpressed in *Pichia*. Protein samples were solubilized with Genapol (1:1, w/v). The majority of channels displayed an average single channel conductance equal to 0.3, 0.6 nS in aqueous phase containing 1 M KCl and at membrane potential of 20 mV. The recordings were done at room temperature. Total 20 insertional events were measured using separate bilayer each time.

The comparison between the single channel conductance measurements of AtPEX11-D and empty vector control showed the significant increase in the percentage abundance of channels corresponding to 0.3 nS as shown in Figure 3-25. The increment of more than 1 fold abundance corresponding to the single channel conductance of 0.3 nS in the purified AtPEX11-D protein samples suggest the possibility that the peroxisomal membrane protein AtPEX11-D act as an ion channel and is perhaps responsible for the 0.3 nS channel activity reported in plant peroxisomes isolated from spinach (Reumann *et al.*, 1995).

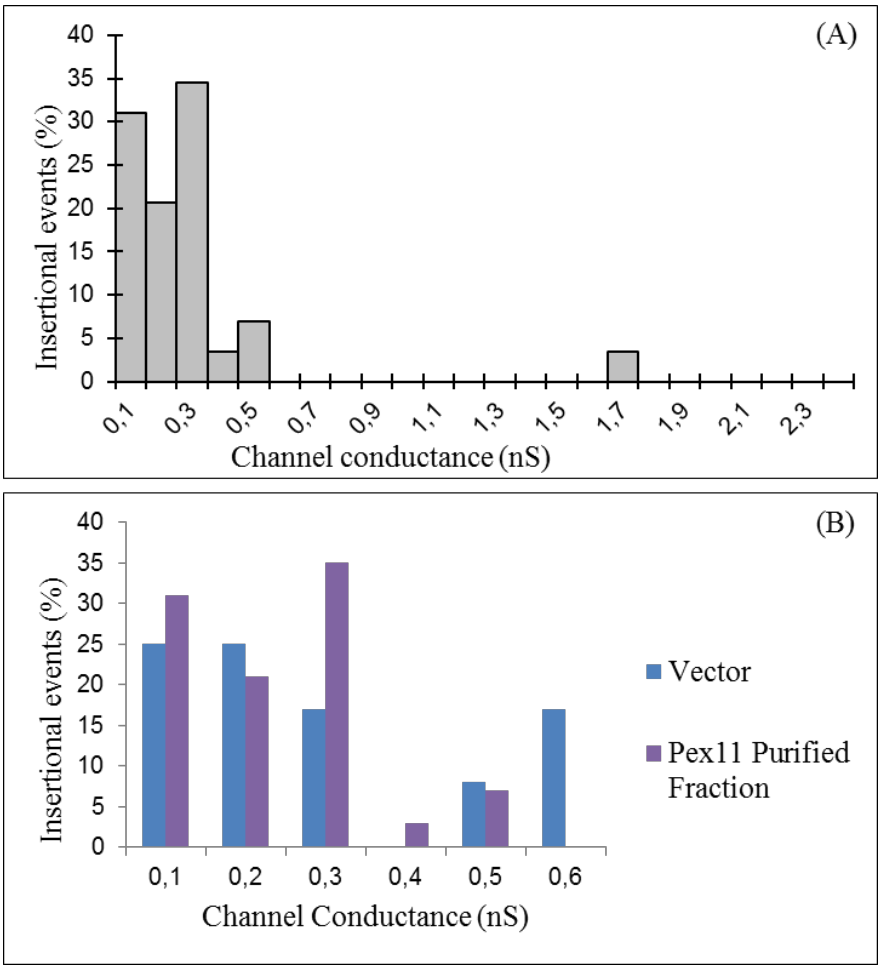

Figure 3-25: Porin activity in purified fraction of AtPEX11-D

Histogram showing the percentage abundance of different single channel conductance measurement observed using purified fraction of AtPEX11-D overexpressed in *Pichia*. Protein samples were solubilized with Genapol (1:1, w/v). The majority of channels displayed average single channel conductance equal to 0.3 nS in aqueous phase containing 1 M KCl. The applied membrane potential was 20 mV and the recordings were done at room temperature. Total 29 insertional events were measured using separate bilayer each time.

The initial results with the purified fractions of AtPMP22 and AtPEX11-D suggest the pore forming activity in the recombinant

protein samples. These finding may improve our current understanding of the presence of ion channels in plant peroxisomes.

Further experiments are required to be done using more purified protein fractions and measuring larger number of insertional events before concluding anything about the kind of ion channels produced by these membrane proteins and to determine the molecular basis of the pore forming activity observed in plant peroxisomes. The additional experiments comprising the ion selectivity determination and the binding assays will be critical to characterize the predicted channels in greater detail.

4. Conclusions and Future Perspectives

Proteome analysis of leaf peroxisomes and evolution of peroxisomal targeting signals

In the present study the several novel peroxisomal proteins have been identified with the help of both prediction and experimental methods. The proteome analysis of the spinach leaf peroxisomes has revealed many unique peroxisomal proteins which were not reported previously. The peroxisomal localization of AAE14 and NS lead to the identification of a new function of plant peroxisomes, in the phylloquinone biosynthesis pathway which was earlier considered to be localized exclusively in chloroplasts. The *in vivo* subcellular localization analysis of the protein sequences from both lower photosynthetic and higher plant orthologs suggested the transition of targeting signals during the course of evolution. Several proteins were identified showing the shift in targeting signal affinity from PTS2 in lower plants to PTS1 in higher plant orthologs. The results also suggest that the climax of evolution in targeting signals of plant peroxisomes may not lead to only PTS1 containing proteins as observed in nematod *C.elegans* and diatom *P.tricornutum* but instead may prefer both the targeting signals either on same protein or on two different proteins which interact with each other. This study involving the evolutionary aspects of targeting signals will assist in better understanding of peroxisomal biology.

Electrophysiological characterization of Arabidopsis leaf peroxisomes and recombinant AtPMP22 and AtPEX11-D proteins

In this thesis, the pore forming activity was demonstrated using leaf peroxisomes of Arabidopsis plants. The planar lipid bilayer analysis of the peroxisome membrane fractions revealed a unique channel with

average single channel conductance of 0.5 nS in 1 M KCl. The channel selectivity towards anions was demonstrated. The initial binding assays predict the substrate specificity of the channel towards carboxylic acid residues. More detailed study by conducting binding assays using different types of metabolic intermediates will be crucial to understand the channel properties in more detail. Like leaf peroxisomes from Arabidopsis, the pore forming activity was also observed in the purified fractions of the Arabidopsis peroxisome membrane proteins AtPMP22 and AtPEX11-D. The single channel conductance measurements suggest the porin like channels of 0.1 nS and 0.3 nS in AtPMP22 and AtPEX11-D respectively. The further electrophysiological characterization of these membrane proteins will be very critical to identify the molecular basis of the channel activity of plant peroxisomes and improve our current knowledge of metabolite-transfer across peroxisomes.

5. References

Agne, B., Meindl, N.M., Niederhoff, K., Einwachter, H., Rehling, P., Sickmann, A., Meyer, H.E., Girzalsky, W., and Kunau, W.H. (2003). Pex8p: an intraperoxisomal organizer of the peroxisomal import machinery. Mol Cell **11,** 635-646.

Akada, R., Murakane, T., and Nishizawa, Y. (2000). DNA extraction method for screening yeast clones by PCR. BioTechniques **28,** 668–670. 672, 674.

Almagro, L., Gómez Ros, L.V., Belchi-Navarro, S., Bru, R., Ros Barceló, A., and Pedreño, M.A. (2009). Class III peroxidases in plant defence reactions. J Exp Bot. **60,** 377-390.

Antonenkov, V.D., and Hiltunen, J.K. (2006). Peroxisomal membrane permeability and solute transfer. Biochim Biophys Acta **1763,** 1697-1706.

Antonenkov, V.D., and Hiltunen, J.K. (2012). Transfer of metabolites across the peroxisomal membrane. Biochim Biophys Acta.

Antonenkov, V.D., Rokka, A., Sormunen, R.T., Benz, R., and Hiltunen, J.K. (2005). Solute traffic across mammalian peroxisomal membrane--single channel conductance monitoring reveals pore-forming activities in peroxisomes. Cell Mol Life Sci **62,** 2886-2895.

Antonenkov, V.D., Mindthoff, S., Grunau, S., Erdmann, R., and Hiltunen, J.K. (2009). An involvement of yeast peroxisomal channels in transmembrane transfer of glyoxylate cycle intermediates. Int J Biochem Cell Biol **41,** 2546-2554.

Ashmarina, L.I., Pshezhetsky, A.V., Branda, S.S., Isaya, G., and Mitchell, G.A. (1999). 3-Hydroxy-3-methylglutaryl coenzyme A lyase: targeting and processing in peroxisomes and mitochondria. J Lipid Res **40,** 70-75.

Aung, K., and Hu, J. (2011). The Arabidopsis tail-anchored protein PEROXISOMAL AND MITOCHONDRIAL DIVISION FACTOR1 is involved in the morphogenesis and proliferation of peroxisomes and mitochondria. Plant Cell **23,** 4446-4461.

Babujee, L., Wurtz, V., Ma, C., Lueder, F., Soni, P., van Dorsselaer, A., and Reumann, S. (2010). The proteome map of spinach leaf peroxisomes

References

indicates partial compartmentalization of phylloquinone (vitamin K1) biosynthesis in plant peroxisomes. J Exp Bot **61,** 1441-1453.

Baron, M., Reynes, J.P., Stassi, D., and Tiraby, G. (1992). A Selectable Bifunctional β-Galactosidase: Phleomycin-resistance Fusion Protein as a Potential Marker for Eukaryotic Cells. Gene **114,** 239-243.

Bartoszewska, M., Opalinski, L., Veenhuis, M., and van der Klei, I.J. (2011). The significance of peroxisomes in secondary metabolite biosynthesis in filamentous fungi. Biotechnol Lett **33,** 1921-1931.

Bauwe, H., Hagemann , M., and Fernie, A.R. (2010). Photorespiration: players, partners and origin. Trends in Plant Science **15,** 330-336.

Behrends, W., Engeland, K., and Kindl, H. (1988). Characterization of two forms of the multifunctional protein acting in fatty acid beta-oxidation. Arch Biochem Biophys **263,** 161-169.

Benz, R., Janko, K., Boos, W., and Läuger, P., (1978). Formation of large, ion-permeable membrane channels by the matrix protein (porin) of *Escherichia coli.* Biochim Biophys Acta **511,** 305-319.

Benz, R., and Hancock, R. E. W. (1987) Mechanism of ion transport through the anion-selective channel of the *Pseudomonas aeruginosa* outer membrane. J Gen Physiol **89**, 275-295.

Benz, R., Schmid, A., and Vos-Scheperkeuter, G. H. (1987). Mechanism of sugar transport through the sugar-specific LamB channel of *E. coli* outer membrane. J Membr Biol **100**, 21-29.

Bradford, M.M. (1976). A rapid and sensitive method for the quantitation of microgram quantities of protein utilizing the principle of protein–dye binding. Analytical Biochemistry **72,** 248–254.

Chang, C.C., Warren, D.S., Sacksteder, K.A., and Gould, S.J. (1999). PEX12 interacts with PEX5 and PEX10 and acts downstream of receptor docking in peroxisomal matrix protein import. J Cell Biol **147,** 761-774.

Chang, J., Fagarasanu, A., and Rachubinski, R.A. (2007). Peroxisomal peripheral membrane protein YlInp1p is required for peroxisome inheritance and influences the dimorphic transition in the yeast Yarrowia lipolytica. Eukaryot Cell **6,** 1528-1537.

Chang, J., Mast, F.D., Fagarasanu, A., Rachubinski, D.A., Eitzen, G.A., Dacks, J.B., and Rachubinski, R.A. (2009). Pex3 peroxisome biogenesis proteins function in peroxisome inheritance as class V myosin receptors. J Cell Biol **187,** 233-246.

References

Clay, N.K., Adio, A.M., Denoux, C., Jander, G., and Ausubel, F.M. (2009). Glucosinolate metabolites required for an Arabidopsis innate immune response. Science **323,** 95-101.

Collins, C.S., Kalish, J.E., Morrell, J.C., McCaffery, J.M., and Gould, S.J. (2000). The peroxisome biogenesis factors pex4p, pex22p, pex1p, and pex6p act in the terminal steps of peroxisomal matrix protein import. Mol Cell Biol **20,** 7516-7526.

Dammai, V., and Subramani, S. (2001). The human peroxisomal targeting signal receptor, Pex5p, is translocated into the peroxisomal matrix and recycled to the cytosol. Cell **105,** 187-196.

Danpure, C.J. (2006). Primary hyperoxaluria type 1: AGT mistargeting highlights the fundamental differences between the peroxisomal and mitochondrial protein import pathways. Biochim Biophys Acta **1763,** 1776-1784.

De Duve, C., and Baudhuin, P. (1966). Peroxisomes (microbodies and related particles). Physiol Rev **46,** 323-357.

Del Rio, L.A. (2011). Peroxisomes as a cellular source of reactive nitrogen species signal molecules. Arch Biochem Biophys **506,** 1-11.

del Rio, L.A., Sandalio, L.M., Corpas, F.J., Palma, J.M., and Barroso, J.B. (2006). Reactive oxygen species and reactive nitrogen species in peroxisomes. Production, scavenging, and role in cell signaling. Plant Physiol **141,** 330-335.

Distel, B., Erdmann, R., Gould, S.J., Blobel, G., Crane, D.I., Cregg, J.M., Dodt, G., Fujiki, Y., Goodman, J.M., Just, W.W., Kiel, J.A., Kunau, W.H., Lazarow, P.B., Mannaerts, G.P., Moser, H.W., Osumi, T., Rachubinski, R.A., Roscher, A., Subramani, S., Tabak, H.F., Tsukamoto, T., Valle, D., van der Klei, I., van Veldhoven, P.P., and Veenhuis, M. (1996). A unified nomenclature for peroxisome biogenesis factors. J Cell Biol **135,** 1-3.

Egawa, K., Shibata, H., Yamashita, S., Yurimoto, H., Sakai, Y., and Kato, H. (2009). Overexpression and purification of rat peroxisomal membrane protein 22, PMP22, in Pichia pastoris. Protein Expr Purif **64,** 47-54.

Elgersma, Y., van Roermund, C.W., Wanders, R.J., and Tabak, H.F. (1995). Peroxisomal and mitochondrial carnitine acetyltransferases of Saccharomyces cerevisiae are encoded by a single gene. Embo J **14,** 3472-3479.

References

Ellis, S.B., Brust, P.F., Koutz, P.J., Waters, A.F., Harpold, M.M., and Gingeras, T.R. (1985). Isolation of Alcohol Oxidase and Two other Methanol Regulatable Genes from the Yeast, *Pichia pastoris*. Mol. Cell. Biol. **5,** 1111-1121.

Erdmann, R., and Schliebs, W. (2005). Peroxisomal matrix protein import: the transient pore model. Nat Rev Mol Cell Biol **6,** 738-742.

Fagarasanu, A., Fagarasanu, M., and Rachubinski, R.A. (2007). Maintaining peroxisome populations: a story of division and inheritance. Annu Rev Cell Dev Biol **23,** 321-344.

Fan, J., Quan, S., Orth, T., Awai, C., Chory, J., and Hu, J. (2005). The Arabidopsis PEX12 gene is required for peroxisome biogenesis and is essential for development. Plant Physiol **139,** 231-239.

Fang, Y., Morrell, J.C., Jones, J.M., and Gould, S.J. (2004). PEX3 functions as a PEX19 docking factor in the import of class I peroxisomal membrane proteins. J Cell Biol **164,** 863-875.

Fransen, M., Vastiau, I., Brees, C., Brys, V., Mannaerts, G.P., and Van Veldhoven, P.P. (2004). Potential role for Pex19p in assembly of PTS-receptor docking complexes. J Biol Chem **279,** 12615-12624.

Fujiki, Y., Rachubinski, R.A., and Lazarow, P.B. (1984). Synthesis of a major integral membrane polypeptide of rat liver peroxisomes on free polysomes. Proc Natl Acad Sci U S A **81,** 7127-7131.

Fujiki, Y., Matsuzono, Y., Matsuzaki, T., and Fransen, M. (2006). Import of peroxisomal membrane proteins: the interplay of Pex3p- and Pex19p-mediated interactions. Biochim Biophys Acta **1763,** 1639-1646.

Fulda, M., Shockey, J., Werber, M., Wolter, F.P., and Heinz, E. (2002). Two long-chain acyl-CoA synthetases from Arabidopsis thaliana involved in peroxisomal fatty acid beta-oxidation. Plant J **32,** 93-103.

Fulda, M., Schnurr, J., Abbadi, A., Heinz, E., and Browse, J. (2004). Peroxisomal Acyl-CoA synthetase activity is essential for seedling development in Arabidopsis thaliana. Plant Cell **16,** 394-405.

Girzalsky, W., Saffian, D., and Erdmann, R. (2010). Peroxisomal protein translocation. Biochim Biophys Acta. **1803,** 724-731.

Goepfert, S., Hiltunen, J.K., and Poirier, Y. (2006). Identification and functional characterization of a monofunctional peroxisomal enoyl-CoA hydratase 2 that participates in the degradation of even cis-unsaturated fatty acids in Arabidopsis thaliana. J Biol Chem **281,** 35894-35903.

References

Goepfert, S., Vidoudez, C., Rezzonico, E., Hiltunen, J.K., and Poirier, Y. (2005). Molecular identification and characterization of the Arabidopsis delta(3,5),delta(2,4)-dienoyl-coenzyme A isomerase, a peroxisomal enzyme participating in the beta-oxidation cycle of unsaturated fatty acids. Plant Physiol **138,** 1947-1956.

Gonzalez, N.H., Felsner, G., Schramm, F.D., Klingl, A., Maier, U.G., and Bolte, K. (2012). A single peroxisomal targeting signal mediates matrix protein import in diatoms. PLoS One **6,** e25316.

Gould, S.G., Keller, G.A., and Subramani, S. (1987). Identification of a peroxisomal targeting signal at the carboxy terminus of firefly luciferase. J Cell Biol **105,** 2923-2931.

Gould, S.J., Keller, G.A., and Subramani, S. (1988). Identification of peroxisomal targeting signals located at the carboxy terminus of four peroxisomal proteins. J Cell Biol **107,** 897-905.

Gould, S.J., Keller, G.A., Hosken, N., Wilkinson, J., and Subramani, S. (1989). A conserved tripeptide sorts proteins to peroxisomes. J Cell Biol **108,** 1657-1664.

Graham, I.A. (2008). Seed storage oil mobilization. Annu Rev Plant Biol **59,** 115-142.

Grunau, S., Mindthoff, S., Rottensteiner, H., Sormunen, R.T., Hiltunen, J.K., Erdmann, R., and Antonenkov, V.D. (2009). Channel-forming activities of peroxisomal membrane proteins from the yeast Saccharomyces cerevisiae. Febs J **276,** 1698-1708.

Gualdron-López, M., Vapola, M.H., Miinalainen, I.J., Hiltunen, J.K., Michels, P.A., and Antonenkov, V.D. (2012). Channel-Forming Activities in the Glycosomal Fraction from the Bloodstream Form of Trypanosoma brucei. PLoS One. **7,** e34530.

Halbach, A., Rucktaschel, R., Rottensteiner, H., and Erdmann, R. (2009). The N-domain of Pex22p can functionally replace the Pex3p N-domain in targeting and peroxisome formation. J Biol Chem **284,** 3906-3916.

Heupel, R., and Heldt, H.W. (1994). Protein organization in the matrix of leaf peroxisomes. A multi-enzyme complex involved in photorespiratory metabolism. Eur J Biochem **220,** 165-172.

Heupel, R., Markgraf, T., Robinson, D.G., and Heldt, H.W. (1991). Compartmentation studies on spinach leaf peroxisomes : evidence for

References

channeling of photorespiratory metabolites in peroxisomes devoid of intact boundary membrane. Plant Physiol **96,** 971-979.

Hiruma, K., Nishiuchi, T., Kato, T., Bednarek, P., Okuno, T., Schulz-Lefert, P., and Takano, Y. (2011). Arabidopsis ENHANCED DISEASE RESISTANCE 1 is required for pathogen-induced expression of plant defensins in nonhost resistance, and acts through interference of MYC2-mediated repressor function. The Plant Journal **67,** 980-992.

Hoagland, D., and Arnon, D. (1950). The water culture method for growing plants without soil. California Agric. Exp. Sta. Circ. **347,** 1-32.

Hoepfner, D., Schildknegt, D., Braakman, I., Philippsen, P., and Tabak, H.F. (2005). Contribution of the endoplasmic reticulum to peroxisome formation. Cell **122,** 85-95.

Hu, J., Baker, A., Bartel, B., Linka, N., Mullen, R.T., Reumann, S., and Zolman, B.K. (2012). Plant peroxisomes: biogenesis and function. Plant Cell **24,** 2279-2303.

Jedd, G., and Chua, N.H. (2000). A new self-assembled peroxisomal vesicle required for efficient resealing of the plasma membrane. Nat Cell Biol **2,** 226-231.

Jones, J.M., Morrell, J.C., and Gould, S.J. (2004). PEX19 is a predominantly cytosolic chaperone and import receptor for class 1 peroxisomal membrane proteins. J Cell Biol **164,** 57-67.

Kamigaki, A., Mano, S., Terauchi, K., Nishi, Y., Tachibe-Kinoshita, Y., Nito, K., Kondo, M., Hayashi, M., Nishimura, M., and Esaka, M. (2003). Identification of peroxisomal targeting signal of pumpkin catalase and the binding analysis with PTS1 receptor. Plant J **33,** 161-175.

Kaur, N., and Hu, J. (2009). Dynamics of peroxisome abundance: a tale of division and proliferation. Curr Opin Plant Biol **12,** 781-788.

Kaur, N., Reumann, S., and Hu, J. (2009). Peroxisome biogenesis and function. Arabidopsis Book **7,** e0123.

Kim, P.K., Mullen, R.T., Schumann, U., and Lippincott-Schwartz, J. (2006). The origin and maintenance of mammalian peroxisomes involves a de novo PEX16-dependent pathway from the ER. J Cell Biol **173,** 521-532.

Klein, A.T., van den Berg, M., Bottger, G., Tabak, H.F., and Distel, B. (2002). Saccharomyces cerevisiae acyl-CoA oxidase follows a novel, non-PTS1, import pathway into peroxisomes that is dependent on Pex5p. J Biol Chem **277,** 25011-25019.

References

Koh, S., Andre, A., Edwards, H., Ehrhardt, D., and Somerville, S. (2005). Arabidopsis thaliana subcellular responses to compatible Erysiphe cichoracearum infections. Plant J **44,** 516-529.

Koo, A.J., Chung, H.S., Kobayashi, Y., and Howe, G.A. (2006). Identification of a peroxisomal acyl-activating enzyme involved in the biosynthesis of jasmonic acid in Arabidopsis. J. Biol. Chem. **281,** 33511-33520.

Kragler, F., Lametschwandtner, G., Christmann, J., Hartig, A., and Harada, J.J. (1998). Identification and analysis of the plant peroxisomal targeting signal 1 receptor NtPEX5. Proc Natl Acad Sci U S A **95,** 13336-13341.

Kunau, W.H. (2001). Peroxisomes: the extended shuttle to the peroxisome matrix. Curr Biol **11,** R659-662.

Labarca, P., Wolff, D., Soto, U., Necochea, C., and Leighton, F. (1986). Large cation-selective pores from rat liver peroxisomal membranes incorporated to planar lipid bilayers. J Membr Biol **94,** 285-291.

Lanyon-Hogg, T., Warriner, S.L., and Baker, A. (2010). Getting a camel through the eye of a needle: the import of folded proteins by peroxisomes. Biol Cell **102,** 245-263.

Lazarow, P.B., and Fujiki, Y. (1985). Biogenesis of peroxisomes. Annu Rev Cell Biol **1,** 489-530.

Lingard, M.J., and Trelease, R.N. (2006). Five Arabidopsis peroxin 11 homologs individually promote peroxisome elongation, duplication or aggregation. J Cell Sci **119,** 1961-1972.

Linka, N., Theodoulou, F.L., Haslam, R.P., Linka, M., Napier, J.A., Neuhaus, H.E., and Weber, A.P. (2008). Peroxisomal ATP import is essential for seedling development in Arabidopsis thaliana. Plant Cell **20,** 3241-3257.

Lipka, V., Dittgen, J., Bednarek, P., Bhat, R., Wiermer, M., Stein, M., Landtag, J., Brandt, W., Rosahl, S., Scheel, D., Llorente, F., Molina, A., Parker, J., Somerville, S., and Schulze-Lefert, P. (2005). Pre- and postinvasion defenses both contribute to nonhost resistance in Arabidopsis. Science **310,** 1180-1183.

Lisenbee, C.S., Lingard, M.J., and Trelease, R.N. (2005). Arabidopsis peroxisomes possess functionally redundant membrane and matrix isoforms of monodehydroascorbate reductase. Plant J **43,** 900-914.

References

Ma, C., and Reumann, S. (2008). Improved prediction of peroxisomal PTS1 proteins from genome sequences based on experimental subcellular targeting analyses as exemplified for protein kinases from Arabidopsis. J Exp Bot **59,** 3767-3779.

Ma, C., Haslbeck, M., Babujee, L., Jahn, O., and Reumann, S. (2006). Identification and characterization of a stress-inducible and a constitutive small heat-shock protein targeted to the matrix of plant peroxisomes. Plant Physiol **141,** 47-60.

Marzioch, M., Erdmann, R., Veenhuis, M., and Kunau, W.H. (1994). PAS7 encodes a novel yeast member of the WD-40 protein family essential for import of 3-oxoacyl-CoA thiolase, a PTS2-containing protein, into peroxisomes. Embo J **13,** 4908-4918.

Matre, P., Meyer, C., and Lillo, C. (2009). Diversity in subcellular targeting of the PP2A B'eta subfamily members. Planta **230,** 935-945.

Maurino, V.G. and Peterhansel, C. (2010). Photorespiration: current status and approaches for metabolic engineering. Current Opinion in Plant Biology **13,** 249-256.

Motley, A.M., and Hettema, E.H. (2007). Yeast peroxisomes multiply by growth and division. J Cell Biol **178,** 399-410.

Motley, A.M., Hettema, E.H., Ketting, R., Plasterk, R., and Tabak, H.F. (2000). Caenorhabditis elegans has a single pathway to target matrix proteins to peroxisomes. EMBO Rep **1,** 40-46.

Mullen, R.T., and Trelease, R.N. (2006). The ER-peroxisome connection in plants: development of the "ER semi-autonomous peroxisome maturation and replication" model for plant peroxisome biogenesis. Biochim Biophys Acta **1763,** 1655-1668.

Murphy, M.A., Phillipson, B.A., Baker, A., and Mullen, R.T. (2003). Characterization of the targeting signal of the Arabidopsis 22-kD integral peroxisomal membrane protein. Plant Physiol **133,** 813-828.

Nguyen, S.D., Baes, M., and Van Veldhoven, P.P. (2008). Degradation of very long chain dicarboxylic polyunsaturated fatty acids in mouse hepatocytes, a peroxisomal process. Biochim Biophys Acta **1781,** 400-405.

Olivier, L.M., Kovacs, W., Masuda, K., Keller, G.A., and Krisans, S.K. (2000). Identification of peroxisomal targeting signals in cholesterol biosynthetic enzymes. AA-CoA thiolase, hmg-coa synthase, MPPD, and FPP synthase. J Lipid Res **41,** 1921-1935.

References

Opperdoes, F.R. (1987). Compartmentation of Carbohydrate Metabolism in Trypanosomes. Annual Review of Microbiology **41,** 127-151.

Orth, T., Reumann, S., Zhang, X., Fan, J., Wenzel, D., Quan, S., and Hu, J. (2007). The PEROXIN11 protein family controls peroxisome proliferation in Arabidopsis. Plant Cell **19,** 333-350.

Oshima, Y., Kamigaki, A., Nakamori, C., Mano, S., Hayashi, M., Nishimura, M., and Esaka, M. (2008). Plant catalase is imported into peroxisomes by Pex5p but is distinct from typical PTS1 import. Plant Cell Physiol **49,** 671-677.

Perry, R.J., Mast, F.D., and Rachubinski, R.A. (2009). Endoplasmic reticulum-associated secretory proteins Sec20p, Sec39p, and Dsl1p are involved in peroxisome biogenesis. Eukaryot Cell **8,** 830-843.

Purdue, P.E., and Lazarow, P.B. (2001). Peroxisome biogenesis. Annu Rev Cell Dev Biol **17,** 701-752.

Reumann, S., Maier, E., Benz, R., and Heldt, H.W. (1995). The membrane of leaf peroxisomes contains a porin-like channel. J Biol Chem **270,** 17559-17565.

Reumann, S., Bettermann, M., Benz, R., and Heldt, H.W. (1997). Evidence for the Presence of a Porin in the Membrane of Glyoxysomes of Castor Bean. Plant Physiol **115,** 891-899.

Reumann, S., Maier, E., Heldt, H.W., and Benz, R. (1998). Permeability properties of the porin of spinach leaf peroxisomes. Eur J Biochem **251,** 359-366.

Reumann, S., Babujee, L., Ma, C., Wienkoop, S., Siemsen, T., Antonicelli, G.E., Rasche, N., Luder, F., Weckwerth, W., and Jahn, O. (2007). Proteome analysis of Arabidopsis leaf peroxisomes reveals novel targeting peptides, metabolic pathways, and defense mechanisms. Plant Cell **19,** 3170-3193.

Rokka, A., Antonenkov, V.D., Soininen, R., Immonen, H.L., Pirila, P.L., Bergmann, U., Sormunen, R.T., Weckstrom, M., Benz, R., and Hiltunen, J.K. (2009). Pxmp2 is a channel-forming protein in Mammalian peroxisomal membrane. PLoS One **4,** e5090.

Rottensteiner, H., Kramer, A., Lorenzen, S., Stein, K., Landgraf, C., Volkmer-Engert, R., and Erdmann, R. (2004). Peroxisomal membrane proteins contain common Pex19p-binding sites that are an integral part of their targeting signals. Mol Biol Cell **15,** 3406-3417.

References

Rucktäschel, R., Girzalsky, W., and Erdmann, R. (2011). Protein import machineries of peroxisomes. Biochim Biophys Acta. **1808,** 892-900.

Sacksteder, K.A., Jones, J.M., South, S.T., Li, X., Liu, Y., and Gould, S.J. (2000). PEX19 binds multiple peroxisomal membrane proteins, is predominantly cytoplasmic, and is required for peroxisome membrane synthesis. J Cell Biol **148,** 931-944.

Schaller, F., Biesgen, C., Mussig, C., Altmann, T., and Weiler, E.W. (2000). 12-Oxophytodienoate reductase 3 (OPR3) is the isoenzyme involved in jasmonate biosynthesis. Planta **210,** 979-984.

Schilmiller, A.L., Koo, A.J., and Howe, G.A. (2007). Functional diversification of acyl-coenzyme A oxidases in jasmonic acid biosynthesis and action. Plant Physiol. **143,** 812-824.

South, S.T., and Gould, S.J. (1999). Peroxisome synthesis in the absence of preexisting peroxisomes. J Cell Biol **144,** 255-266.

Sparkes, I.A., Hawes, C., and Baker, A. (2005). AtPEX2 and AtPEX10 are targeted to peroxisomes independently of known endoplasmic reticulum trafficking routes. Plant Physiol **139,** 690-700.

Strader, L.C., Wheeler, D.L., Christensen, S.E., Berens, J.C., Cohen, J.D., Rampey, R.A., and Bartel, B. (2011). Multiple facets of Arabidopsis seedling development require indole-3-butyric acidderived auxin. Plant Cell **23,** 984–999.

Subramani, S. (1993). Protein import into peroxisomes and biogenesis of the organelle. Annu Rev Cell Biol **9,** 445-478.

Sulter, G.J., Verheyden, K., Mannaerts, G., Harder, W., and Veenhuis, M. (1993). The in vitro permeability of yeast peroxisomal membranes is caused by a 31 kDa integral membrane protein. Yeast **9,** 733-742.

Taler, D., Galperin, M., Benjamin, I., Cohen, Y., and Kenigsbuch, D. (2004). Plant eR genes that encode photorespiratory enzymes confer resistance against disease. Plant Cell **16,** 172-184.

Tanaka, A., and Ueda, M. (2000). Sorting of peroxisomal and mitochondrial carnitine acetyltransferase isozymes in the diploid yeast, Candida tropicalis. Cell Biochem Biophys **32,** 139-146.

Theodoulou, F.L., Job, K., Slocombe, S.P., Footitt, S., Holdsworth, M., Baker, A., Larson, T.R., and Graham, I.A. (2005). Jasmonic acid levels are reduced in COMATOSE ATP-binding cassette transporter mutants.

Implications for transport of jasmonate precursors into peroxisomes. Plant Physiol. **137,** 835-840.

Till, A., Lakhani, R., Burnett, S.F., and Subramani, S. (2012). Pexophagy: the selective degradation of peroxisomes. Int J Cell Biol.

Tugal, H.B., Pool, M., and Baker, A. (1999). Arabidopsis 22-kilodalton peroxisomal membrane protein. Nucleotide sequence analysis and biochemical characterization. Plant Physiol **120,** 309-320.

Van Ael, E., and Fransen, M. (2006). Targeting signals in peroxisomal membrane proteins. Biochim Biophys Acta **1763,** 1629-1638.

van der Klei, I.J., Yurimoto, H., Sakai, Y., and Veenhuis, M. (2006). The significance of peroxisomes in methanol metabolism in methylotrophic yeast. Biochim Biophys Acta **1763,** 1453-1462.

van der Zand, A., Braakman, I., and Tabak, H.F. (2010). Peroxisomal membrane proteins insert into the endoplasmic reticulum. Mol Biol Cell **21,** 2057-2065.

van Roermund, C.W., Tabak, H.F., van Den Berg, M., Wanders, R.J., and Hettema, E.H. (2000). Pex11p plays a primary role in medium-chain fatty acid oxidation, a process that affects peroxisome number and size in Saccharomyces cerevisiae. J Cell Biol **150,** 489-498.

Wanders, R.J., Ferdinandusse, S., Brites, P., and Kemp, S. (2010). Peroxisomes, lipid metabolism and lipotoxicity. Biochim Biophys Acta **1801,** 272-280.

Wessel, D., and Flügge, U.I. (1984). A method for the quantitative recovery of protein in dilute solution in the presence of detergents and lipids. Anal Biochem. **138,** 141-143.

Yamaguchi, K., Mori, H., and Nishimura, M. (1995). A novel isoenzyme of ascorbate peroxidase localized on glyoxysomal and leaf peroxisomal membranes in pumpkin. Plant Cell Physiol. **36,** 1157-1162.

Yan, M., Rayapuram, N., and Subramani, S. (2005). The control of peroxisome number and size during division and proliferation. Curr Opin Cell Biol **17,** 376-383.

Yang, X., Purdue, P.E., and Lazarow, P.B. (2001). Eci1p uses a PTS1 to enter peroxisomes: either its own or that of a partner, Dci1p. Eur J Cell Biol **80,** 126-138.

Zolman, B.K., Silva, I.D., and Bartel, B. (2001). The Arabidopsis pxa1 mutant is defective in an ATP-binding cassette transporter-like protein

References

required for peroxisomal fatty acid beta-oxidation. Plant Physiol **127,** 1266-1278.

Zolman, B.K., Nyberg, M., and Bartel, B. (2007). IBR3, a novel peroxisomal acyl-CoA dehydrogenase-like protein required for indole-3-butyric acid response. Plant Mol Biol **64,** 59-72.

Zolman, B.K., Monroe-Augustus, M., Silva, I.D., and Bartel, B. (2005). Identification and functional characterization of Arabidopsis PEROXIN4 and the interacting protein PEROXIN22. Plant Cell **17,** 3422-3435.

Zolman, B.K., Martinez, N., Millius, A., Adham, A.R., and Bartel, B. (2008). Identification and characterization of Arabidopsis indole-3-butyric acid response mutants defective in novel peroxisomal enzymes. Genetics **180,** 237-251.

6. Appendix

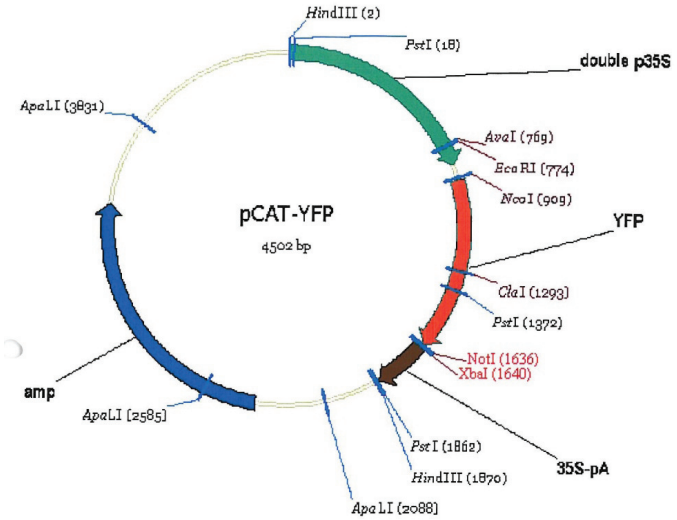

Figure 6-1: pCAT-YFP vector map

The vector contains EYFP as a reporter protein which is under the control of a double 35S CaMV promoter. The plasmid has been used to clone genes in both front and back of EYFP to study their transient expression in onion epidermal cells and to validate the targeting signals *in vivo* by subcellular localization analysis using fluorescence microscope.

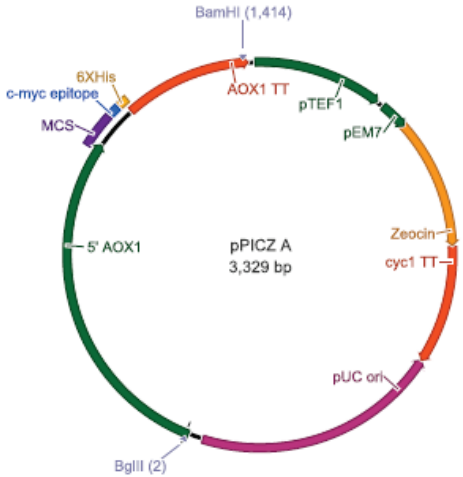

Figure 6-2: pPICZ A vector map

pPICZ A is a 3.3 kb expression vector (Invitrogen ™) used in cloning genes which are required to be expressed in *Pichia pastoris*. The Recombinant proteins are expressed as fusions to a C-terminal peptide containing the *c-myc* epitope and/or a polyhistidine tag. The vector carries a inducible AOX1 promoter for high-level expression in Pichia pastoris, AOX1 transcription termination sequence for efficient polyadenylation and 3' transcript processing. The Zeocin resistance gene is driven by the EM7 promoter for selection in *E.coli* and the TEF1 promoter for selection in *Pichia pastoris.*

Table 6-1: List of oligonucleotide primers used for gene-cloning

Primer	Construct name	Template vector	Destination vector	Primer sequence (5'to 3')	R.E.
PS1f	EYFP with NcoI and SacII	pCAT-EYFP-CKI	pCAT-SKL137	CACCATGGCAGCCGCGGCAATGGTGA GCAAGGGCGAGGAG	NcoI, SacII
PS2f	DECR with NcoI and SacI	DECR cDNA	pCAT-EYFP	CACCATGGGAGCTCTCATGGACTCTCC GTTCAAACC	NcoI SacI
PS3r	DECR with NotI and SacII	DECR cDNA	pCAT-EYFP	CTGCCGCGGCAGCGGCCGCCAGCTTGC TGGTTGGGAGACC	NotI, SacII
PS4f	PTS2 domain vector	pCAT-EYFP-CKI	pCAT-EYFP	CAGGAGCTCTCGATAACCGTCGTTTTC TCCATGTTGTCTACCGCGCCGCGGCAA TGGTGAGCAAG	SacI, SacII
PS7f	AT4G04470.1/ AtPMP22 for	pENTR223	pPICZ A	AGCTTCGAAATGGGCCATCATCATCAT CATCATCATCATCATCACATGGGATCT TCACCACCGAAG	SfuI
PS8r	AT4G04470.1/ AtPMP22 rev	pENTR223	pPICZ A	GCTGGGCCCTCACTTAGCCTTTGCCAA	ApaI

PS9f	AT2G45740.2/ AtPEX11-D for	pda04235/RIKEN	pPICZ A	GGC TTC GAA ATG GGC CAT CAT CAC CAC CAT CAC CAC CAT CAT CAC ATG GGG ACG ACG TTA GAT GTA	SfuI
PS10r	AT2G45740.2/ AtPEX11-D rev	pda04235/RIKEN	pPICZ A	GCT GGG CCC TCA GGG TGT TTT GAT CTT	ApaI
PS11f	AT4G14305.1/ PMP22Hom for	pda16488/RIKEN	pCAT-EYFP-Hin1R	AAG ACT GCG GCC GCT ATG TCG GAT CTT GCT AAA GAC	NotI
PS12r	AT4G14305.1/ PMP22Hom rev	pda16488/RIKEN	pCAT-EYFP-Hin1R	CAAGTCTAGAGCTACGCGTTTTTGATC ACCGG	XbaI
XC45f	SDM NS for	pCAT-NS	pCAT-EYFP	CGAGCCGACGACTCTCCGTCGTCACCA ACGTTCTCATCCCTATCGGATTCAGTCC AGC	AclI
XC46r	SDM NS rev	pCAT-NS	pCAT-EYFP	GCTGGACTGAATCCGATAGGGATGAGA ACGTTGGTGACGACGGAGAGTCGTCGG CTCG	AclI
GC21r	EYFP-Ct 10 aa-Mp LACS6/7	pCAT-EYFP-CKI	pCAT-SKL137	TATGTCTAGAGTCACCGCCCCGCGTTC AACTCGCGATACATTCTCTTGTACAGC TCGTCCATGCC	NcoI
GC22f	Nt 15 aa-	pCAT-PTD2-EYFP	pCAT-DECR	CA GGA GCT CTC TCC GCG CGT AGG	SacI

	Mp LACS6/7-EYFP			TTA GAC GTC CTC CGT GGG CAC GTC GTC AAC ACG GCC GCG GCA ATG GTG AGC AAG	
GC25r	EYFP-Ct 10 aa-Sm Acd 32.1	pCAT-EYFP-CKI	pCAT-SKL137	TATGTCTAGAGTCAAGACTTCGGAATG ATCACACGCAAAAACCCCTTGTACAGC TCGTCCATGCC	NcoI
GC26f	Nt 15 aa-Sm Acd 32.1-EYFP	pCAT-PTD2-EYFP	pCAT-DECR	CA GGA GCT CTC GCG CGC GCG AGG ATG TAT CAC CTG GCG TGC CAT CTC GAG GAC GGG GCC GCG GCA ATG GTG AGC AAG	SacI
GC33r	EYFP-Ct 10 aa-Ol CSY	pCAT-EYFP-CKI	pCAT-SKL137	TATGTCTAGAGTCATTTTCGTCCGAGAT AGTTCTCCACGCCGCTCTTGTACAGCTC GTCCATGCC	NcoI
GC34f	Nt 15 aa-Ol CSY-EYFP	pCAT-PTD2-EYFP	pCAT-DECR	CA GGA GCT CTC GCG AAT CGG CGG CTG GGA CAA ATC AAC GAT CAC GTC CGC GGC GAC GCC GCG GCA ATG GTG AGC AAG	SacI
GC37r	EYFP-Ct 10 aa-Pp ACX 3/6	pCAT-EYFP-CKI	pCAT-SKL137	TATGTCTAGAGTCACTGCACATTGCTC CAGGAGTTATATTCAACCTTGTACAGC TCGTCCATGCC	NcoI
GC38f	Nt 15 aa-	pCAT-PTD2-EYFP	pCAT-DECR	CA GGA GCT CTC GCA GCA CGG CGC	SacI

	Pp ACX 3/6-EYFP			GCT GGC GTC TTA GCC AGA CAC CTT GCG CAT GAAGCC GCG GCA ATG GTG AGC AAG	
GC43r	EYFP-Ct 10 aa-At PKT3	pCAT-EYFP-CKI	pCAT-SKL137	TATGTCTAGAGTCAGCGAGCGTCCTTG GACAAAAGACCTTGCGCCTTGTACAGC TCGTCCATGCC	NcoI
GC44r	EYFP-Ct 10 aa-At NS	pCAT-EYFP-CKI	pCAT-SKL137	TATGTCTAGAGTCAAGGTCGCCGGTGA AATTTAGAGAAGTCCGGCTTGTACAGC TCGTCCATGCC	NcoI
GC45f	Nt 50 aa-AtPfkB-EYFP	ABRC cDNA clone	pCAT-DECR-EYFP	TACACCATGGAACCGGTTATAATCGGT	NcoI
GC94r	Nt 50 aa-AtPfkB-EYFP	ABRC cDNA clone	pCAT-DECR-EYFP	GCTAGCGGCCGCTCCAAGCTTGAAGAT GCAATC	NotI

Journal of Experimental Botany, Page 1 of 13
doi:10.1093/jxb/erq014

RESEARCH PAPER

The proteome map of spinach leaf peroxisomes indicates partial compartmentalization of phylloquinone (vitamin K1) biosynthesis in plant peroxisomes

Lavanya Babujee[1,†], Virginie Wurtz[2], Changle Ma[1,‡], Franziska Lueder[1,§], Pradeep Soni[3], Alain van Dorsselaer[2] and Sigrun Reumann[1,3,*]

[1] Georg-August-University of Goettingen, Albrecht-von-Haller-Institute for Plant Sciences, Department of Plant Biochemistry, Justus-von-Liebig-Weg 11, D-37077 Goettingen, Germany
[2] Laboratoire de Spectrométrie de Masse Bio-Organique, ECPM, UMR/CNRS 7178, Institut Pluridisciplinaire Hubert CURIEN, Universite Louis Pasteur Strasbourg, France
[3] Centre for Organelle Research, Faculty of Science and Technology, University of Stavanger, N-4036 Stavanger, Norway

[†] Present address: Department of Plant Pathology, University of Wisconsin, Madison, WI, USA.
[‡] Present address: Section of Molecular Biology, Division of Biological Sciences, University of California, San Diego, La Jolla, CA, USA.
[§] Present address: Department of Biochemistry and Molecular Biology, Bio21 Molecular Science and Biotechnology Institute, University of Melbourne, 30 Flemington Road Parkville, Victoria 3010, Australia.
* To whom correspondence should be addressed. E-mail: sigrun.reumann@uis.no

Received 24 September 2009; Revised 16 December 2009; Accepted 14 January 2010

Abstract

Leaf peroxisomes are fragile, low-abundance plant cell organelles that are difficult to isolate from one of the few plant species whose nuclear genome has been sequenced. Leaf peroxisomes were enriched at high purity from spinach (*Spinacia oleracea*) and ~100 protein spots identified from 2-dimensional gels by a combination of liquid chromatography–tandem mass spectrometry (LC-MS/MS) and *de novo* sequencing. In addition to the predominant enzymes involved in photorespiration and detoxification, several minor enzymes were detected, underscoring the high sensitivity of the protein identification. The tryptic peptides of three unknown proteins shared high sequence similarity with *Arabidopsis* proteins that carry putative peroxisomal targeting signals type 1 or 2 (PTS1/2). The apparent *Arabidopsis* orthologues are a short-chain alcohol dehydrogenase (SDRa/IBR1, At4g05530, SRL>) and two enoyl-CoA hydratases/isomerases (ECHIa, At4g16210, SKL>; NS/ECHId, At1g60550, RLx$_5$HL). The peroxisomal localization of the three proteins was confirmed *in vivo* by tagging with enhanced yellow fluorescent protein (EYFP), and the targeting signals were identified. The single *Arabidopsis* isoform of naphthoate synthase (NS) is orthologous to MenB from cyanobacteria, which catalyses an essential reaction in phylloquinone biosynthesis, a pathway previously assumed to be entirely compartmentalized in plastids in higher plants. In an extension of a previous study, the present *in vivo* targeting data furthermore demonstrate that the enzyme upstream of NS, chloroplastic acyl-CoA activating enzyme isoform 14 (AAE14, SSL>), is dually targeted to both plastids and peroxisomes. This proteomic study, extended by *in vivo* subcellular localization analyses, indicates a novel function for plant peroxisomes in phylloquinone biosynthesis.

Key words: Acyl-activating enzyme, enoyl-CoA hydratase/isomerase, mass spectrometry, phylloquinone, proteome analysis, short-chain dehydrogenase, subcellular targeting.

Abbreviations: AAE14, acyl-CoA activating enzyme isoform 14; ASB-14, amidosulphobetaine-14; CaMV, cauliflower mosaic virus; CAT, catalase; CFP, cyan fluorescent protein; CHAPS, (3-[(3-cholamidopropyl)-dimethyalmino]-propanesulphate); CHY1, hydroxyisobutyryl-CoA hydrolase 1; 2-DE, 2-dimensional gel electrophoresis; DHNA-CoA, 1,4-dihydroxy-2- naphthoyl-CoA; DTT, dithiothreitol; ECHI, enoyl-CoA hydratase/isomerase; EST, expressed sequence tag; EYFP, enhanced yellow fluorescent protein; GFP, green fluorescent protein; IEF, isoelectric focusing; IEP, isoelectric point; LC-MS/MS, liquid chromatography–tandem mass spectrometry; MALDI, matrix-assisted laser desorption/ionization; MFP, multifunctional protein; MS, mass spectrometry; NS, naphthoate synthase; PMF, peptide mass fingerprinting; PTD, peroxisome targeting domain; PTS1/2, peroxisomal targeting signal type 1/2; RFP, red fluorescent protein; ROS, reactive oxygen species; SDR, short-chain dehydrogenase/reductase; YFP, yellow fluorescent protein.

Introduction

Technical advances in 2-dimensional gel electrophoresis (2-DE), mass spectrometry, and shotgun proteomics laid the foundation for the first plant organellar proteome studies (Peltier *et al.*, 2000; Kruft *et al.*, 2001; Millar *et al.*, 2001). The proteome in its entirety is the expressed complement of the genome and varies with tissue and organ, the developmental stage, and biotic and abiotic factors. Proteomics technology is, for instance, able to identify novel organellar proteins, characterize protein complexes, and detect post-translational protein modifications on a large scale, which is hardly possible with other methods. The bottleneck of organellar proteomics, however, is the high enrichment of the desired cell compartment.

Peroxisomes are ubiquitous cell organelles that compartmentalize oxidative metabolic reactions by a single boundary membrane. A characteristic property of peroxisomes is their functional flexibility, as their protein content varies depending on the organism, the type of tissue, and the environmental conditions. Peroxisomes are often part of distinct metabolic networks that are spread over different subcellular compartments, including the cytosol, mitochondria, and plastids in plants. For instance, the recycling of 2-phosphoglycolate during photorespiration involves the co-ordinated functioning of at least 11 chloroplastic, peroxisomal, and mitochondrial enzymes and 14–18 distinct transmembrane transport steps for intermediate transfer between cell compartments (Reumann and Weber, 2006). Hydrogen peroxide produced by peroxisomal oxidases, as well as other reactive oxygen species (ROS), can be immediately degraded by catalase (CAT) and other peroxisomal antioxidative enzymes (del Rio *et al.*, 2002).

Intensive research during recent years using complementary approaches, including forward and reverse genetics, has revealed an unexpected metabolic complexity of plant peroxisomes. For instance, plant peroxisomes play a physiological role in the biosynthesis of the signalling molecule jasmonic acid, β-oxidation of indole butyric acid (IBA), and sulphur and polyamine metabolism (for a review, see Kaur *et al.*, 2009). Moreover, evidence is emerging from recent studies that peroxisomes have important functions in specific defence mechanisms, conferring resistance against pathogen attack (for a review, see Kaur *et al.*, 2009). Additional physiological functions of plant peroxisomes are probably as yet uncovered.

Given their fragility *in vitro*, their limited abundance under standard growth conditions, and their pronounced physical association with mitochondria and chloroplasts, proteomic studies of peroxisomes have been reported only in the past few years, for example in *Saccharomyces cerevisiae* (Schafer *et al.*, 2001; Marelli *et al.*, 2004), in mammals (Kikuchi *et al.*, 2004; Wiese *et al.*, 2007), and in plants (for a review, see Saleem *et al.*, 2006; Palma *et al.*, 2009). Proteomic analyses of plant peroxisomes are made difficult by the fact that the genomes of only a few plant species have been sequenced to date, none of which represents established model organisms for the isolation of leaf peroxisomes. Also, large expressed sequence tag (EST) sequencing projects have not been realized for plant species such as *Spinacia*, from which leaf peroxisomes can be enriched in high quality and considerable quantity (Yu and Huang, 1986; Lopez-Huertas *et al.*, 1995).

Complementarily or alternatively to experimental proteomic studies, peroxisomal matrix proteins can be predicted from genome sequences by taking advantage of the sequence conservation of matrix targeting signals (Emanuelsson *et al.*, 2003; Kamada *et al.*, 2003; Neuberger *et al.*, 2003; Reumann, 2004; Reumann *et al.*, 2004; Boden and Hawkins, 2005). Peroxisomal matrix proteins are synthesized on free ribosomes and generally targeted to the matrix by one of two conserved targeting sequences, namely the C-terminal peroxisomal targeting signal type 1 (PTS1) of the prototype SKL> (where > indicates the C-terminal end), or the cleavable PTS2 nonapeptide of the prototype RLx_5HL (Gould *et al.*, 1987; Swinkels *et al.*, 1991). When these conserved targeting peptides are applied to genomic screens, most known and many novel matrix proteins can be identified. The AraPerox database (www3.uis.no/AraPeroxV1/), for instance, currently lists ~400 candidate proteins that are potentially targeted to peroxisomes in *Arabidopsis thaliana* (Reumann *et al.*, 2004, 2007). However, because these PTS peptides and auxiliary or even essential targeting elements surrounding the small targeting peptides have not yet been precisely defined, peroxisomal targeting cannot be predicted with sufficient accuracy, reiterating the need for experimental approaches to reveal the proteome of peroxisomes.

In the present study, a previously utilized method to purify leaf peroxisomes from *Spinacia oleracea* L. was extended by the addition of a second density gradient to allow for proteomic analysis. *De novo* sequencing of three unknown proteins permitted the identification of the corresponding *Arabidopsis* homologues. The *Arabidopsis* cDNAs were cloned by reverse transcription-PCR (RT-PCR), and peroxisomal localization was verified for fusion proteins with enhanced yellow fluorescent protein (EYFP) by fluorescence microscopy in epidermal cells of *Allium cepa* L. The peroxisomal localization of naphthoate synthase (NS), which catalyses an essential step in phylloquinone biosynthesis, prompted the investigation of the subcellular targeting of the enzyme immediately upstream in this pathway, chloroplastic acyl-CoA activating enzyme isoform 14 (AAE14), in greater detail. Upon N-terminal fusion of the protein with EYFP, placing the predicted PTS1 of AAE14, SSL>, at the free C-terminus, the fusion protein indeed targeted plant peroxisomes. The data thus indicate that at least two reactions of phylloquinone biosynthesis have been transferred from chloroplasts to peroxisomes during the evolution of higher plants.

Materials and methods

Plant growth

Spinach plants (*S. oleracea* L., cv. Monopa) were grown hydroponically in nutrient solution under a light intensity of ~300–350 μmol

m^{-2} s^{-1} (9/15 h light/dark cycle, 21 °C/18 °C day/night temperature) for up to 8 or 12 weeks (Reumann *et al.*, 1994).

Isolation of leaf peroxisomes

The basic protocol described by Yu and Huang (1986) that involves a Percoll density gradient separation of sedimented leaf peroxisomes in 0.25 M sucrose was adapted for the large-scale isolation of leaf peroxisomes for preparative purposes (Reumann *et al.*, 1995). The stability and purity of leaf peroxisomes was further improved by the addition of protease inhibitors, by increasing the concentration of Percoll from 45% to 48% (v/v), and by the addition of a second density gradient. After Percoll density gradient centrifugation and washing, the peroxisome suspension was homogenized using a tight-fitting Potter–Elvehjem homogenizer, layered on a discontinuous sucrose density gradient [small layers of 2 ml each of 18, 25, and 35% (w/w) sucrose over a linear 40–50% (w/w) gradient on a 60% (w/w) sucrose cushion (all in 10 mM HEPES-NaOH pH 7.5, 1 mM EDTA)], and spun for 2 h at 83 000 *g* (SW 28 rotor, Beckman Coulter ultracentrifuge). The peroxisome band, visible as a yellowish-white layer, was harvested, supplemented with protease inhibitors, and frozen at –80 °C until use.

2-DE and SDS–PAGE

Protein content was estimated using bovine serum albumin (BSA) as standard (Lowry *et al.*, 1951; Bradford, 1976). Prior to 2-DE, proteins from peroxisomes were generally precipitated using methanol and chloroform (Wessel and Flugge, 1984). The proteins were solubilized for 2 h in 350 µl of immunoelectrofocusing (IEF) buffer [7 M urea, 2 M thiourea, 4% (w/v) CHAPS (3-[(3-cholamidopropyl)-dimethylamino]-propanrsulphate), 0.5% (v/v) IPG buffer, 3 mg ml^{-1} dithiothreitol (DTT), and trace amounts of bromophenol blue], and the solution was clarified by centrifugation (20 min, 20 000 *g*). Immobiline 18 cm pH gradient (IPG) strips were actively rehydrated with the protein solution, and IEF was carried out for 20 h for a total of 60 kVh (IPG Phor, APB, Sweden). The proteins were then reduced and alkylated by equilibration for 12 min each in buffers [6 M urea, 50 mM TRIS-HCl pH 8.8, 30% (v/v) glycerol, 2% (w/v) SDS, and 0.001% (w/v) bromophenol blue] containing either 10 mg ml^{-1} DTT or 25 mg ml^{-1} iodoacetamide, respectively. The equilibrated strips were positioned over vertical polyacrylamide gels of the desired concentration and sealed in place with 1% (w/v) agarose prepared in SDS running buffer for separation in the second dimension. Post-electrophoretic staining of the gels was carried out according to described protocols using colloidal Coomassie solution (Herbert *et al.*, 2001).

In-gel digestion for automated application

In-gel digestion with trypsin was performed according to published methods (Jeno *et al.*, 1995) modified for use with a robotic digestion system (MassPREP, Micromass, Manchester, UK). Each gel slice was decolourized by washing with 50 µl of 25 mM ammonium hydrogen carbonate followed by washing with 50 µl of acetonitrile. This step was repeated twice. The gel pieces were then dehydrated with acetonitrile and dried at 60 °C, prior to the addition of modified trypsin (Promega, Madison, WI, USA; 10 µl at a concentration of 12.5 ng μl^{-1} in 25 mM ammonium hydrogen carbonate). The digestion was performed at 37 °C overnight followed by extraction in 5 µl of 30% (v/v) water/65% (v/v) acetronitrile/5% (v/v) formic acid.

ZipTip® Pipette Tips (Millipore Corporation) were used for the rapid purification and concentration of peptides prior to mass spectrometry. The C18 columns (ZipTips) were pre-wetted by washing (3× 10 µl) with 10 µl of 50% (v/v) acetonitrile. The tips were equilibrated with 1% (v/v) formic acid (3× 10 µl). Next, 10 µl of 1% formic acid was added to the peptide extract. The peptides were bound to the equilibrated C18 column by drawing the sample slowly through it. The columns were washed with the loading solvent (3× 10 µl) to remove the non-peptide impurities. The desalted peptides were concentrated by eluting in 2–5 µl of 60% (v/v) acetonitrile/1% (v/v) formic acid.

Matrix-assisted laser desorption ionization mass spectrometry (MALDI-MS)

Mass measurements were carried out on a Biflex (Bruker, Wissenbourg, Germany) matrix-assisted laser desorption time-of-flight mass spectrometer (MALDI-TOF). A saturated solution of α-cyano-4-hydroxycinnamic acid in acetone was used as the matrix. The first layer of fine matrix crystals was obtained by spreading and fast evaporation of 0.5 µl of matrix solution. On this fine layer of crystals, a droplet of 0.5 µl of aqueous formic acid (5% v/v) was deposited. Afterwards, 0.5 µl of the peptide sample was added, and a second 0.25 µl droplet of saturated matrix solution (in 50% water/50% acetonitrile) was added. The preparation was dried under vacuum and washed in 1 µl of 5% (v/v) formic acid. All mass spectra were internally calibrated with trypsin autolysis peaks. The resulting peptide mass fingerprints (PMFs) were searched against a local copy of the non-redundant database SWISS-PROT (http://www.expasy.ch/sprot) using the MASCOT (Perkins *et al.*, 1999) search program. The parameters used in the search were as follows: peptide mass tolerance 50 ppm, one missed cleavage, carboxymethylated cysteine, methionine oxidation, and N-terminal acetylation.

Liquid chromatography–tandem mass spectrometry (LC-MS/MS)

Samples were injected into a CapLC System (Waters, Milford, MA, USA) equipped with an autosampler, gradient, and auxiliary pump. A volume of 6.4 µl was injected via 'microliter pickup' mode and desalted online through a 300 µm×5 mm C_{18} trapping cartridge (LC Packings, San Francisco, CA, USA). The samples were desalted at a high flow rate of 30 µl min^{-1} for 3 min. The peptides were separated on a 75 µm×15 cm, 3 µm particle size, 100 Å pore size C_{18} PepMap™ column (LC Packings, CA, USA) prior to introduction into the mass spectrometer. A typical reversed-phase was used from low to high organic over ~35 min. Mobile phase A was 0.1% formic acid, and B was 95% acetonitrile and 0.1% formic acid. The flow rate was 5 µl min^{-1}. The system utilized a split flow, resulting in a column flow rate of ~400–500 µl min^{-1}. MS/MS data were obtained using a Q-Tof 2 (Micromass) fitted with a Z-spray nanoflow electrospray ion source. The mass spectrometer was operated in positive ion mode with a potential of 3500 V applied to the nanoflow probe body. The collision energy was determined 'on the fly' based on the mass and charge state of peptide. Charge state recognition was used to switch into MS/MS mode only for double- and triple-charged ions. Several trypsin autolysis ions were excluded. The data were processed by Protein Lynx Version (Micromass) to generate searchable peak lists. Initial protein identifications were made by the correlation of uninterpreted tandem mass spectra to entries in SWISS-PROT using Global Server (Version 1.1, Micromass).

Gene cloning by RT-PCR and subcellular localization analysis in Allium cepa *L.*

Total RNA was isolated from different tissues of *A. thaliana* cv. Columbia using the Invisorb Spin Plant Mini Kit (Invitek GmbH, Berlin, Germany). Full-length cDNAs of a short-chain dehydrogenase/reductase (SDRa, At4g05530, 254 residues, SRL>) and two monofunctional enoyl-CoA hydratases/isomerases (ECHIa, At4g16210, 265 residues; SKL>, NS/ECHId, At1g60550, 337 residues, RLx_5HL) were isolated from RNA using appropriate oligonucleotide primers (Supplementary Table SII available at *JXB* online). Total RNA was converted to single-stranded cDNA by reverse transcriptase (Superscript II, Invitrogen, Karlsruhe,

Germany) and used as the template for PCR using a proofreading DNA polymerase (Thermozyme, Invitrogen, Karlsruhe, Germany). Amplification products were subcloned into pGEMT using the pGEM®-T Easy Vector System (Promega, Madison, WI, USA) and sequenced. Site-directed mutagenesis (PTS2 of NS, RLx_5HL to RLx_5VL) was performed using *Pfu*Ultra high-fidelity DNA polymerase for mutagenic primer-directed replication of both plasmid strands of NS-EYFP in the pCAT vector using the Quick-Change II site-directed mutagenesis kit (Stratagene; Supplementary Table SII). The cDNA of AAE14 was obtained from the Arabidopsis Biological Resource Center (ABRC, OH, USA). Gene-specific subcloning primers are listed in Supplementary Table SII.

To verify peroxisomal localization in plant cells, the cDNAs were subcloned into plant expression vectors (Supplementary Table SII). Those encoding proteins with predicted PTS1s (SDRa, SRL>; ECHIa, SKL>) were cloned in-frame with and downstream of the EYFP gene in the plant expression vector pCAT-YFP-C, whereas NS/ECHId carrying a predicted N-terminal PTS2 (RLx_5HL) was cloned in-frame with and upstream of EYFP in pCAT-YFP-Nfus. The expression of both fusion genes was under the control of a double 35S cauliflower mosaic virus (CaMV) promoter (Fulda *et al.*, 2002; Ma *et al.*, 2006). Onion epidermal cells were transformed by cell bombardment with gold particles coated with plasmid DNA, and the subcellular localization of the fusion proteins was analysed by fluorescence microscopy (Olympus BX51, SDRa, ECHIa, NS/ECHId, Ma *et al.*, 2006; Nikon TE-2000U, AAE14). In double-labelling experiments, a PTS2 sequence fused to cyan fluorescent protein (ECFP) was used as a peroxisomal marker (Fulda *et al.*, 2002; Ma *et al.*, 2006). For analysis of PTS2 proteins, another peroxisomal marker, red fluorescent protein (RFP)–SKL, was used (Matre *et al.*, 2009).

Results

Isolation of spinach leaf peroxisomes and protein identification

The bottleneck of organellar proteomics is generally the isolation of highly purified organelles from organisms with fully sequenced genomes. Different protocols have been established for the isolation of leaf peroxisomes from model plants of biochemical research. These methods, however, could not be transferred to *Arabidopsis*, probably due to high concentrations of secondary metabolites and a pronounced physical association of leaf peroxisomes with mitochondria and plastids in Brassicaceae. Investigations were therefore carried out to determine whether leaf peroxisomes can be isolated from *S. oleracea* L. at a sufficient purity for in-depth proteome analyses and whether sufficient sequence information can be obtained from representative tryptic peptides by LC-MS/MS and *de novo* sequencing, to facilitate the *in silico* identification of the corresponding *Arabidopsis* orthologues.

Leaf peroxisomes from *S. oleracea* L. isolated by Percoll density gradient centrifugation according to reported protocols are largely devoid of chloroplastic and mitochondrial contaminations, as indicated by sensitive biochemical methods and estimated by chlorophyll content and fumarase activity, respectively (Yu and Huang, 1986; Reumann *et al.*, 1995). Ther initial proteome analyses of such a fraction of enriched leaf peroxisomes by 2-DE, however, identified prominent protein spots as the small and large subunits of ribulose-bisphosphate carboxylase/oxygenase (RubisCO) and other plastidic enzymes. Measurement of the plastidic enzyme NADP-dependent glyceraldehyde dehydrogenase (NADP-GAPDH) confirmed a partial co-purification of a non-green plastid variant with leaf peroxisomes (data not shown) that most probably represented partially differentiated proplastids. To improve leaf peroxisome purification, the Percoll concentration was increased. Moreover, the washed organelle fraction was laid on top of a second density gradient, i.e. a linear high-resolution sucrose gradient, and subjected to ultracentrifugation. As analysed by sucrose fractionation, the proplastid-like organelles had a slightly lower density than the leaf peroxisomes (Supplementary Fig. S1 at *JXB* online). A significant separation of these proplastid-like organelles from leaf peroxisomes was achieved, and their contamination was reduced to a minimum (Fig. 1, Supplementary Table SI at *JXB* online).

Proteins of highly enriched spinach leaf peroxisomes were analysed by 2-DE. Optimal protein solubilization and representation on 2-D gels was achieved in the presence of thiourea and the zwitterionic detergent CHAPS alone or in combination with amidosulphobetaine-14 (ASB14). The majority of the leaf peroxisomal proteins represented on 2-D gels had a slightly acidic to strongly alkaline isoelectric point (IEP) (pH 6.5–9.5). Individual protein spots were subjected to tryptic in-gel digestion and the peptides analysed by a combination of MALDI, LC-MS/MS, and *de novo* sequencing by electrospray ionisation/tandem mass spectrometry (ESI-MS/MS). For MALDI-TOF-MS, at least five matching peptides with an m/z error <50 ppm were considered minimal requirements for reliable protein identification. For nano-LC-MS/MS, only identifications presenting high-quality MS/MS spectra (MS/MS ion scores >40) were retained.

Some protein spots were identified as plastidic enzymes, for instance the large subunit of RubisCO and RubisCO activase (Supplementary Table SI at *JXB* online), indicating the persistence of minor contamination by partially differentiated proplastid-like organelles. In contrast, neither proteins from mitochondria, which are the major contaminant of peroxisomes from mammals and fungi, nor endoplasmic reticulum (ER) or nuclear proteins were detected. Known proteins of plant peroxisomes were identified based on high sequence coverage of the full-length polypeptide by tryptic peptides and high sequence similarity of the peptides with homologues cloned from various plant species (Supplementary Table SI). In many cases, the proteins of highest sequence similarity derived from *Arabidopsis*, but proteins from other plant species (e.g. *Citrullus lanatus*, *Fritillaria agrestis*, and *Medicago sativa*) were also detected (Supplementary Table SI). The most dominant protein spots included two enzymes from the antioxidative system, CAT and ascorbate peroxidase (APX), and several enzymes involved in the photorespiratory C_2 cycle [glycolate oxidase (GOX), serine-glyoxylate aminotransferase, glutamate-glyoxylate aminotransferase (GGT), hydroxypyruvate reductase (HPR), and malate dehydrogenase]. Several protein spots were identified as enzymes involved in fatty acid

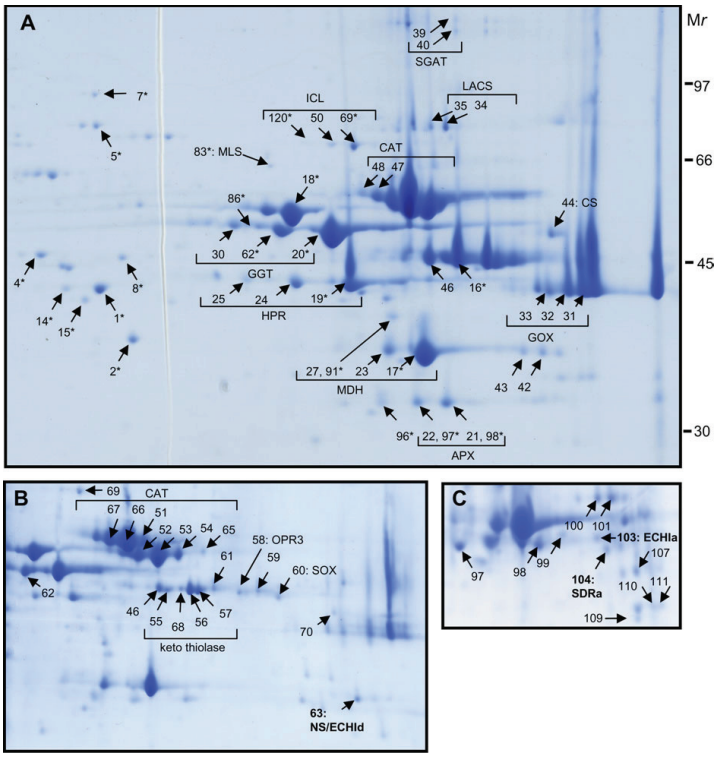

Fig. 1. Proteomic analysis of leaf peroxisomes isolated from *Spinacia oleracea* L. Proteins of isolated spinach leaf peroxisomes were separated by 2-DE and identified by mass spectrometry. Three different gels with optimal resolution in different areas are shown (A–C). Proteins spots labelled by asterisks (*) were identified from another gel (see Supplementary Table SI at *JXB* online).

β-oxidation or the glyoxylate cycle, including, for instance, long-chain acyl-CoA synthetase isoform 6, thiolase, citrate synthase, isocitrate lyase (ICL), and malate synthase (Fig. 1, Supplementary Table SI). Other proteins included 12-oxo-phytodienoic acid reductase isoform 3, which is involved in the biosynthesis of jasmonic acid, and sulphite oxidase.

Some enzymes were found in multiple spots arranged in a horizontal line, indicating different IEPs but similar molecular masses. These proteins included some proteins that are encoded by small gene families in *Arabidopsis*, such as CAT (three genes in *Arabidopsis*), GOX (three genes in *Arabidopsis*), and GGT (two genes in *Arabidopsis*). Additionally, the same horizontal spot pattern was observed for some proteins that are encoded by single genes in *Arabidopsis*, including HPR, ICL, and APX, suggesting that these proteins may differ in IEP due to post-translational modifications.

Unknown proteins of spinach leaf peroxisomes

Sequence information of three unknown proteins of spinach leaf peroxisomes permitted the identification of *Arabidopsis* homologues, which had unknown functions at the time of investigation. One of the three proteins is a member of the superfamily of short-chain alcohol dehydrogenases (spot 104, SDRa, 254 residues, At4g05530). Two other proteins are novel monofunctional enoyl-CoA hydratases/isomerases (ECHIs) of the superfamily of peroxisomal ECHIs that contains five known plant peroxisomal members (Reumann *et al.*, 2004). The first ECHI, referred to as isoform a (spot 103, ECHIa, 264 residues, At4g16210), belongs to clade VI of putative plant enoyl-CoA hydratases (Reumann *et al.*, 2004). The second enoyl-CoA hydratase/isomerase is annotated as naphthoate synthase (spot 63, NS/ECHId, 337 residues, At1g60550) and represents the single orthologue of cyanobacterial MenB, which participates in phylloquinone biosynthesis (Johnson *et al.*, 2001; Gross *et al.*, 2008). Remarkably, all three novel *Arabidopsis* proteins that share significant sequence similarity with the tryptic spinach proteins carry predicted targeting signals for peroxisomes: either C-terminal PTS1 tripeptides (SDRa, SRL>; ECHIa, SKL>) or a putative PTS2 nonapeptide in the N-terminal domain (NS/ECHId, RLx_5HL). All three PTS peptides have previously been classified as major PTS peptides and are high-probability predictors of peroxisomal targeting in unknown proteins (Reumann, 2004).

Subcellular localization analysis of EYFP fusion proteins in vivo

To provide conclusive evidence for the localization of these unknown proteins in peroxisomes, the cDNAs of the *Arabidopsis* homologues were cloned by RT-PCR. The cDNAs encoding proteins with putative C-terminal PTS1 tripeptides (SDRa and ECHIa) or an N-terminal PTS2 nonapeptide (NS/ECHId) were fused at their 5′ or 3′ ends, respectively, in-frame with EYFP in the plant expression vector pCAT. The expression of these fusion genes was under the control of two copies of the 35S promoter of the CaMV (Fulda *et al.*, 2002; Ma *et al.*, 2006). Onion epidermal cells were transformed by bombardment with gold particles coated with plasmid DNA, and the subcellular localization of the fusion proteins was analysed by fluorescence microscopy upon transient gene expression.

The fusion protein EYFP–SDRa, which carried a predicted PTS1 tripeptide (SRL>), was targeted to small subcellular structures that moved quickly along cytoplasmic strands in living cells in single transformants (Fig. 2A1). These punctate structures coincided with peroxisomes labelled with a control fusion protein containing the PTS2 domain of glyoxysomal malate dehydrogenase (gMDH) and ECFP (gMDH–CFP; Fulda *et al.*, 2002), as shown in double transformants expressing *EYFP-SDRa* and *gMDH-CFP*

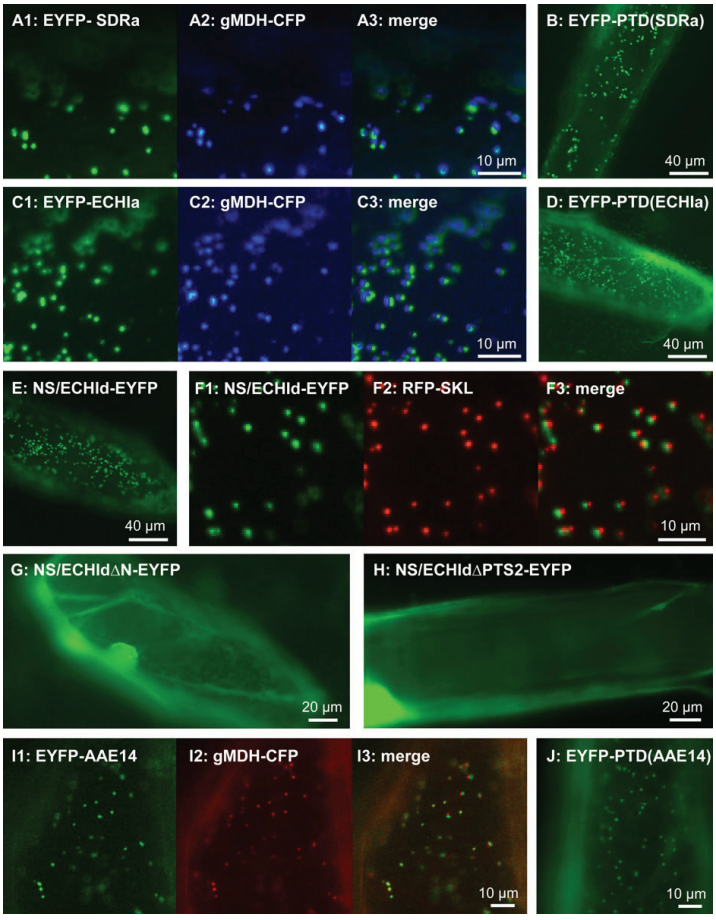

Fig. 2. *In vivo* subcellular localization analysis of novel leaf peroxisomal enzymes tagged with EYFP in onion epidermal cells. The cDNAs of four *Arabidopsis* proteins that were homologous to novel matrix proteins from spinach leaf peroxisomes were fused, depending on the predicted presence of PTS1 or PTS2, in-frame either N-terminally (SDRa, At4g05530, SRL>; ECHIa, At4g16210, SKL>; AAE14, At1g30520, SSL>) or C-terminally (NS/ECHId, At1g60550, RLx_5HL) to enhanced yellow fluorescent protein (EYFP) under the control of a double 35S CaMV promoter. Onion epidermal cells were transformed by bombardment with gold particles coated with plasmid DNA, and protein localization was analysed by fluorescence microscopy. For imaging, either YFP- (A1, B, C1, D, E, F1, G, H, I1, J), CFP- (A2, C2, F2, I2), or RFP-specific filters were used (F2). In I2, cyan fluorescence is shown as red for the image overlay (I3).

simultaneously (Fig. 2A). To investigate whether the predicted C-terminal tripeptide of SDRa, SRL>, was indeed a functional PTS1, the predicted peroxisome targeting domain (PTD) of SDRa, comprising the C-terminal 10 amino acid residues, was fused to EYFP. The resulting construct, referred to as EYFP–PTD(SDRa), was localized to punctate subcellular structures, demonstrating that SRL> is the PTS1 of SDRa (Fig. 2B). Likewise, EYFP–ECHIa, with the accessible C-terminal tripeptide SKL>, was localized to subcellular structures that coincided with peroxisomes (Fig. 2C). Consistent with the targeting prediction, EYFP appended C-terminally with the 10 amino acid domain of ECHIa was detected in organelle-like structures, thereby identifying SKL> as the PTS1 of ECHIa (Fig. 2D).

To investigate the subcellular localization of NS/ECHId carrying the predicted PTS2 RLx_5HL, a reporter protein fusion construct was created, leaving the N-terminal domain of NS/ECHId accessible. NS/ECHId–EYFP was clearly localized to peroxisome-like structures that were distinguishable in size and shape from plastids (Fig. 2E). In double transformants expressing two PTS2 proteins simultaneously, i.e. NS/ECHId–EYFP and gMDH–CFP, cyan fluorescent organelles could barely be detected next to numerous bright-yellow fluorescent peroxisomes (data not shown). The most likely explanation is that the higher expression level of NS/ECHId–EYFP and competition between both proteins for binding to the cytosolic PTS2 receptor, Pex7p, reduced peroxisomal import of gMDH–CFP below the detection limit. However, in double transformants expressing NS/ECHId–EYFP and RFP–SKL, the yellow and red fluorescent organelles co-localized, conclusively demonstrating that NS–EYFP was localized to peroxisomes (Fig. 2F).

Upon deletion of the putative N-terminal targeting domain of ~40 residues from NS/ECHId, the shortened fusion protein (NS/ECHIdΔN–EYFP) remained cytosolic (Fig. 2G). To investigate the subcellular targeting of NS/ECHId by the predicted PTS2 in more detail, the N-terminal domain was altered by site-directed mutagenesis. The exchange of the essential histidien residue to valine (H20→V) was predicted to render the putative PTS2 dysfunctional. The mutated construct remained cytosolic (NS/ECHIdΔPTS2–EYFP, Fig. 2H). These data demonstrate that the nonapeptide RLx_5HL is indeed the PTS2 of NS/ECHId and that the enzyme is, unlike AAE14 (see below), exclusively targeted to peroxisomes.

Thus, all three *Arabidopsis* homologues of the novel proteins identified in spinach leaf peroxisomes were verified to be peroxisome localized as EYFP fusion proteins *in vivo*, and the predicted PTS1/2 signals were conclusively demonstrated to be responsible for peroxisomal targeting.

NS is encoded by a single gene in *Arabidopsis* that is orthologous to MenB from cyanobacteria, chlorobi, and red algae (Gross *et al.*, 2008; Kim *et al.*, 2008). The enzyme catalyses an essential step in phylloquinone biosynthesis, the conversion of *o*-succinylbenzoyl-coenzyme A to 1,4-dihydroxy-2-naphthoyl-CoA (DHNA-CoA) (Fig. 3). Based on gene clustering in cyanobacteria, algae, and higher plants, and experimental subcellular localization data for most enzymes (see Discussion), phylloquinone biosynthesis was previously thought to be exclusively compartmentalized in plastids in higher plants. The present peroxisomal localization data on the *Arabidopsis* orthologue (see above) cast doubt on this view. Kim *et al.* (2008) showed that AAE14 catalyses the reaction upstream of that of MenB, the activation of *o*-succinyl benzoate to *o*-succinyl benzoyl-CoA (Fig. 3). When fused C-terminally with green fluorescent protein (GFP) (AAE14–GFP), AAE14 localizes to chloroplasts (Kim *et al.*, 2008). However, AAE14 ends with SSL>, which has recently been characterized as a functional PTS1 (Reumann *et al.*, 2007), suggesting that the enzyme might be dually targeted to both plastids and peroxisomes. These data prompted the investigation of the subcellular localization of AAE14 in more detail as an N-terminal EYFP fusion protein (EYFP–AAE14) that permitted the C-terminal tripeptide of AAE14, SSL>, to function as a subcellular targeting signal. The fusion protein indeed localized to small punctate structures that were clearly distinct from plastids. The identity of the EYFP-labelled organelles as peroxisomes was demonstrated by double labelling the peroxisomes with CFP (Fig. 2I). Moreover, the C-terminal 10 amino acid residues of AAE14 directed EYFP to small subcellular organelles indicative of peroxisomes, identifying SSL> as the PTS1 of AAE14 (Fig. 2J). In summary and in an extension of the study by Kim *et al.* (2008), the present *in vivo* targeting data demonstrate that AAE14 is dually targeted to both plastids and peroxisomes. The extended subcellular localization analyses of this proteomic study thus indicate that at least two steps of phylloquinone biosynthesis are compartmentalized in peroxisomes in higher plants (Fig. 3).

Discussion

Proteomic studies are generally restricted to organisms with sequenced genomes to facilitate protein identification from high-resolution 2-D gels by mass spectrometry. Even though apparent tissue limitations of the diminutive *Arabidopsis* weed can be overcome by large-scale plant growth, it was not possible to isolate leaf peroxisomes of satisfactory quality and quantity from *Arabidopsis* by applying methods established for other plants species or *Arabidopsis* itself. In a parallel approach, an attempt was therefore made to analyse the proteome of leaf peroxisomes from *S. oleracea* L.

The isolates of leaf peroxisomes from spinach following published methods (Yu and Huang, 1986) were virtually free of chloroplasts and mitochondria, as indicated by sensitive measurements based on the chlorophyll content and the activity of the mitochondrial marker enzyme fumarase (Supplementary Fig. S1 at *JXB* online). However, the leaf peroxisomes were still contaminated by partially differentiated 'proplastid-like' organelles that contained RubisCO and Calvin cycle enzymes. Due to their similar equilibrium density in Percoll and sucrose density gradients, these

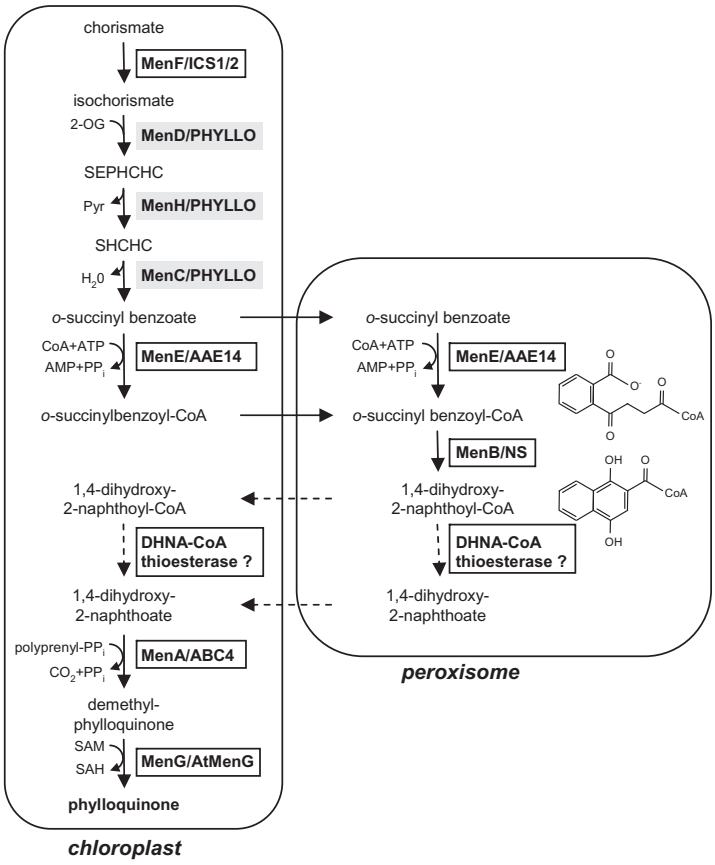

Fig. 3. Model of the compartmentalization of phylloquinone biosynthesis between chloroplasts and peroxisomes in higher plants. Of eight predicted *Arabidopsis* homologues of cyanobacterial enzymes involved in phylloquinone biosynthesis (MenA–G), three are expressed as a fusion protein from the trifunctional PHYLLO locus (MenC, D, H, light grey shading) and targeted to chloroplasts (Gross *et al.*, 2006). In this study the *Arabidopsis* AAE14 and NS homologues have been identified as peroxisomal enzymes, demonstrating that at least two steps of phylloquinone biosynthesis are compartmentalized in peroxisomes in higher plants. SEPHCHC, 2-succinyl-5-enolpyruvyl-6-hydroxy-3-cyclohexene-1-carboxylic acid; SHCHC, (1*R*,6*R*)-2-succinyl-6-hydroxy-2,4-cyclohexadiene-1-carboxylic acid; 2-OG, 2-oxoglutarate.

proplastids and leaf peroxisomes were difficult to separate. The plastidic contamination was reduced to a minimum by the application of two successive density gradients, but it could not be completely eliminated, a problem shared by recent studies of the peroxisomal proteome (Fukao *et al.*, 2002, 2003; Reumann *et al.*, 2007, 2009; Arai *et al.*, 2008; Eubel *et al.*, 2008). As a result, some plastidic proteins were still present on the 2-D gels. *In vivo* subcellular localization analyses are thus essential to validate the putative peroxisomal localization of candidate proteins identified in enriched spinach leaf peroxisomes.

Remarkably, a comparison of the proteomic data of this study with recent studies of leaf peroxisomes from *Arabidopsis* (Reumann *et al.*, 2007, 2009) shows that some proteins were identified in leaf peroxisomes from *Spinacia* but not in *Arabidopsis*, for instance malate synthase and ICL. These data support the necessity of analysing organelles from different plant species before drawing generalized conclusions about organelle constituents (Fukao *et al.*, 2002, 2003; Reumann *et al.*, 2007, 2009; Arai *et al.*, 2008; Eubel *et al.*, 2008).

Since plant peroxisomes cannot be isolated in absolute purity, additional independent lines of evidence were provided that the novel proteins indeed reside in peroxisomes. One efficient method to verify protein targeting to peroxisomes by the PTS1/2 pathways is *in silico* analysis for conservation of the predicted PTS in homologous plant proteins and ESTs (Reumann, 2004). For instance, all full-length protein sequences of ECHIa homologues from higher plants and from *Physcomitrella* terminate with putative

PTS1s. Likewise, the PTS2 nonapeptide of NS/ECHId has previously been shown to be highly conserved (Reumann *et al.*, 2007, see also Supplementary Fig. S2 at *JXB* online). Many apparent orthologues of AAE14 terminate with SSL> or SNL>, with two sequences even carrying the prototypical PTS1s, SRL> and SKL>. Only a single EST carries a C-terminal tripeptide, CSL> (*Manihot esculenta*), that has not (yet) been described as a functional plant PTS1 (Fig. 4). In summary, all four candidate proteins carry conserved PTS peptides, strongly supporting peroxisomal protein functions across higher plant species.

Conclusive evidence for peroxisome localization of the unknown proteins was provided by *in vivo* subcellular targeting analysis. It was demonstrated by double labelling subcellular organelles that SDRa is targeted to peroxisomes *in vivo*. Similar data have been obtained for *Arabidopsis* SDRa (Eubel *et al.*, 2008; Wiszniewski *et al.*, 2009) and for the orthologue from soybean (Gm SDRa; Arai *et al.*, 2008). By fusing the 10 C-terminal amino acid residues of SDRa to EYFP, it was further confirmed that the predicted PTS, SRL>, indeed targets SDRa to peroxisomes. The characterization of the targeting signals of predicted PTS1 proteins is important because it enables those proteins to be included as positive control sequences in the development of PTS1 prediction algorithms (T Lingner, G E Antonicelli, P Meinicke, and S Reumann, unpublished data).

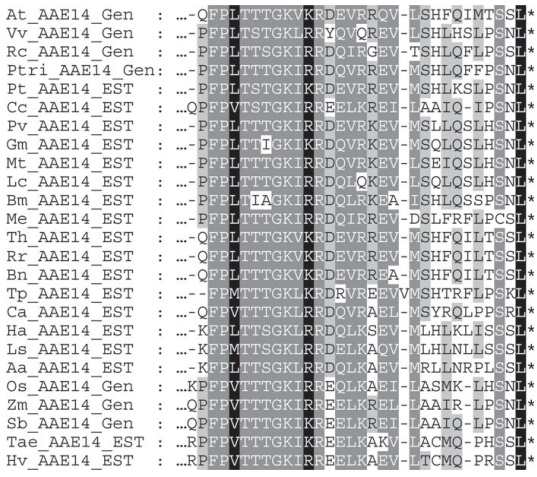

Fig. 4. PTS1 conservation analysis in AAE14 orthologues. Orthologous protein sequences were retrieved from the protein and EST databases at NCBI by homology analysis (Reumann, 2004), aligned by ClustalX, and shaded by Genedoc. Selected plant species with the most divergent C-terminal PTS1 tripeptides are shown. At, *Arabidopsis thaliana*; Aa, *Artemisia annua*; Bm, *Burma mangrove*; Bn, *Brassica napus*; Ca, *Capsicum annuum*; Cc, *Cenchrus ciliaris*; Gm, *Glycine max*; Ha, *Helianthus annuus*; Hc, *Hedyotis centranthoides*; Hv, *Hordeum vulgare*; Lc, *Lotus corniculatus*; Ls, *Lactuca serriola*; Me, *Manihot esculenta*; Mt, *Medicago truncatula*; Os, *Oryza sativa*; Pt, *Poncirus trifoliata*; Ptri, *Populus trichocarpa*; Pv, *Phaseolus vulgaris*; Rc, *Ricinus communis*; Sb, *Sorghum bicolor*; Tae, *Triticum aestivum*; Th, *Thellungiella halophila*; Tp, *Triphysaria pusilla*; Vv, *Vitis vinifera*; Zm, *Zea mays*.

Members of the superfamily of SDRs form a universal superfamily of metabolically important oxidoreductases. In *Arabidopsis* leaf peroxisomes, three further SDR homologues were identified, including the predicted DECR orthologue (SDRb; Reumann *et al.*, 2007). The oxidoreductase SDRa is the plant orthologue of vertebrate peroxisomal NADP-dependent carbonyl reductase, which participates in arachidonic acid metabolism (Fransen *et al.*, 1999). Cofactor specificity for NADP appears to be conserved in SDRa (Reumann *et al.*, 2007). In an ethylmethane sulphonate (EMS) screen, a strong IBA-response mutant, *ibr1*, was recently isolated that is deficient in IBR1/SDRa (Zolman *et al.*, 2008). Like *ibr3* (Zolman *et al.*, 2007), the mutant does not have apparent defects in peroxisomal fatty acid β-oxidation, indicating that IBR1/SDRa is specifically involved in shortening the side chain of IBA to indole acetic acid (IAA) rather than the β-oxidation of straight-chain fatty acids. These present data complement this study by confirming that IBR1/SDRa is indeed a peroxisomal enzyme.

Furthermore, it was verified that ECHIa is targeted to peroxisomes *in vivo*, as shown previously (Eubel *et al.*, 2008). By fusing its C-terminal 10 residues to EYFP, it was confirmed that the predicted PTS, SKL>, is indeed the peroxisomal targeting signal of ECHIa. Well-characterized members of the *Arabidopsis* superfamily of peroxisomal ECHIs are the multifunctional proteins MFP2 and AIM1 and the branched-chain amino acid catabolic enzyme CHY1 (Zolman *et al.*, 2001; for a review, see Graham and Eastmond, 2002). Additional members of this protein family include Δ(3,5),Δ(2,4)-dienoyl-coenzyme A (CoA) isomerase (Goepfert *et al.*, 2005) and Δ(3),Δ(2)-enoyl CoA isomerases 1 and 2 (Goepfert *et al.*, 2008), both of which participate in the degradation of unsaturated fatty acids through the β-oxidation cycle. ECHIa is plant-specific among eukaryotes and is closely related to some poorly characterized prokaryotic ECHIs. The physiological function of ECHIa in plant peroxisomal metabolism remains to be elucidated.

Among plant peroxisomal isomerases, NS/ECHId has a unique role. The fusion protein NS–EYFP, with a predicted N-terminal PTS2 (RLx_5HL), was localized to small subcellular organelles that were clearly distinguishable in size and shape from non-green plastids with their characteristic stromuli in onion epidermal cells (Reumann *et al.*, 2007). Upon removal of the N-terminal domain, NS/ECHIdΔN-EYFP remained cytosolic. The peroxisomal proteomics and subcellular localization of NS, supplemented by PTS2 conservation in plant orthologues (Reumann *et al.*, 2007; Supplementary Fig. S2 at *JXB* online), demonstrate that NS/ECHId is a plant peroxisomal protein that is targeted to peroxisomes by the PTS2 pathway. Moreover, NS lacks a predicted transit peptide and has not been identified in any chloroplast proteome study (SUBA II; Heazlewood *et al.*, 2007). Site-directed mutagenesis of

RLx_5HL to RLx_5VL in the putative PTS2 did not significantly lower the prediction score for plastidic targeting (TargetP: wild type, 0.543; mutated version, 0.508; Emanuelsson *et al.*, 2000) but rendered the fusion protein entirely cytosolic. Therefore, it is concluded that NS is exclusively localized to peroxisomes.

The annotation of NS/ECHId as naphthoate synthase is derived from facultative anaerobic bacteria and cyanobacteria, where the orthologues are involved in the biosynthesis of menaquinone (vitamin K2) and phylloquinone (vitamin K1), respectively (Johnson *et al.*, 2001; see also references therein). Phylloquinone, a substituted 1,4-naphthoquinone with an 18-carbon-saturated phytyl tail, functions as a bound one-electron carrier cofactor at the A1 site of photosystem I (PSI; Fig. 3). Plants are the only eukaryotes possessing orthologues of prokaryotic NS. Detailed phylogenetic analyses have demonstrated that *Arabidopsis* NS/ECHId is orthologous to MenB from red algae, chlorobi, cyanobacteria, and anaerobic bacteria (Gross *et al.*, 2008).

In higher plants, all nine reactions of phylloquinone biosynthesis have previously been demonstrated or assumed to be compartmentalized exclusively in chloroplasts for several reasons. First, several *men* genes, including *menB*, are plastid encoded in red algae, and the gene products are unlikely to be exported. Secondly, the first four enzymes of the pathway (MenF, D, H, and C), which convert chorismate to *o*-succinylbenzoate (Fig. 3), are nuclear encoded in higher plants and localized to chloroplasts; the MenD, H, and C domains are encoded as a trifunctional fusion protein in *Arabidopsis* (Gross *et al.*, 2006). Thirdly, MenA/ABC4 and MenG are also plastid localized (Shimada *et al.*, 2005; Lohmann *et al.*, 2006). For MenB, neither subcellular localization nor functional data have been reported for any plant homologue to date. In light of the lack of any evidence for the existence of additional MenB paralogues in *Arabidopsis* or additional transcriptional or translational variants, it is concluded that *Arabidopsis* NS/ECHId is exclusively peroxisomal in *Arabidopsis* and in most other higher plant species.

The localization of NS/ECHId to peroxisomes sheds new light on the compartmentalization of phylloquinone biosynthesis in higher plants and raises further questions, regarding, for instance, the evolution of phylloquinone compartmentalization. In red algae such as *Cyanidioschyzon merolae* and *Cyanidium caldarium*, the (single) homologue of NS is still plastid encoded and thus plastid localized. After the divergence of rhodophyta, the *menB* gene was transferred to the nucleus. The acquisition of an N-terminal extension and a PTS2 seems to have happened twice independently in the lineage of streptophyta and chlorophyta. While the orthologues of both *Ostreococcus* (RVx_5HV) and higher plants carry N-terminal extensions harbouring predicted or related PTS2s, those of *Chlamydomonas* and *Physcomitrella* are shorter, similar to those of prokaryotic homologues (*Mycobacterium*, *Pelodictyon*; Supplementary Fig. S2 at *JXB* online), and lack PTS2-like nonapeptides. Thus, the NS gene inherited from cyanobacteria has been transferred from the plastid to the nuclear genome at a rather late stage of streptophyta evolution, and its protein product has probably been redirected from plastids to peroxisomes via an intermediate, cytosolic stage, as found nowadays in *Physcomitrella*.

MenE/AAE14 is the ligase that activates *o*-succinyl benzoate to *o*-succinyl-CoA in phylloquinone biosynthesis. Even though the presence of a transit peptide is not predicted for AAE14, the C-terminal full-length fusion protein (AAE14–EYFP) and a GFP with the first 120 residues of AAE14 appended to its N-terminus localized to chloroplasts (Kim *et al.*, 2008). However, similarly to NS, AAE14 has not been identified in any of the numerous high-sensitivity proteomic analyses of chloroplasts (SUBA II). Moreover, analogously to peroxisomal fatty acid catabolism and jasmonic acid biosynthesis, it might be postulated that *o*-succinylbenzoate, rather than its CoA derivative, is imported into peroxisomes and activated in the matrix (Fig. 3) by transport and reaction processes similar to those for straight-chain fatty acids and OPDA by LACS6/7 and OPCL1, respectively (Fulda *et al.*, 2004; Koo *et al.*, 2006). Indeed, both full-length AAE14 and EYFP appended with the C-terminal 10 residues of AAE14 localized to peroxisomes (Fig. 2), indicating that AAE14 is dually targeted to both chloroplasts and peroxisomes. Future studies need to address the regulation and possible species specificity of the dual targeting of AAE14. The present proteomic and localization data thus indicate that at least two enzymes of phylloquinone biosynthesis are peroxisomal, and that phylloquinone biosynthesis is partially compartmentalized in peroxisomes in higher plants (Fig. 3).

The peroxisomal localization of AAE14 and NS/ECHId raises the question of whether additional enzymes involved in phylloquinone biosynthesis might be localized in peroxisomes and which intermediates are transported across the peroxisomal and the chloroplast envelope membranes. The enzyme immediately upstream of AAE14, MenC, is part of the trifunctional PHYLLO locus and is chloroplast localized. The enzyme downstream of NS, DHNA-CoA thioesterase, has recently been characterized biochemically and cloned from *Synechocystis* but lacks closely related homologues in higher plants (Widhalm *et al.*, 2009). In light of the recent identification of four small thioesterases in *Arabidopsis* leaf peroxisomes and the peroxisomal targeting prediction of additional paralogues (Reumann *et al.*, 2004, 2007, 2009), DHNA-CoA thioesterase may well be a peroxisomal enzyme that releases DHNA in the peroxisomal matrix, which is then transported across the peroxisomal membrane back to the chloroplast for attachment of the phytol chain and completion of phylloquinone biosynthesis (Fig. 3).

Supplementary data

Supplementary data are available at *JXB* online.

Figure S1. Improved separation of Percoll-purified leaf peroxisomes and proplastid-like organelles from *Spinacia oleracea* L. by a second sucrose density gradient.

Figure S2. Multiple sequence alignment of NS/MenB orthologues.

Table SI. Proteins identified in isolated leaf peroxisomes from *Spinacia oleracea* L. by mass spectrometry.

Table SII. Oligonucleotide primers used for cDNA subcloning.

Acknowledgements

We thank Aline Benichou, Dr Xiong-Yan Chen, Alena Liavonchanka, and Nora Valeur for experimental contributions, Gilles Basset for comments, and the Arabidopsis Biological Resource Center (ABRC) for provision of the cDNA clone of AAE14. The research was supported by a grant from the Deutsche Forschungsgemeinschaft (RE1304/2), a Dorothea-Erxleben stipend from the government of Lower Saxony (to SR), and UiS funding.

References

Arai Y, Hayashi M, Nishimura M. 2008. Proteomic analysis of highly purified peroxisomes from etiolated soybean cotyledons. *Plant and Cell Physiology* **49,** 526–539.

Boden M, Hawkins J. 2005. Prediction of subcellular localization using sequence-biased recurrent networks. *Bioinformatics* **21,** 2279–2286.

Bradford MM. 1976. A rapid and sensitive method for the quantitation of microgram quantities of protein utilizing the principle of protein–dye binding. *Analytical Biochemistry* **72,** 248–254.

del Rio LA, Corpas FJ, Sandalio LM, Palma JM, Gomez M, Barroso JB. 2002. Reactive oxygen species, antioxidant systems and nitric oxide in peroxisomes. *Journal of Experimental Botany* **53,** 1255–1272.

Emanuelsson O, Elofsson A, von Heijne G, Cristobal S. 2003. In silico prediction of the peroxisomal proteome in fungi, plants and animals. *Journal of Molecular Biology* **330,** 443–456.

Emanuelsson O, Nielsen H, Brunak S, von Heijne G. 2000. Predicting subcellular localization of proteins based on their N-terminal amino acid sequence. *Journal of Molecular Biology* **300,** 1005–1016.

Eubel H, Meyer EH, Taylor NL, Bussell JD, O'Toole N, Heazlewood JL, Castleden I, Small ID, Smith SM, Millar AH. 2008. Novel proteins, putative membrane transporters, and an integrated metabolic network are revealed by quantitative proteomic analysis of Arabidopsis cell culture peroxisomes. *Plant Physiology* **148,** 1809–1829.

Fransen M, Van Veldhoven PP, Subramani S. 1999. Identification of peroxisomal proteins by using M13 phage protein VI phage display: molecular evidence that mammalian peroxisomes contain a 2,4-dienoyl-CoA reductase. *Biochemica Journal* **340,** 561–568.

Fukao Y, Hayashi M, Hara-Nishimura I, Nishimura M. 2003. Novel glyoxysomal protein kinase, GPK1, identified by proteomic analysis of glyoxysomes in etiolated cotyledons of Arabidopsis thaliana. *Plant and Cell Physiology* **44,** 1002–1012.

Fukao Y, Hayashi M, Nishimura M. 2002. Proteomic analysis of leaf peroxisomal proteins in greening cotyledons of Arabidopsis thaliana. *Plant and Cell Physiology* **43,** 689–696.

Fulda M, Schnurr J, Abbadi A, Heinz E, Browse J. 2004. Peroxisomal Acyl-CoA synthetase activity is essential for seedling development in Arabidopsis thaliana. *The Plant Cell* **16,** 394–405.

Fulda M, Shockey J, Werber M, Wolter FP, Heinz E. 2002. Two long-chain acyl-CoA synthetases from Arabidopsis thaliana involved in peroxisomal fatty acid beta-oxidation. *The Plant Journal* **32,** 93–103.

Goepfert S, Vidoudez C, Rezzonico E, Hiltunen JK, Poirier Y. 2005. Molecular identification and characterization of the Arabidopsis delta(3,5), delta(2,4)-dienoyl-coenzyme A isomerase, a peroxisomal enzyme participating in the beta-oxidation cycle of unsaturated fatty acids. *Plant Physiology* **138,** 1947–1956.

Goepfert S, Vidoudez C, Tellgren-Roth C, Delessert S, Hiltunen JK, Poirier Y. 2008. Peroxisomal Delta(3), Delta(2)-enoyl CoA isomerases and evolution of cytosolic paralogues in embryophytes. *The Plant Journal* **56,** 728–742.

Gould SG, Keller GA, Subramani S. 1987. Identification of a peroxisomal targeting signal at the carboxy terminus of firefly luciferase. *Journal of Cell Biology* **105,** 2923–2931.

Graham IA, Eastmond PJ. 2002. Pathways of straight and branched chain fatty acid catabolism in higher plants. *Progress in Lipid Research* **41,** 156–181.

Gross J, Cho WK, Lezhneva L, Falk J, Krupinska K, Shinozaki K, Seki M, Herrmann RG, Meurer J. 2006. A plant locus essential for phylloquinone (vitamin K1) biosynthesis originated from a fusion of four eubacterial genes. *Journal of Biological Chemistry* **281,** 17189–17196.

Gross J, Meurer J, Bhattacharya D. 2008. Evidence of a chimeric genome in the cyanobacterial ancestor of plastids. *BMC Evolutionary Biology* **8,** 117.

Heazlewood JL, Verboom RE, Tonti-Filippini J, Small I, Millar AH. 2007. SUBA: the Arabidopsis Subcellular Database. *Nucleic Acids Research* **35,** D213–D218.

Herbert B, Galvani M, Hamdan M, Olivieri E, MacCarthy J, Pedersen S, Righetti PG. 2001. Reduction and alkylation of proteins in preparation of two-dimensional map analysis: why, when, and how? *Electrophoresis* **22,** 2046–2057.

Jeno P, Mini T, Moes S, Hintermann E, Horst M. 1995. Internal sequences from proteins digested in polyacrylamide gels. *Analytical Biochemistry* **224,** 75–82.

Johnson TW, Zybailov B, Jones AD, Bittl R, Zech S, Stehlik D, Golbeck JH, Chitnis PR. 2001. Recruitment of a foreign quinone into the A1 site of photosystem I. *In vivo* replacement of plastoquinone-9 by media-supplemented naphthoquinones in phylloquinone biosynthetic pathway mutants of Synechocystis sp. PCC 6803. *Journal of Biological Chemistry* **276,** 39512–39521.

Kamada T, Nito K, Hayashi H, Mano S, Hayashi M, Nishimura M. 2003. Functional differentiation of peroxisomes revealed by expression profiles of peroxisomal genes in Arabidopsis thaliana. *Plant and Cell Physiology* **44,** 1275–1289.

Kaur N, Reumann S, Hu J. 2009. Peroxisome biogenesis and function. *The Arabidopsis book,* The American Society of Plant Biologists 1–41.

Kikuchi M, Hatano N, Yokota S, Shimozawa N, Imanaka T, Taniguchi H. 2004. Proteomic analysis of rat liver peroxisome: presence of peroxisome-specific isozyme of Lon protease. *Journal of Biological Chemistry* **279,** 421–428.

Kim HU, van Oostende C, Basset GJ, Browse J. 2008. The AAE14 gene encodes the Arabidopsis o-succinylbenzoyl-CoA ligase that is essential for phylloquinone synthesis and photosystem-I function. *The Plant Journal* **54,** 272–283.

Koo AJ, Chung HS, Kobayashi Y, Howe GA. 2006. Identification of a peroxisomal acyl-activating enzyme involved in the biosynthesis of jasmonic acid in Arabidopsis. *Journal of Biological Chemistry* **281,** 33511–33520.

Kruft V, Eubel H, Jansch L, Werhahn W, Braun HP. 2001. Proteomic approach to identify novel mitochondrial proteins in Arabidopsis. *Plant Physiology* **127,** 1694–1710.

Lohmann A, Schottler MA, Brehelin C, Kessler F, Bock R, Cahoon EB, Dormann P. 2006. Deficiency in phylloquinone (vitamin K1) methylation affects prenyl quinone distribution, photosystem I abundance, and anthocyanin accumulation in the Arabidopsis AtmenG mutant. *Journal of Biological Chemistry* **281,** 40461–40472.

Lopez-Huertas E, Sandalio LM, Del Rio LA. 1995. Integral membrane polypeptides of pea leaf peroxisomes: characterization and response to plant stress. *Plant Physiology and Biochemistry* **33,** 295–302.

Lowry OH, Rosebrough NJ, Farr AL, Randall RJ. 1951. Protein measurement with the Folin phenol reagent. *Journal of Biological Chemistry* **193,** 265–275.

Ma C, Haslbeck M, Babujee L, Jahn O, Reumann S. 2006. Identification and characterization of a stress-inducible and a constitutive small heat-shock protein targeted to the matrix of plant peroxisomes. *Plant Physiology* **141,** 47–60.

Marelli M, Smith JJ, Jung S, *et al*. 2004. Quantitative mass spectrometry reveals a role for the GTPase Rho1p in actin organization on the peroxisome membrane. *Journal of Cell Biology* **167,** 1099–1112.

Matre P, Meyer C, Lillo C. 2009. Diversity in subcellular targeting of the PP2A B′eta subfamily members. *Planta* **230,** 935–945.

Millar AH, Sweetlove LJ, Giege P, Leaver CJ. 2001. Analysis of the Arabidopsis mitochondrial proteome. *Plant Physiology* **127,** 1711–1727.

Neuberger G, Maurer-Stroh S, Eisenhaber B, Hartig A, Eisenhaber F. 2003. Prediction of peroxisomal targeting signal 1 containing proteins from amino acid sequence. *Journal of Molecular Biology* **328,** 581–592.

Palma JM, Corpas FJ, Del Rio LA. 2009. Proteome of plant peroxisomes: new perspectives on the role of these organelles in cell biology. *Proteomics* **9,** 2301–2312.

Peltier JB, Friso G, Kalume DE, Roepstorff P, Nilsson F, Adamska I, van Wijk KJ. 2000. Proteomics of the chloroplast: systematic identification and targeting analysis of lumenal and peripheral thylakoid proteins. *The Plant Cell* **12,** 319–341.

Perkins DN, Pappin DJ, Creasy DM, Cottrell JS. 1999. Probability-based protein identification by searching sequence databases using mass spectrometry data. *Electrophoresis* **20,** 3551–3567.

Reumann S. 2004. Specification of the peroxisome targeting signals type 1 and type 2 of plant peroxisomes by bioinformatics analyses. *Plant Physiology* **135,** 783–800.

Reumann S, Babujee L, Ma C, Wienkoop S, Siemsen T, Antonicelli GE, Rasche N, Luder F, Weckwerth W, Jahn O. 2007. Proteome analysis of Arabidopsis leaf peroxisomes reveals novel targeting peptides, metabolic pathways, and defense mechanisms. *The Plant Cell* **19,** 3170–3193.

Reumann S, Heupel R, Heldt HW. 1994. Compartmentation studies on spinach leaf peroxisomes. II. Evidence for the transfer of reductant from the cytosol to the peroxisomal compartment via a malate shuttle. *Planta* **193,** 167–173.

Reumann S, Ma C, Lemke S, Babujee L. 2004. AraPerox. A database of putative Arabidopsis proteins from plant peroxisomes. *Plant Physiology* **136,** 2587–2608.

Reumann S, Maier E, Benz R, Heldt HW. 1995. The membrane of leaf peroxisomes contains a porin-like channel. *Journal of Biological Chemistry* **270,** 17559–17565.

Reumann S, Quan S, Aung K, *et al*. 2009. In-depth proteome analysis of Arabidopsis leaf peroxisomes combined with *in vivo* subcellular targeting verification indicates novel metabolic and regulatory functions of peroxisomes. *Plant Physiology* **150,** 125–143.

Reumann S, Weber AP. 2006. Plant peroxisomes respire in the light: some gaps of the photorespiratory C2 cycle have become filled—others remain. *Biochimica et Biophysica Acta* **1763,** 1496–1510.

Saleem RA, Smith JJ, Aitchison JD. 2006. Proteomics of the peroxisome. *Biochimica et Biophysica Acta* **1763,** 1541–1551.

Schafer H, Nau K, Sickmann A, Erdmann R, Meyer HE. 2001. Identification of peroxisomal membrane proteins of *Saccharomyces cerevisiae* by mass spectrometry. *Electrophoresis* **22,** 2955–2968.

Shimada H, Ohno R, Shibata M, Ikegami I, Onai K, Ohto MA, Takamiya K. 2005. Inactivation and deficiency of core proteins of photosystems I and II caused by genetical phylloquinone and plastoquinone deficiency but retained lamellar structure in a T-DNA mutant of Arabidopsis. *The Plant Journal* **41,** 627–637.

Swinkels BW, Gould SJ, Bodnar AG, Rachubinski RA, Subramani S. 1991. A novel, cleavable peroxisomal targeting signal at the amino-terminus of the rat 3-ketoacyl-CoA thiolase. *EMBO Journal* **10,** 3255–3262.

Wessel D, Flugge UI. 1984. A method for the quantitative recovery of protein in dilute solution in the presence of detergents and lipids. *Analytical Biochemistry* **138,** 141–143.

Widhalm JR, van Oostende C, Furt F, Basset GJ. 2009. A dedicated thioesterase of the Hotdog-fold family is required for the biosynthesis of the naphthoquinone ring of vitamin K1. *Proceedings of the Natoional Academy of Sciences, USA* **106,** 5599–5603.

Wiese S, Gronemeyer T, Ofman R, *et al*. 2007. Proteomics characterization of mouse kidney peroxisomes by tandem mass spectrometry and protein correlation profiling. *Molecular and Cellular Proteomics* **6,** 2045–2057.

Wiszniewski AA, Zhou W, Smith SM, Bussell JD. 2009. Identification of two Arabidopsis genes encoding a peroxisomal oxidoreductase-like protein and an acyl-CoA synthetase-like protein

that are required for responses to pro-auxins. *Plant Molecular Biology* **69,** 503–515.

Yu C, Huang AH. 1986. Conversion of serine to glycerate in intact spinach leaf peroxisomes: role of malate dehydrogenase. *Archives of Biochemistry and Biophysics* **245,** 125–133.

Zolman BK, Martinez N, Millius A, Adham AR, Bartel B. 2008. Identification and characterization of Arabidopsis indole-3-butyric acid response mutants defective in novel peroxisomal enzymes. *Genetics* **180,** 237–251.

Zolman BK, Monroe-Augustus M, Thompson B, Hawes JW, Krukenberg KA, Matsuda SP, Bartel B. 2001. chy1, an Arabidopsis mutant with impaired beta-oxidation, is defective in a peroxisomal beta-hydroxyisobutyryl-CoA hydrolase. *Journal of Biological Chemistry* **276,** 31037–31046.

Zolman BK, Nyberg M, Bartel B. 2007. IBR3, a novel peroxisomal acyl-CoA dehydrogenase-like protein required for indole-3-butyric acid response. *Plant Molecular Biology* **64,** 59–72.

The Proteome Map of Spinach Leaf Peroxisomes Indicates Partial Compartmentalization of Phylloquinone (Vitamin K1) Biosynthesis in Plant Peroxisomes

Lavanya Babujee, Virginie Wurtz, Changle Ma, Franziska Lueder, Pradeep Soni, Alain van Dorsselaer, Sigrun Reumann

Suppl. Figure 1: Improved separation of Percoll-purified leaf peroxisomes and proplastid-like organelles from *Spinacia oleracea* L. by a second sucrose density gradient.

Based on fumarase activity (mitochondrium marker) and chlorophyll content (chloroplast marker) the contamination of peroxisomes was estimated approximately 0.5% and 0.03%, respectively (data not shown). To improve the separation of proplastid-like organelles spinach leaf peroxisomes enriched by Percoll density gradient centrifugation were homogenized by a tight fitting Potter-Elvehjem homogenizer, layered on top of a linear 40-60 %(w/w) sucrose density gradient and ultracentrifuged. The enzyme activities of HPR (peroxisome marker) and NADP-GAPDH (proplastid-like organelles) were measured in the crude extract (676 U HPR and 1075 U NADP-GAPDH activity) and the gradient fractions. Peroxisomes equilibrated at their typical equilibrium density of 52.5 % (w/w) sucrose in the gradient. Fractions 12-14 were significantly purified over proplastid-like organelles and subjected to proteome analysis. A representative gradient from three independent experiments is shown (n=3).

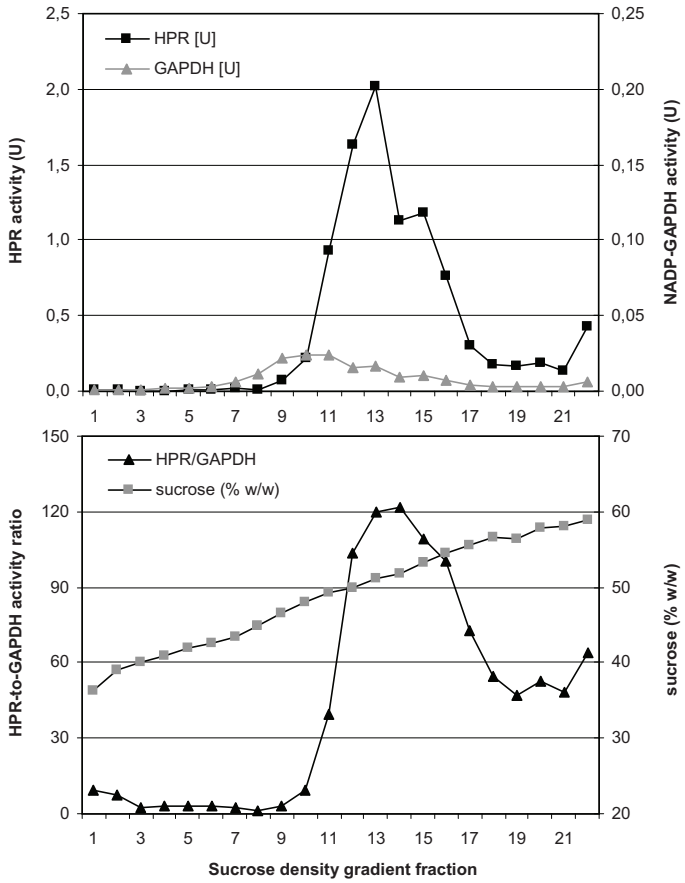

The Proteome Map of Spinach Leaf Peroxisomes Indicates Partial Compartmentalization of Phylloquinone (Vitamin K1) Biosynthesis in Plant Peroxisomes

Lavanya Babujee, Virginie Wurtz, Changle Ma, Franziska Lueder, Pradeep Soni, Alain van Dorsselaer, Sigrun Reumann

Suppl. Figure 2

Multiple sequence alignment of MenB/NS orthologs. Active site (!) and conserved residues implicated in substrate binding (*) in MenB of *Mycobacterium tuberculosis* (Truglio *et al.*, 2003) are indicated. Predicted PTS2s are printed bold. At, *Arabidopsis thaliana*; Cr, *Chlamydomonas reinhardtii*; Gm, *Glycine max*; *Mycobacterium tuberculosis* H37Rv; Ol, *Ostreococcus lucimarinus* CCE9901; Os, *Oryza sativa*; Pl, *Pelodictyon phaeoclathratiforme* BU-1 (Chlorobiaceae); Ppat, *Physcomitrella patens* subsp. patens; Ptri, *Populus trichocarpa*; Ps, *Picea sitchensis*; Rc, *Ricinus communis*; Sb, *Sorghum bicolor*; Vv, *Vitis vinifera*; Zm, *Zea mays*.

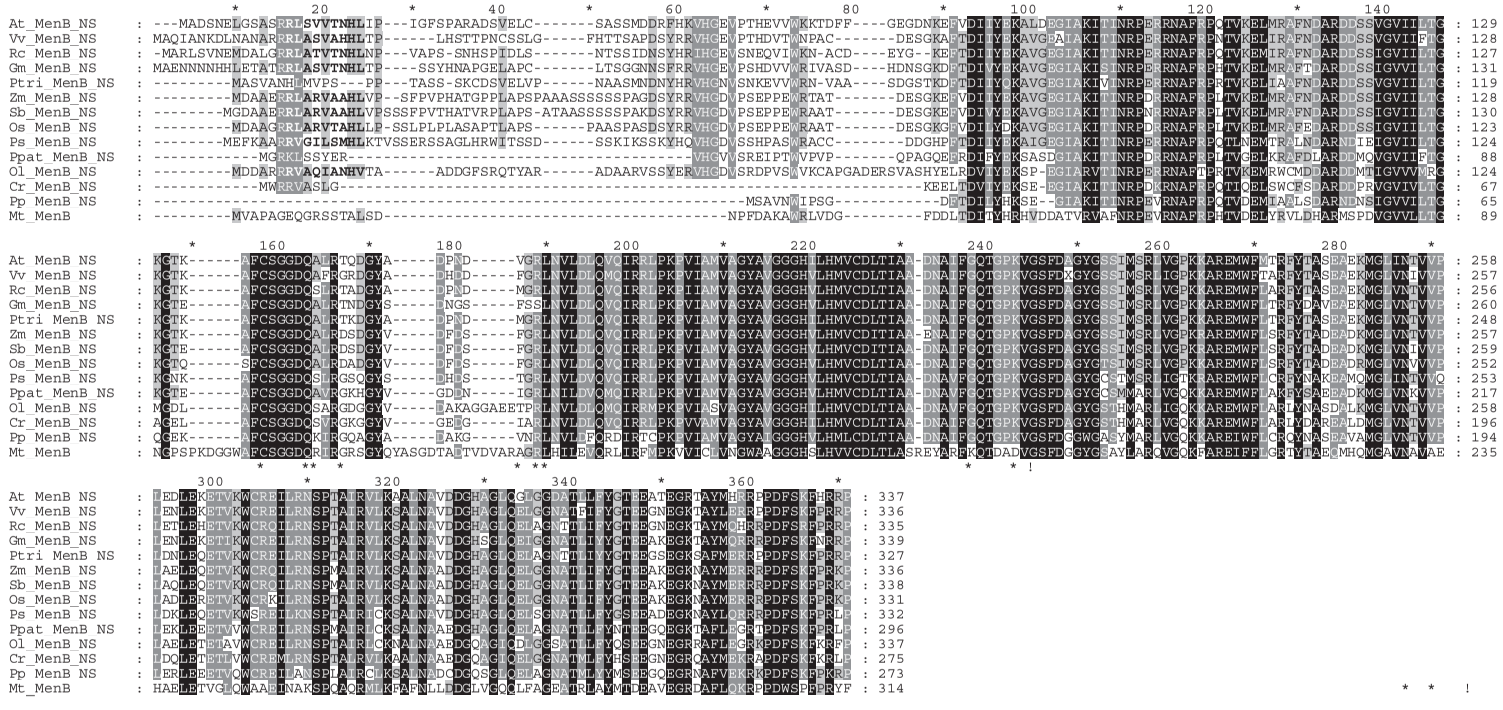

Suppl. Table I: Proteins identified in isolated leaf peroxisomes from *Spinacia oleracea* L. by mass spectrometry

Protein spots indicated by an asterics (*) in gel A were identified from gel spots located outside of the areas shown for gel B (62, 69) or gel C (83, 91, 97, 98, 120) or derived from a forth gel (1, 2, 4, 5, 7, 8, 14-18, 20). M., *Mesembryanthemum*

Spot No.	Acronym	Protein ID	Organism	Accession number	Mol mass / pI	Sequence coverage / peptide sequence
Leaf peroxisomal proteins						
16	SGT/AGT	Serine (alanine)-glyoxylate aminotransferase	*Arabidopsis thaliana*	At2g13360	44.2/7.69	4%
17	MDH	Malate dehydrogenase	*Citrullus lanatus*	P19446	35.5/7.06	25%
19	HPR	Hydroxypyruvate reductase	*Cucumis savitus*	P13443	41.7/5.95	21%
20	GGT1	Glutamate-glyoxylate aminotransferase isoform 1	*Arabidopsis thaliana*	At1g23310	53.3/6.91	25%
21	APX	(Cytosolic) ascorbate peroxidase	*M. crystallinum*	Q9XFC0	31.5/8.25	7%
22	APX	(Cytosolic) ascorbate peroxidase	*M. crystallinum*	Q9XFC0	31.5/8.25	7%
23	MDH	Malate dehydrogenase	*Citrullus lanatus*	P19446	35.5/7.06	23%
24	HPR	Hydroxypyruvate reductase	*Cucurbita*	Q42708	42.3/5.87	25%
25	HPR	Hydroxypyruvate reductase	*Cucurbita*	Q42708	42.3/5.87	20%
27	MDH	Malate dehydrogenase	*Medicago sativa*	O48903	38.1/8.,5	16 %
30	GGT1	Glutamate-glyoxylate aminotransferase isoform 1	*Arabidopsis thaliana*	Q9C5K2 (At1g23310)	53.3/6.91	18%
31	GOX	Glycolate oxidase	*Spinacia oleracea*	P05414	40.2/9.16	62%
32	GOX	Glycolate oxidase	*Spinacia oleracea*	P05414	40.2/9.16	39%
33	GOX	Glycolate oxidase	*Spinacia oleracea*	P05414	40.2/9.16	59%
34	LACS6	Long chain acyl-CoA synthetase isoform 6	*Arabidopsis thaliana*	Q8LKS6 (At3g05970)	76.6/8.11	3%
35	LACS6	Long chain acyl-CoA synthetase isoform 6	*Arabidopsis thaliana*	Q8LKS6 (At3g05970)	76.6/8.11	2%
39	SGT/AGT	Serine (alanine)-glyoxylate aminotransferase	*Fritillaria agrestis*	O49124	44/7.63	TNNLTAVR
40	SGT/AGT	Serine (alanine)-glyoxylate aminotransferase	*Fritillaria agrestis*	O49124	44/7.63	LFVPGPVNIPEPVIR
42	Uri	Uricase (or)	*Arabidopsis thaliana*	O04420 (At2g26230)	34.9/8.6	3%
	pMDH2	Malate dehydrogenase	*Arabidopsis thaliana*	Q9ZP05 (At5g09660)	37.3/8.1	3%
43	MDH	Malate dehydrogenase (or)	*Medicago sativa*	O48903	38.1/8.5	16%
	Uri	Uricase	*Arabidopsis thaliana*	O04420 (At2g26230)	34.9/8.6	3%
44	CSY2	Citrate synthase-like protein	*Arabidopsis thaliana*	Q9LXS6 (At3g58750)	56.5/8.73	11%
46	SGT	Serine (alanine)-glyoxylate aminotransferase	*Arabidopsis thaliana*	O81248 (At2g13360)	44.1/7.69	6%
	HPR	Hydroxypyruvate reductase	*Arabidopsis thaliana*	Q9C9W5 (At1g68010)	42.2/6.68	6%
47	CAT	Catalase	*Suaeda salsa*	Q941J0	33.3/6.4	27%
48	CAT4	Catalase isoform 4	*Helianthus annuus*	Q9M502	56.9/6.62	14%
50	ICL	Isocitrate lyase	*Solanum lycopersicum*	P49297	64.7/6.56	9%
51	CAT1	Catalase isozyme 1	*Nicotiana plumbaginifolia*	P49315	55.82/6.75	15%

52	CAT2	Catalase 2	*Arabidopsis thaliana*	P25819 (At4g35090)	56.9/6.63	26%
53	CAT2	Catalase 2	*Arabidopsis thaliana*	P25819 (At4g35090)	56.9/6.63	23%
54	CAT2	Catalase 2	*Arabidopsis thaliana*	P25819 (At4g35090)	56.9/6.63	23%
55	PED1/KAT2	3-ketoacyl-CoA thiolase	*Arabidopsis thaliana*	Q9S7M3 (At2g33150)	48.5/8.62	17%
56	PED1/KAT2	3-ketoacyl-CoA thiolase	*Arabidopsis thaliana*	Q9S7M3 (At2g33150)	48.5/8.62	17%
57	PED1/KAT2	3-ketoacyl-CoA thiolase	*Arabidopsis thaliana*	Q9S7M3 (At2g33150)	48.5/8.62	17%
58	OPR3	12-oxophytodienoate reductase 3	*Solanum lycopersicum*	Q9FEW9	43.5/8.51	4%
59	SOX	Sulphite oxidase (or)	*Oryza sativa*	Q8LP96	43.8/8.13	7%
	SGT	Serine (alanine)-glyoxylate aminotransferase	*Fritillaria agrestis*	O49124	44.1/7.63	6%
60	SOX	Sulphite oxidase	*Oryza sativa*	Q8LP96	43.8/8.13	11%
61	SGT/AGT	Serine (alanine)-glyoxylate aminotransferase	*Fritillaria agrestis*	O49124	44.1/7.63	6%
	Thiol.	3-Ketoacyl-CoA thiolase	*Cucurbita*	P93112	48.6/8.21	4%
62	GGT1	Glutamate-glyoxylate aminotransferase isoform 1	*Arabidopsis thaliana*	Q9C5K2 (At1g23310)	53.3/6.91	27%
63	NS/ECHId	Naphthoate synthase/Enoyl-CoA hydratase/ isomerase isoform d (or)	*Arabidopsis thaliana*	Q8GYN9 (At1g60550)	37.1/6,77	7%
	NS	Putative naphthoate synthase menB	*Oryza sativa*	Q8LR33	35.9/8.88	7%
65	CAT	Catalase	*Suaeda salsa*	Q94EV9	56.7/6.76	15%
66	CAT4	Catalase 4	*Helianthus annuus*	Q9M502	56.9/6.62	13%
67	CAT	Catalase	*Suaeda salsa*	Q94EV9	56.7/6.76	22%
68	PED1/KAT2	3-Ketoacyl-CoA thiolase	*Arabidopsis thaliana*	Q9S7M3 (At2g33150)	48.5/8.62	11%
69	ICL	Isocitrate lyase	*Ipomoea batatas*	Q9FQD2	64.4/7.25	9%
70	GOX	Glycolate oxidase (or)	*Spinacia oleracea*	P05414	40.3/9.16	18%
		Cytosolic Aspartate aminotransferase	*Arabidopsis thaliana*	P46645 (At5g19550)	44.2/6.8	13%
83	MLS	Malate synthase	*Cucumis sativus*	P08216 (At3g21720)	64.9/8.45	11%
91	MDH	Malate dehydrogenase, glyoxysomal (or)	*Citrullus lanatus*	P19446	37.6/8.67	23%
	SGT	Serine (alanine)-glyoxylate aminotransferase	*Fritillaria agrestis*	O49124	44.1/7.63	6%
95	SOX	Sulfite oxidase	*Oryza sativa*	Q8LP96	43.8/8.13	9%
97	MDH	Malate dehydrogenase, (or)	*Citrullus lanatus*	P19446	37.6/8.67	23%
	APX	(cytosolic) ascorbate peroxidase	*M. crystallinum*	Q9XFC0	31.5/8.25	10%
98	APX3	Ascorbate peroxidase isoform 3	*Arabidopsis thaliana*	Q42564 (At4g35000)	31.6/6.47	17%
99	APX3	Ascorbate peroxidase isoform 3 (or)	*Arabidopsis thaliana*	Q42564 (At4g35000)	31.6/6.47	12%
	CSY	Citrate synthase (or)	*Cucurbita maxima*	P49299	56.7/8.84	4%
	MDH	Malate dehydrogenase	*Arabidopsis thaliana*	Q9ZP05	37.3/8.14	3%
100	MDH	Malate dehydrogenase (glyoxysomal)(or)	*Citrullus lanatus*	P19446	37.6/8.67	7%
	Uri	Uricase	*Arabidopsis thaliana*	O04420 (At2g26230)	34.9/8.6	3%
101	GOX	Glycolate oxidase	*Spinacia oleracea*	P05414	40.3/9.16	7%
103	ECHI	Monofunctional enoyl CoA hydratase/ isomerase	*Cicer arietinum*	Q9SMK7	29.0/9,02	7%
104	SDRa	Short-chain alcohol dehydrogenase /reductase isoform a	*Arabidopsis thaliana*	Q9S9W2 (At4g05530)	26.7/8.46	12%
107	GOX	Glycolate oxidase	*Spinacia oleracea*	P05414	40.3/9.16	20%
109	GOX	Glycolate oxidase	*Spinacia oleracea*	P05414	40.3/9.16	25%

110	GOX	Glycolate oxidase	*Spinacia oleracea*	P05414	40.3/9.16	25%
111	GOX	Glycolate oxidase	*Spinacia oleracea*	P05414	40.3/9.16	21%
120	ICL	Isocitrate lyase	*Solanum lycopersicum*	P49297	64.7/6.56	8%
Chloroplast proteins						
1		RubisCO activase	*Spinacia oleracea*	P10871	51.5/6.62	55%
2		Fructose-bisphosphate aldolase	*Spinacia oleracea*	P16096	42.4/6.85	26%
4		RubisCO activase	*Spinacia oleracea*	P10871	51.5/6.62	65%
5		Transketolase	*Solanum tuberosum*	Q43848	79.9/5.94	8%
7		ATP-dependent clp protease	*Lycopersicon esculentum*	P31542	102/5.86	34%
8		Phosphoglycerate kinase	*Spinacia oleracea*	P29409	45.5/5.83	17%
14		RubisCO activase	*Spinacia oleracea*	P10871	45.4/5.4	55%
15		Phosphoribulokinase	*Spinacia oleracea*	P09559	44,9/5,82	38%
18		RubisCO LSU	Spinacia oleracea	P00875	52,7/6,13	46 %

Suppl. Table II: Oligonucleotide primers used for cDNA subcloning

Construct	PTS1 protein	AGI code	Primer	Primer sequence (5' to 3')
EYFP-SDRa	SDRa	At4g05530	for (NotI)	CACCAAGACTGCGGCCGCTATGGAGAAGAAGCTACC
			rev (NotI)	TGAAGAATTAGCGGCCGCTTAGAGTCTTGAAGGCATTCC
EYFP-PTD(SDRa)	SDRa	At4g05530	for (NcoI)	AAGTCCATGGTGAGCAAGGGCGAGGA
			rev (XbaI)	TATATCTAGATTAGAGTCTTGAAGGCATTCCTCCAGCGACAACCTTGTACAGCTCGTCCATGCC
EYFP-ECHIa	ECHIa	At4g16210	for (NotI)	AAGATTGCGGCCGCTATGGATCAAACAGTATCGG
			rev (SacII)	TATACCGCGGCTACAACTTAGAAGAAGGTTTC
EYFP-PTD(ECHIa)	ECHIa	At4g16210	for (NcoI)	AAGTCCATGGTGAGCAAGGGCGAGGA
			rev (XbaI)	TATATCTAGACTACAACTTAGAAGAAGGTTTCTTGGATCCACGCTTGTACAGCTCGTCCATGCC
NS-EYFP	NS/ECHId	At1g60550	for (NcoI)	CACCATGGCGGATTCCAATGAGCTTG
			rev (NcoI)	GAGCTCCATGGAAGGTCGCCGGTGAAATTTA
NSΔN-EYFP	NS/ECHId	At1g60550	for (NcoI)	CACCATGGATGATAGATTCCATAAG
			rev (NcoI)	GAGCTCCATGGAAGGTCGCCGGTGAAATTTA
NSΔPTS2(H→V)-EYFP	NS/ECHId	At1g60550	for (AclI)	CGAGCCGACGACTCTCCGTCGTCACCAACGTTCTCATCCCTATCGGATTCAGTCCAGC
			rev (AclI)	GCTGGACTGAATCCGATAGGGATGAGAACGTTGGTGACGACGGAGAGTCGTCGGCTCG
EYFP-AAE14	AAE14	At1g30520	for (NotI)	aagactgcggccgctatggctaatcactctcgg
			rev (XbaI)	caagtctagatcagagagagctagtcat
EYFP-PTD(AAE14)	AAE14	At1g30520	for (NcoI)	AAGTCCATGGTGAGCAAGGGCGAGGA
			rev (XbaI)	TATGTCTAGAGTCAGAGAGAGCTAGTCATGATTTGGAAATGAGACTTGTACAGCTCGTCCATGCC